18.S996 Hydrodynamic quantum analogs

Lecture 14: Orbital pilot-wave dynamics

Walkers in a rotating frame

Path-memory induced quantization of classical orbits

Emmanuel Fort[a,1], Antonin Eddi[b], Arezki Boudaoud[c], Julien Moukhtar[b], and Yves Couder[b]

[a]Institut Langevin, Ecole Supérieure de Physique et de Chimie Industrielles ParisTech and Université Paris Diderot, Centre National de la Recherche Scientifique Unité Mixte de Recherche 7587, 10 Rue Vauquelin, 75 231 Paris Cedex 05, France; [b]Matières et Systèmes Complexes, Université Paris Diderot, Centre National de la Recherche Scientifique Unité Mixte de Recherche 7057, Bâtiment Condorcet, 10 Rue Alice Domon et Léonie Duquet, 75013 Paris, France; and [c]Laboratoire de Physique Statistique, Ecole Normale Supérieure, 24 Rue Lhomond, 75231 Paris Cedex 05, France

J. Fluid Mech. (2014), vol. 739, pp. 444–464. © Cambridge University Press 2013
doi:10.1017/jfm.2013.627

Droplets walking in a rotating frame: from quantized orbits to multimodal statistics

Daniel M. Harris and John W. M. Bush†

Department of Mathematics, Massachusetts Institute of Technology, Cambridge, MA 02139, USA

J. Fluid Mech. (2014), vol. 744, pp. 404–429. © Cambridge University Press 2014 40
doi:10.1017/jfm.2014.50

Pilot-wave dynamics in a rotating frame: on the emergence of orbital quantization

Anand U. Oza, Daniel M. Harris, Rodolfo R. Rosales and John W. M. Bush†

Department of Mathematics, Massachusetts Institute of Technology, Cambridge, MA 02139, USA

PHYSICS OF FLUIDS 26, 082101 (2014)

Pilot-wave hydrodynamics in a rotating frame: Exotic orbits

Anand U. Oza,[1] Øistein Wind-Willassen,[2] Daniel M. Harris,[1] Rodolfo R. Rosales,[1] and John W. M. Bush[1,a)]

[1]Department of Mathematics, Massachusetts Institute of Technology, 77 Massachusetts Avenue, Cambridge, Massachusetts 02139, USA
[2]Department of Applied Mathematics and Computer Science, Technical University of Denmark, 2800 Kongens Lyngby, Denmark

J. Fluid Mech. (2023), vol. 973, A4, doi:10.1017/jfm.2023.742

JFM PAPERS

Pilot-wave dynamics in a rotating frame: the onset of orbital instability

Nicholas Liu[1], Matthew Durey[2] and John W.M. Bush[1,†]

[1]Department of Mathematics, Massachusetts Institute of Technology, Cambridge, MA 02139, USA
[2]School of Mathematics and Statistics, University of Glasgow, University Place, Glasgow G12 8QQ, UK

Quick review: Dynamics in a rotating frame

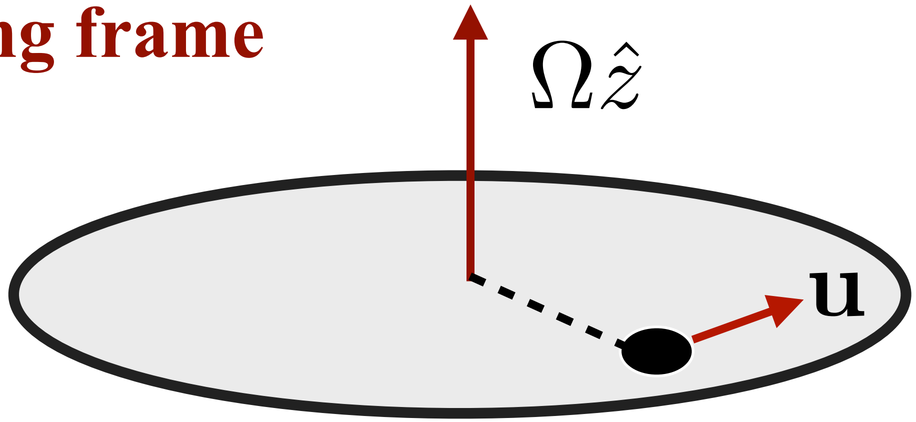

I. Particle motion in a rotating frame

- fictitious forces result from interpretation of inertial forces in rotating frame
- stationary particles subject to centrifugal force $\mathbf{F_{cent}} = m\Omega^2 r\ \hat{r}$
- moving particles subject to Coriolis force $\mathbf{F_C} = 2m\mathbf{u} \wedge \mathbf{\Omega}$

Trajectory equation in a rotating frame

$$m\ddot{\mathbf{x}}_{\mathbf{p}} = \mathbf{F_{ext}} + 2m\dot{\mathbf{x}}_{\mathbf{p}} \wedge \mathbf{\Omega} + m\Omega^2 r\hat{r}$$

Inertia Coriolis Centrifugal

II. Navier-Stokes equations in a rotating frame

- consider frame rotating with uniform angular velocity $\boldsymbol{\Omega} = \Omega\hat{z}$
- velocity, $\mathbf{u}$, in rotating frame related to that, $\mathbf{v}$, in lab frame by $\mathbf{u} = \mathbf{v} - \boldsymbol{\Omega} \wedge \mathbf{r}$
- sub into Navier-Stokes for $\mathbf{v}$ to deduce their form in the rotating frame:

$$\frac{D\mathbf{u}}{Dt} = -\frac{1}{\rho}\nabla p_d + \nu\nabla^2\mathbf{u} + \mathbf{g} - 2\boldsymbol{\Omega} \wedge \mathbf{u} \quad , \quad \nabla \cdot \mathbf{u} = 0$$

where the dynamic pressure $p_d = p - \rho\mathbf{g}\cdot\mathbf{x} - \frac{1}{2}\rho\Omega^2 r^2$

Statics: $\mathbf{u} = 0 \longrightarrow \nabla p_d = 0$

$$p = p_0 + \rho\mathbf{g}\cdot\mathbf{x} - \frac{1}{2}\rho\Omega^2 r^2$$

Isobar on free surface:

$$z = \frac{\Omega^2}{2g} r^2$$

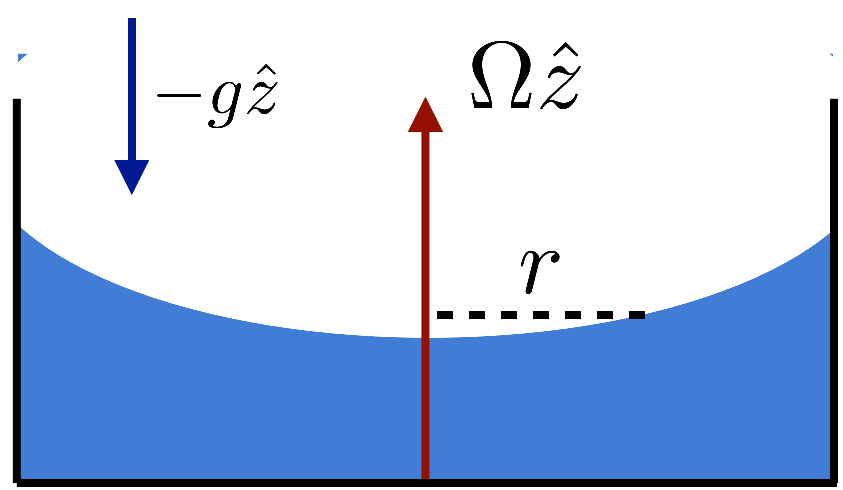

Experimental setup

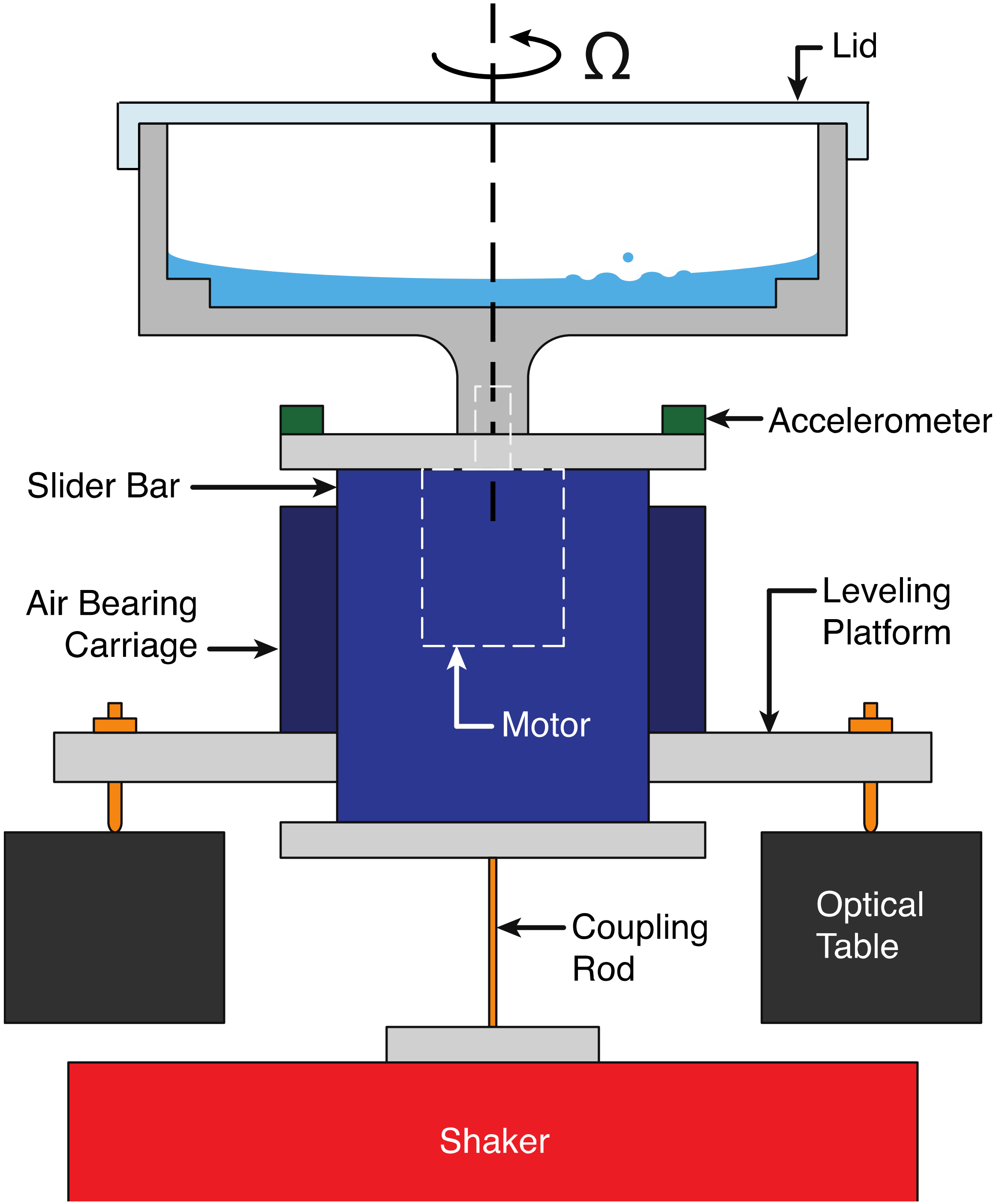

Control parameters:

γ/γ_F Memory

Ω Rotation rate

Fort et al, *PNAS* **107** (41) 17515-17520 (2010).

Harris & Bush, *JFM* **739**, 444-464 (2014).

III. Walking droplets in a rotating frame

$$z = \frac{\Omega^2}{2g} r^2$$

- interface represents a parabolic isopotential, weakly curved
- a stationary bouncer bounces perpendicular to the curved free surface
- the outward centrifugal force is precisely balanced by the inward curvature force
- trajectory equation for a walking droplet need only be augmented by Coriolis force
- walkers translate at free walking speed, but transform to bouncers at high Ω
- tend to execute *anticyclonic* orbits, for which centripetal and Coriolis forces balance

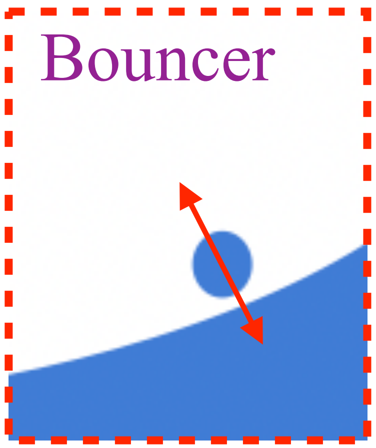

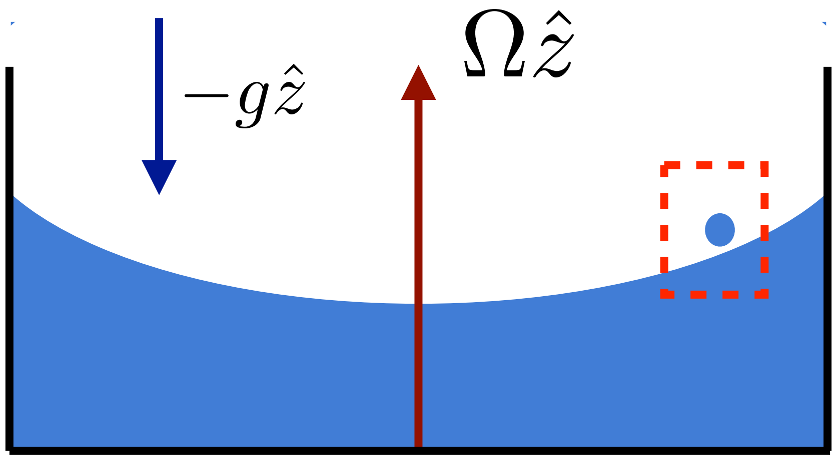

Inertial orbits: *anticyclonic*

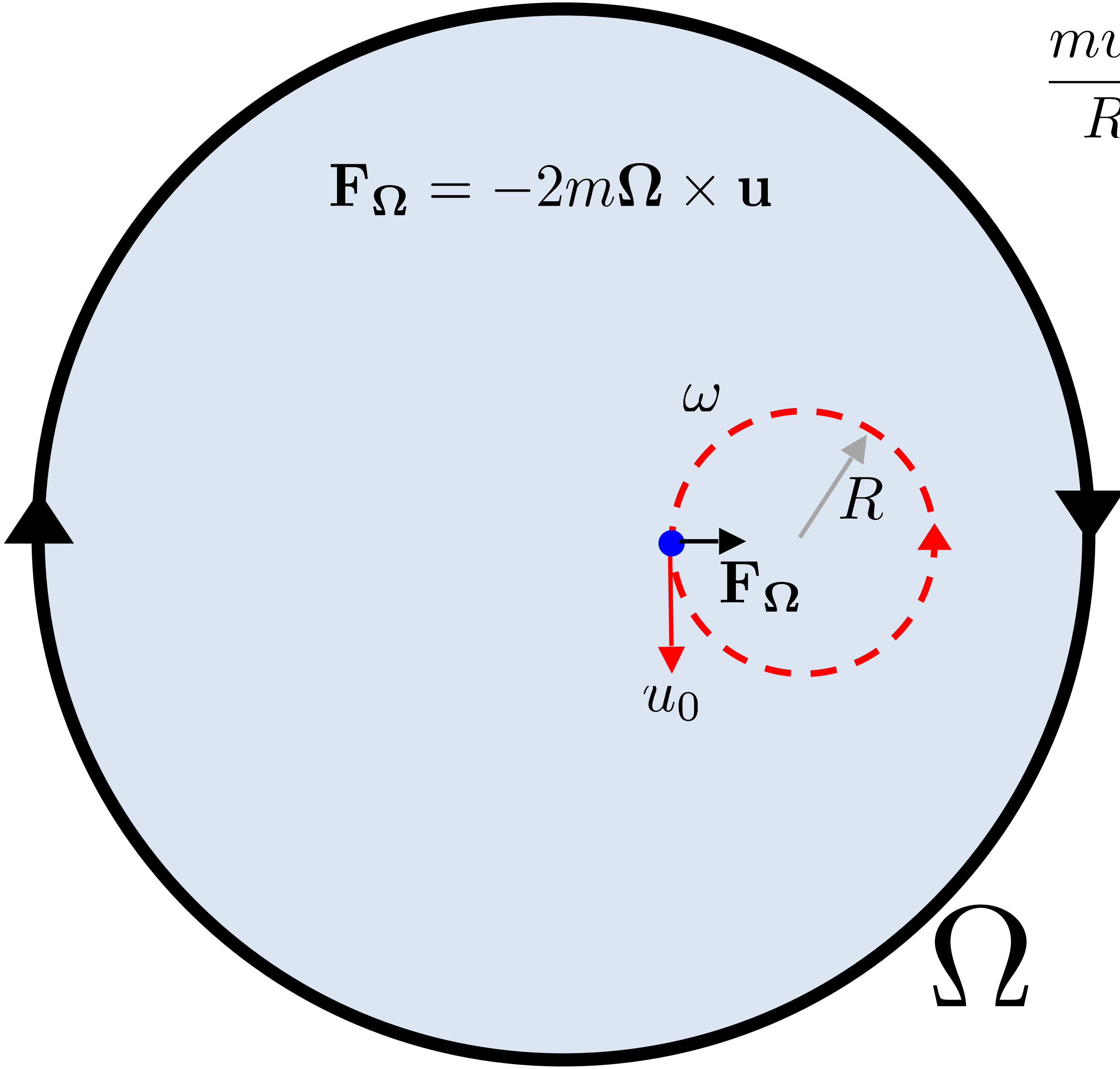

$$\frac{mu_0^2}{R} = |\mathbf{F}_{\boldsymbol{\Omega}}| = 2m\Omega u_0$$

$$R = \frac{u_0}{2\Omega}$$

$$\omega = \frac{u_0}{R} = -2\Omega$$

Coriolis force:

$$\mathbf{F} = -2m\boldsymbol{\Omega} \times \dot{\mathbf{x}}_p$$

Force on charged particle:

$$\mathbf{F} = -q\boldsymbol{B} \times \dot{\mathbf{x}}_p$$

Walker on a rotating bath

Lab frame

Rotating frame

$$\omega = \frac{u_0}{R} = -2\Omega$$

Wave fields generated by orbiting walkers

Centered on drop

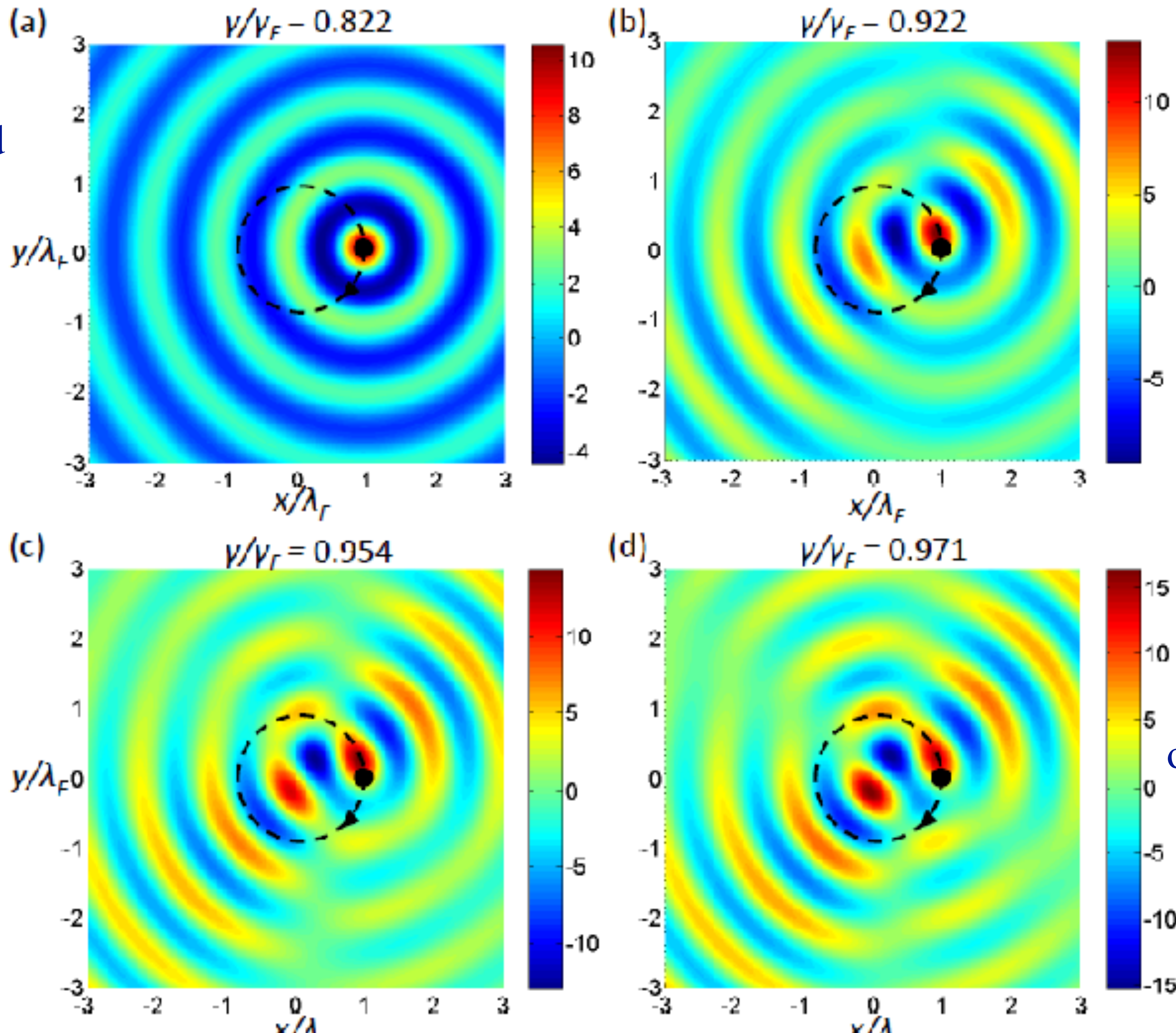

Centered on orbital center

Orbital quantization

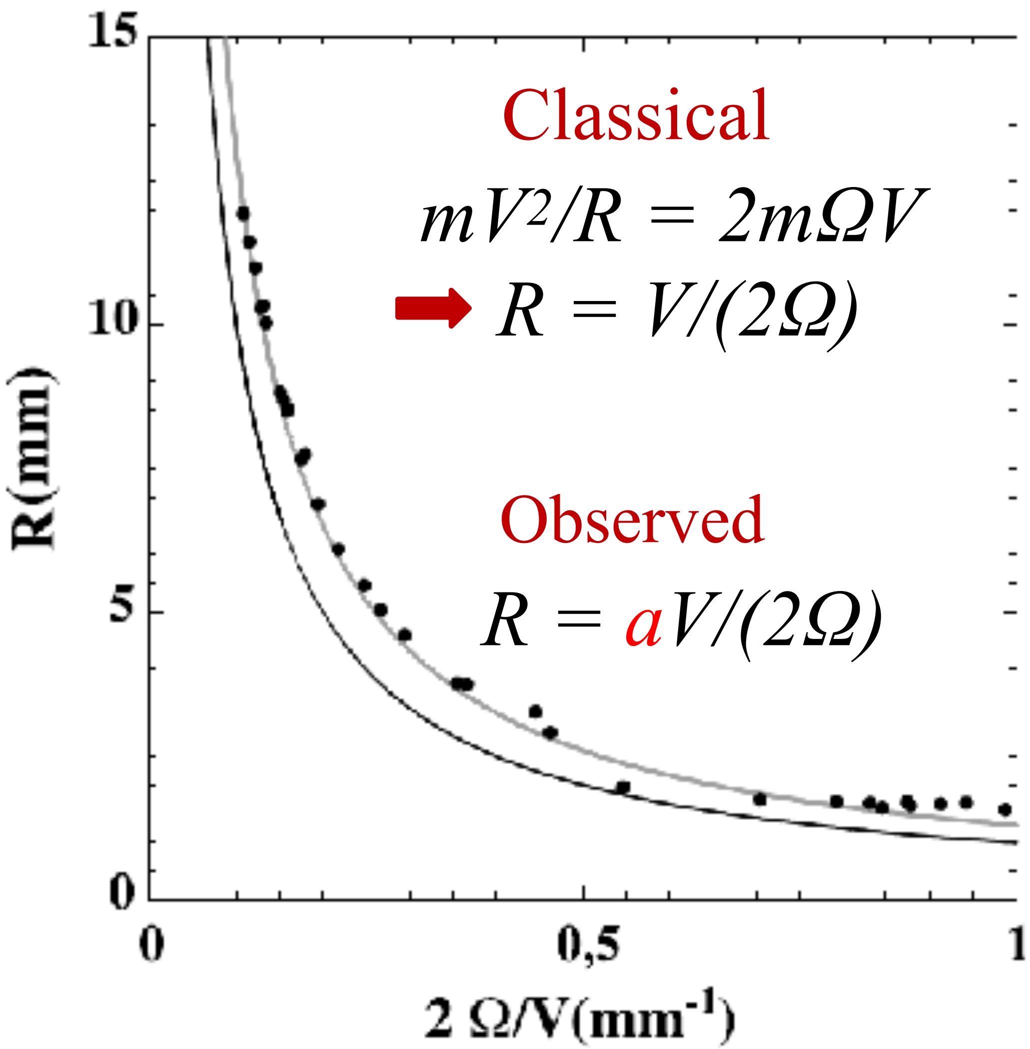

low memory

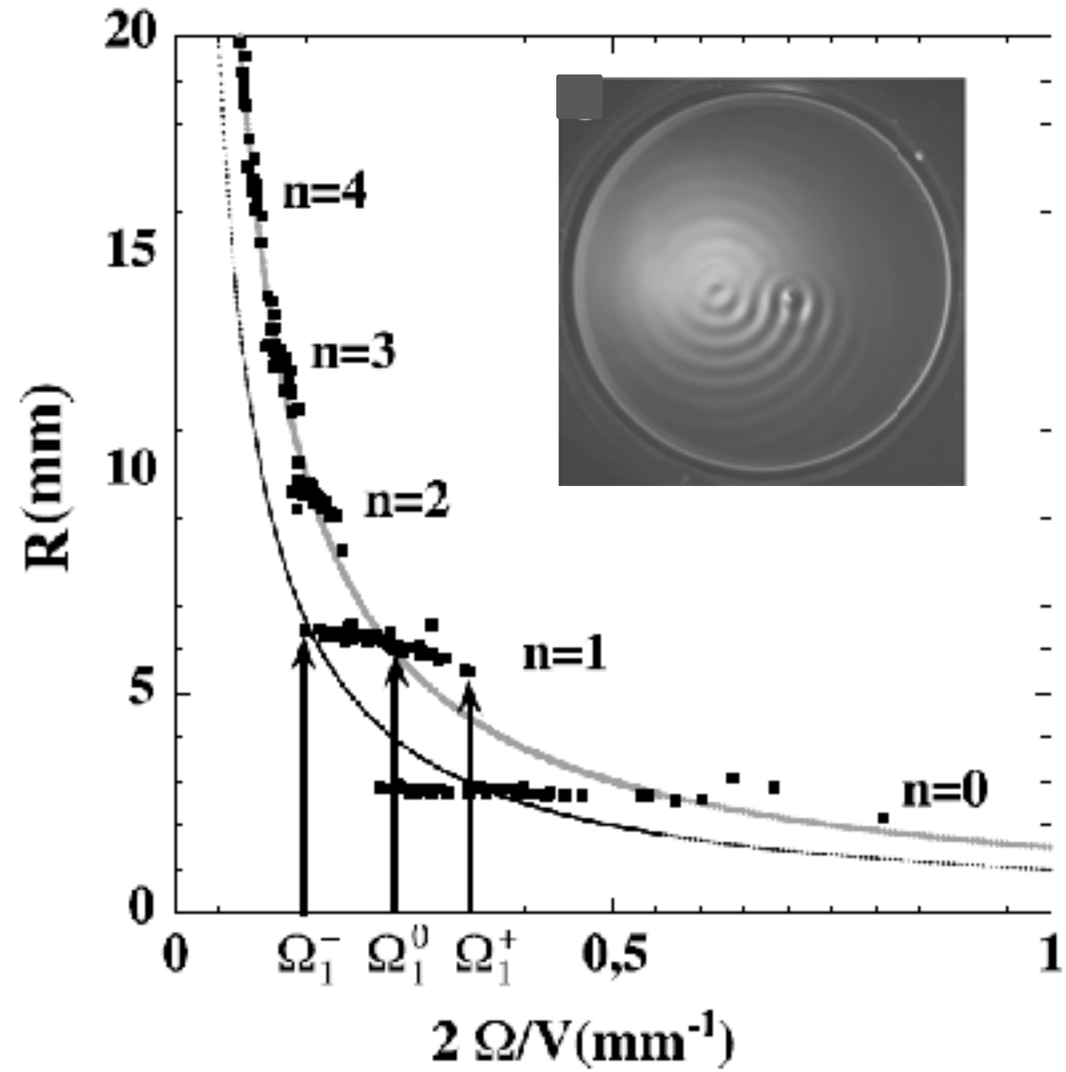

high memory

Fort et al, *PNAS* **107** (41) 17515-17520 (2010)

Pilot-wave dynamics in a rotating frame

Oza, Harris, Rosales & Bush (2013)

$$m\ddot{\mathbf{x}} + D\dot{\mathbf{x}} = \frac{F}{T_F}\int_{-\infty}^{t} \frac{J_1(k_F|\mathbf{x}(t)-\mathbf{x}(s)|)}{|\mathbf{x}(t)-\mathbf{x}(s)|}(\mathbf{x}(t)-\mathbf{x}(s))\, e^{-(t-s)/(T_F M_e)}\, ds - 2m\mathbf{\Omega}\times\dot{\mathbf{x}}$$

Coriolis force

Seek orbital solutions: $r_p(t) = r_0\ ,\ \theta_p(t) = \omega t$

Pilot-wave dynamics in a rotating frame

Oza, Harris, Rosales & Bush (2013)

$$m\ddot{\mathbf{x}} + D\dot{\mathbf{x}} = \frac{F}{T_F}\int_{-\infty}^{t} \frac{J_1(k_F\,|\mathbf{x}(t)-\mathbf{x}(s)|)}{|\mathbf{x}(t)-\mathbf{x}(s)|}\,(\mathbf{x}(t)-\mathbf{x}(s))\,e^{-(t-s)/(T_F M_e)}\,ds - 2m\boldsymbol{\Omega}\times\dot{\mathbf{x}}$$

Coriolis force

Seek orbital solutions: $r_p(t) = r_0\ ,\ \theta_p(t) = \omega t$

$$\begin{aligned} -mr_0\omega^2 &= \frac{F}{T_F}\int_0^\infty J_1\left(2k_F r_0 \sin\frac{\omega z}{2}\right)\sin\frac{\omega z}{2} e^{-z/(M_e T_F)}\,dz + 2mr_0\Omega\omega \\ Dr_0\omega &= \frac{F}{T_F}\int_0^\infty J_1\left(2k_F r_0 \sin\frac{\omega z}{2}\right)\cos\frac{\omega z}{2} e^{-z/(M_e T_F)}\,dz \end{aligned}$$

nonlinear system of equations in *(r_0, ω)*

Stability of orbital solutions

Oza, Rosales & Bush (2013)

$$m\ddot{\mathbf{x}} + D\dot{\mathbf{x}} = \frac{F}{T_F}\int_{-\infty}^{t} \frac{J_1(k_F|\mathbf{x}(t)-\mathbf{x}(s)|)}{|\mathbf{x}(t)-\mathbf{x}(s)|}(\mathbf{x}(t)-\mathbf{x}(s))\,e^{-(t-s)/(T_F M_e)}\,ds - 2m\mathbf{\Omega}\times\dot{\mathbf{x}}$$

- write equation in polar coordinates
- linearize around orbital solutions:

$$r(t) = r_0 + \varepsilon r_1(t), \quad \theta(t) = \omega t + \varepsilon\theta_1(t) \qquad (0 < \varepsilon << 1)$$

- Laplace transform linearized equation

$$\mathcal{L}[r_1] = R(s), \quad \mathcal{L}[\theta_1] = \Theta(s)$$

and obtain solutions

$$R(s) = a(s)/F(s), \quad \Theta(s) = b(s)/F(s)$$

- zeros of *F(s)* determine stability of orbital solution
  - Stable if Re(s) < 0, unstable if Re(s) > 0

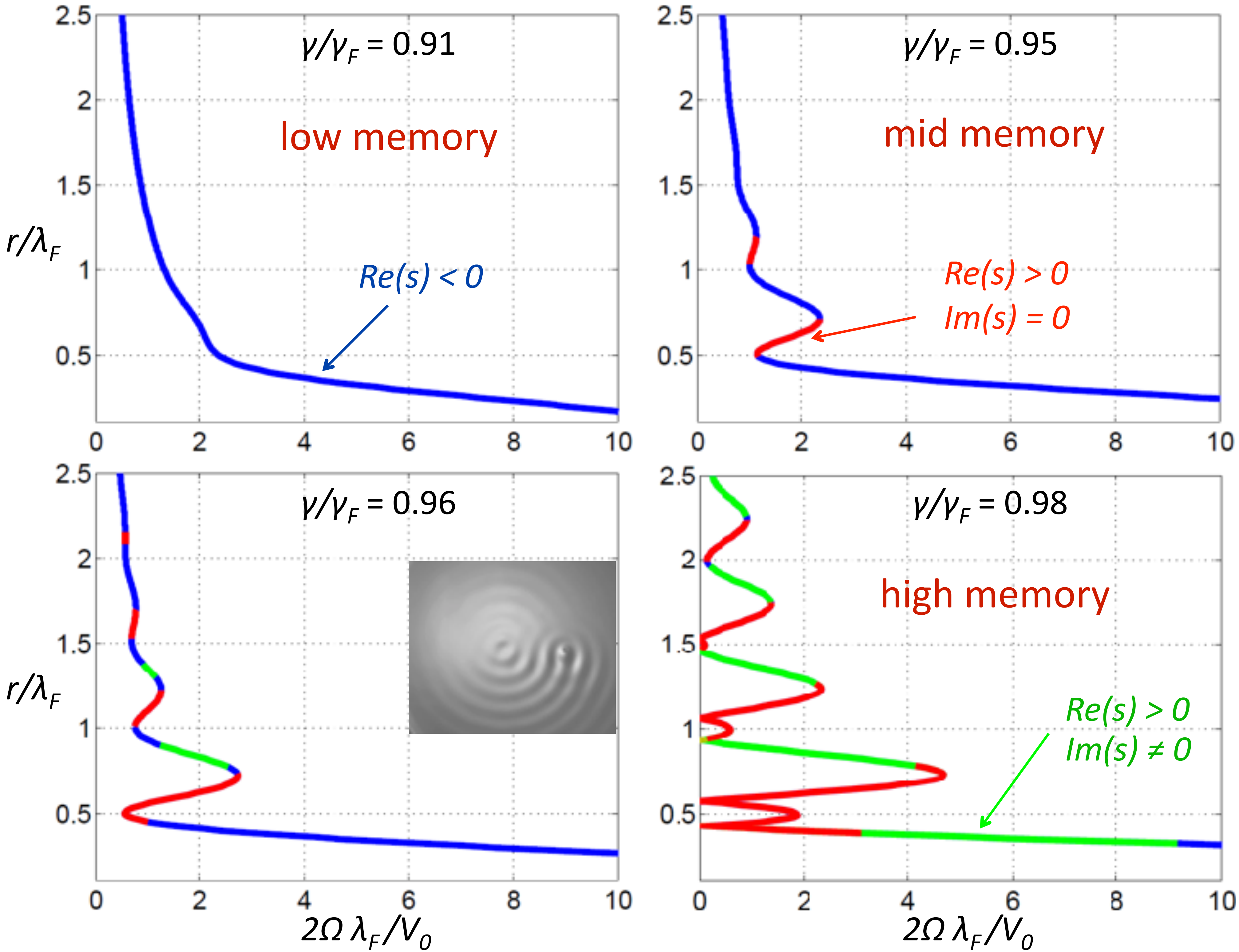

$\gamma/\gamma_F = 0.91$
low memory
Re(s) < 0
$\gamma/\gamma_F = 0.95$
mid memory
Re(s) > 0
Im(s) = 0
$\gamma/\gamma_F = 0.96$
$\gamma/\gamma_F = 0.98$
high memory
Re(s) > 0
Im(s) ≠ 0
r/λ_F
$2\Omega\,\lambda_F/V_0$

Low-memory results

$$\gamma/\gamma_F = 0.822 \pm 0.006$$

Deduced: $$\frac{\tilde{m}}{m} = a = 1 + \frac{4FM_e^3T_F^2k_F}{m\left(-1+\sqrt{1+4FM_e^2T_Fk_F/D}\right)^3}$$

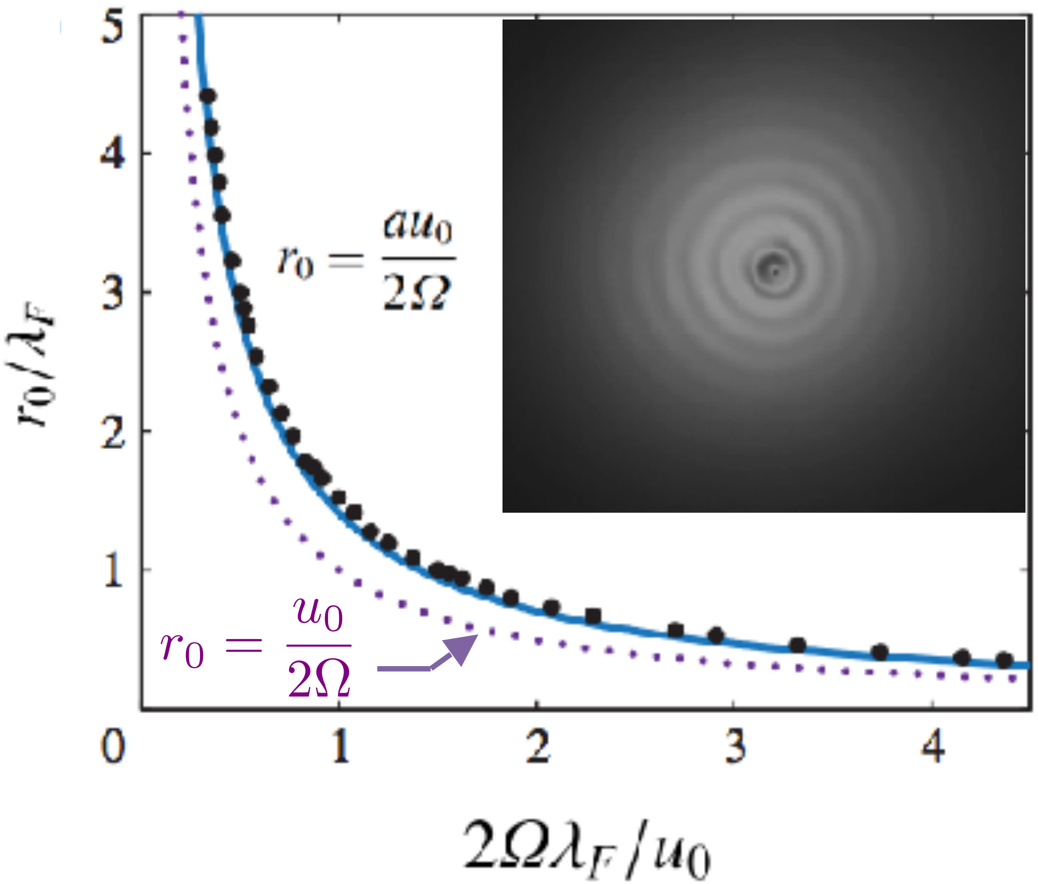

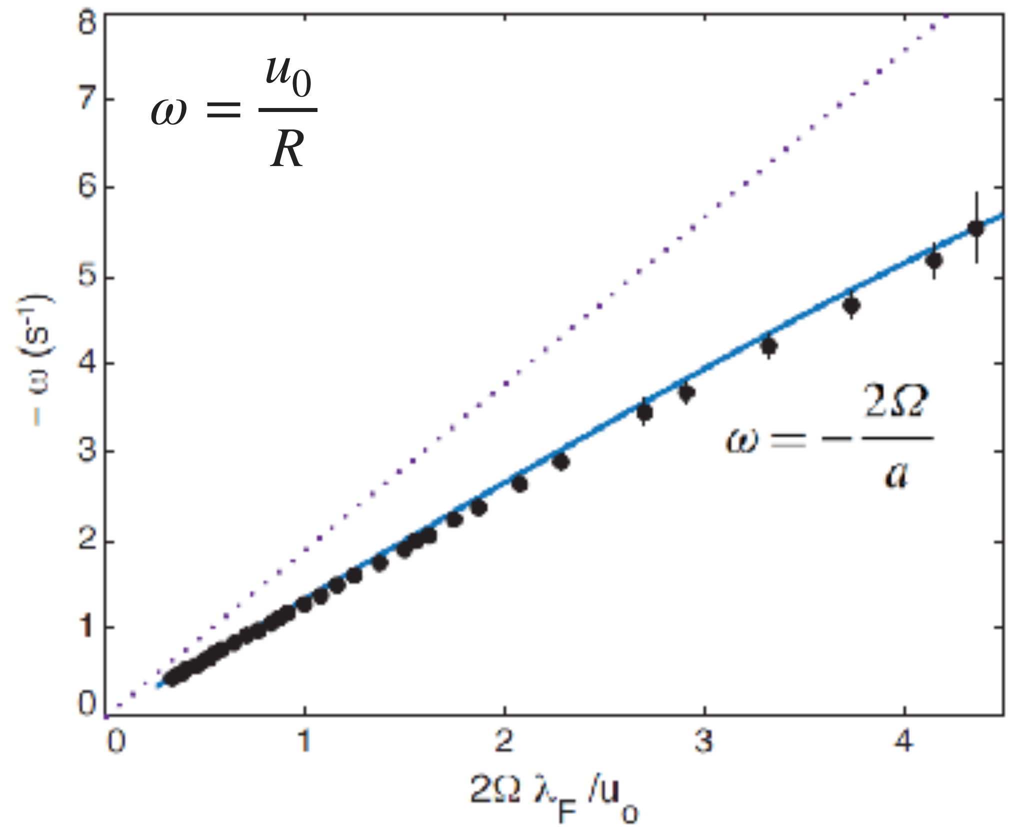

- **continuous** variation of orbital radius and frequency with rotation rate
- offset from classical prediction can be understood as a wave-induced added mass (Bush, Oza, Molacek 2014)

Mid-memory regime

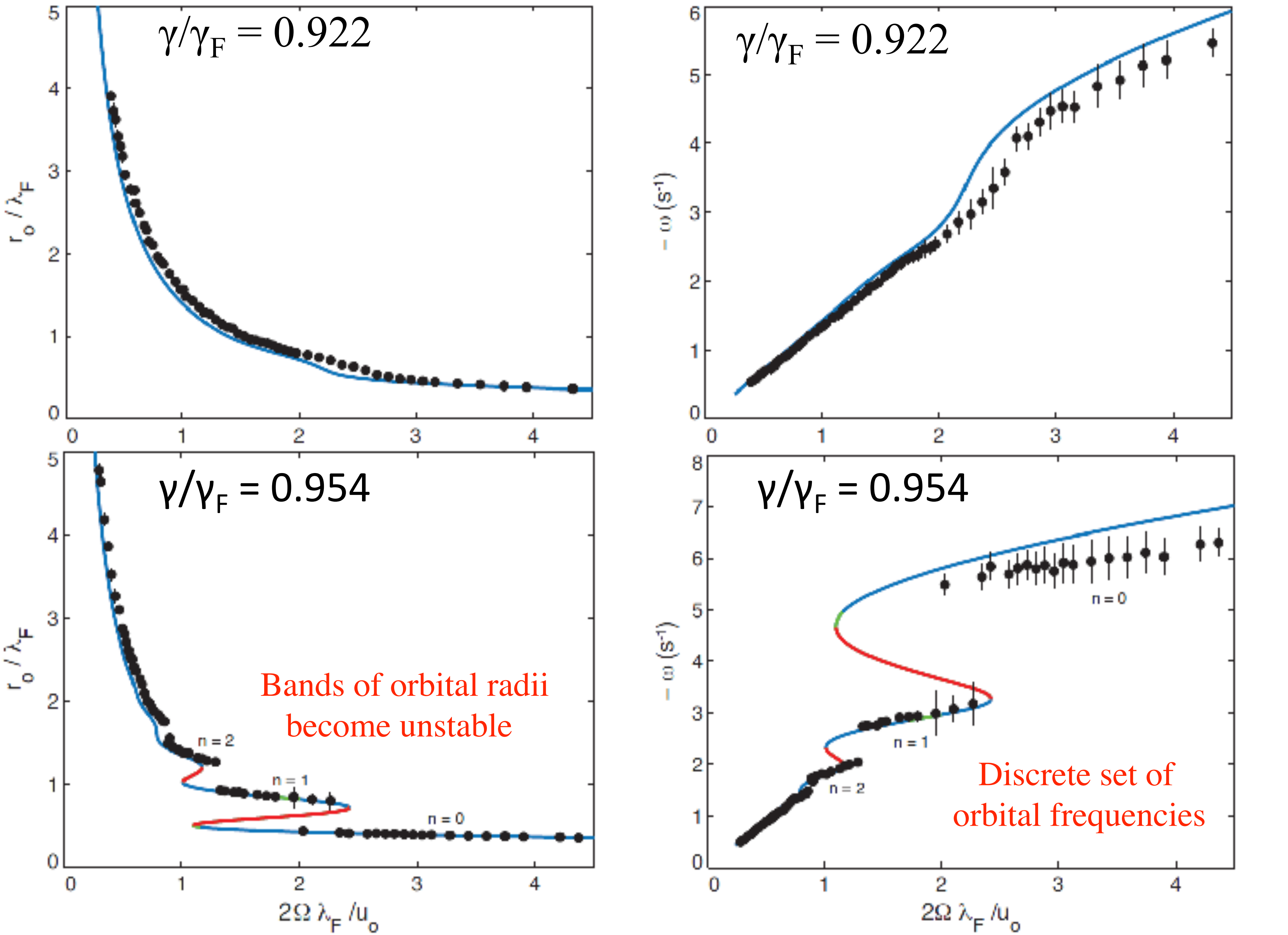

High memory regime

$\gamma/\gamma_F = 0.971$

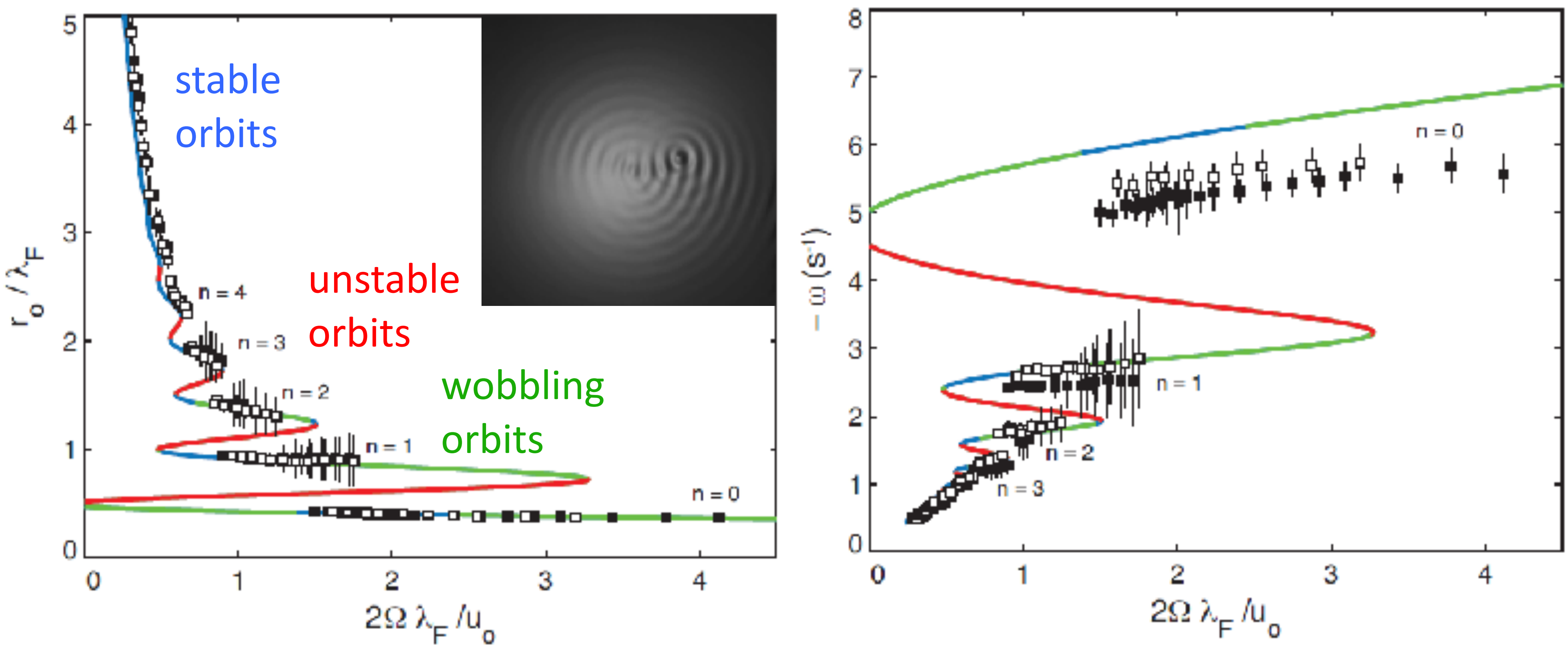

- more bands of radii become inaccessible
- multiple radii accessible for fixed rotation rate
- periodic fluctuations in orbital radius observed

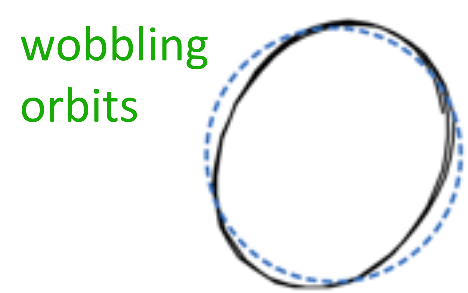

Stability of circular orbits: high memory

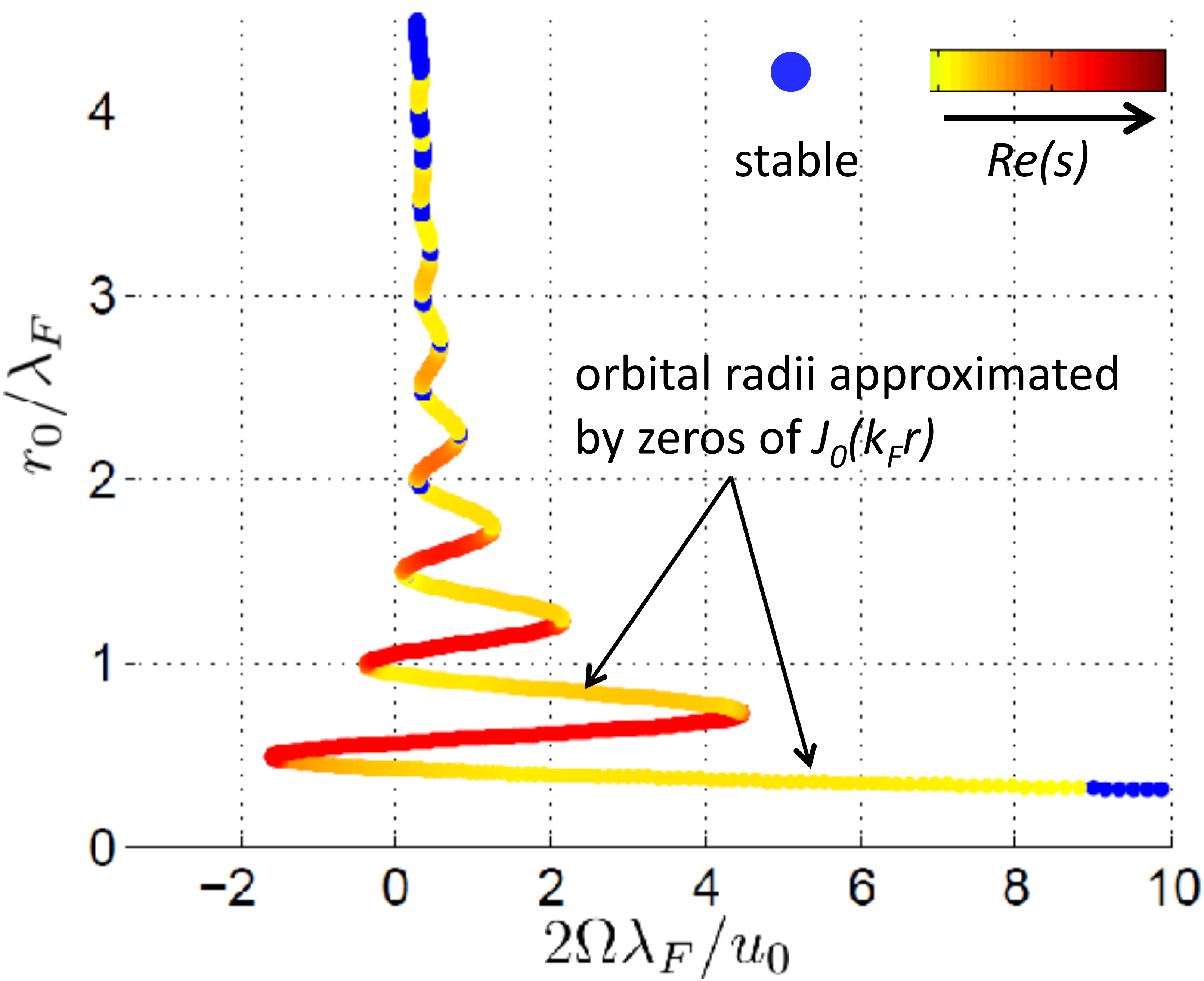

Hydrodynamic spin states at ultra-high memory?

UNSTABLE!

Balance between inertial and wave force.

Orbital radii split by applied rotation.

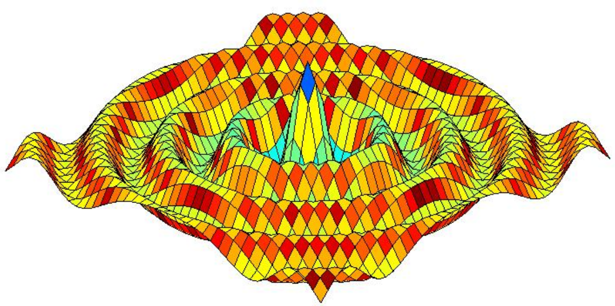

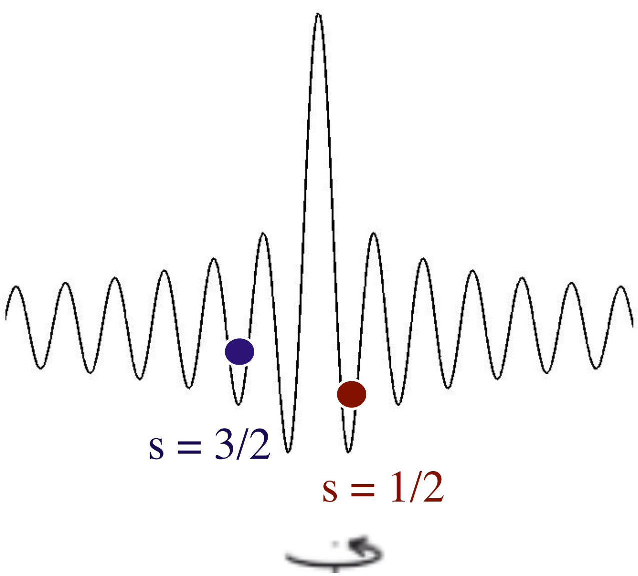

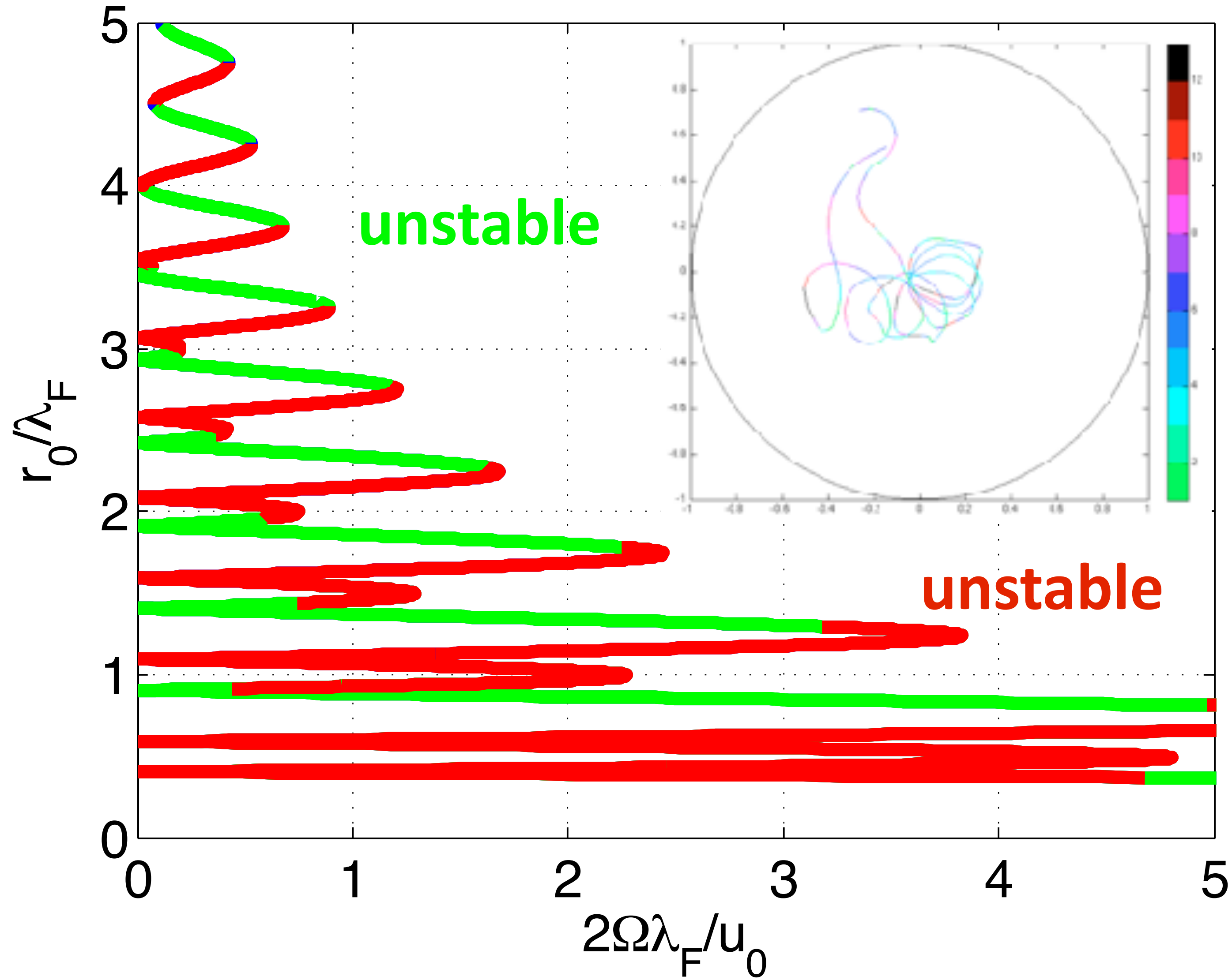

Oza, Rosales & Bush (2018)

Ultra-high memory limit ($M_e >> 1$)

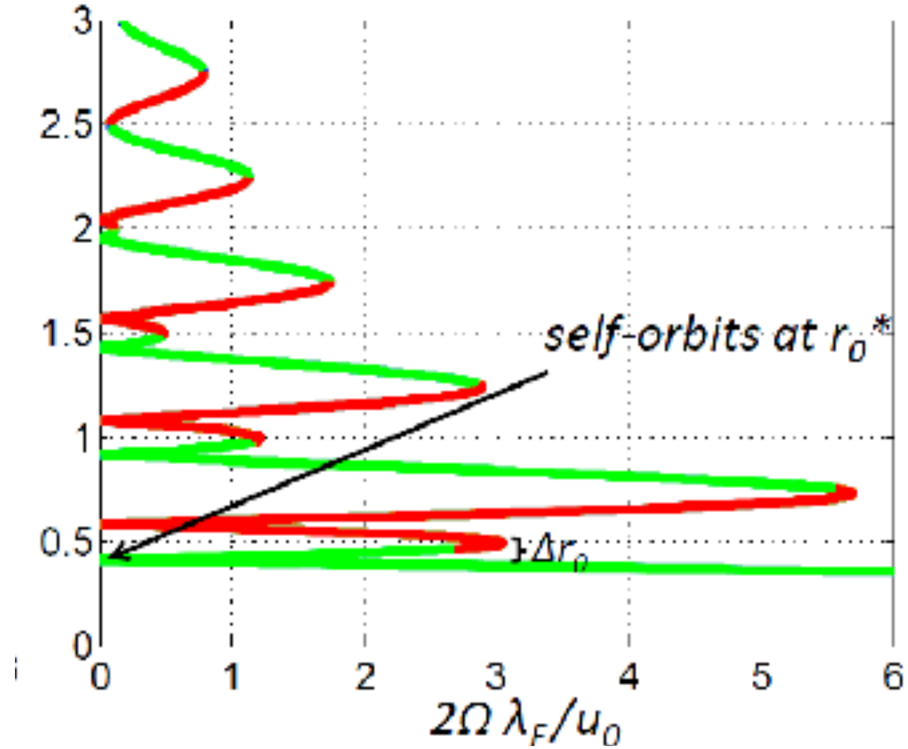

Approximate governing equations in high-memory limit:

Radial: $$-mr_0\omega^2 = FM_e J_0(k_F r_0) J_1(k_F r_0) + 2m\Omega r_0 \omega + O\left(M_e^{-1}\right)$$

Tangential: $$Dr_0\omega = \frac{F}{k_F T_F r_0 \omega}\left(1 - J_0^2(k_F r_0)\right) + O\left(M_e^{-2}\right)$$

As $M_e \to \infty$: r_0 satisfies $J_0(k_F r_0) = 0$ or $J_1(k_F r_0) = 0$

$$\frac{\Delta r_0}{\lambda_F} = \frac{2mr_0^*|\omega^*|}{FM_e\pi J_1(k_F r_0^*)^2}\Omega$$

Zeeman-like splitting

Eddi *et al.*, *PRL* (2012)

Analog Zeeman splitting of orbiting pairs

- the Zeeman effect is the splitting of spectral lines in the presence of a uniform **B**
- invoke Coriolis-Lorentz equivalence: orbital radii split by applied rotation
- for orbiting pairs, change proportional to applied rotation $\frac{\Delta r}{\lambda_F} \sim \Omega$

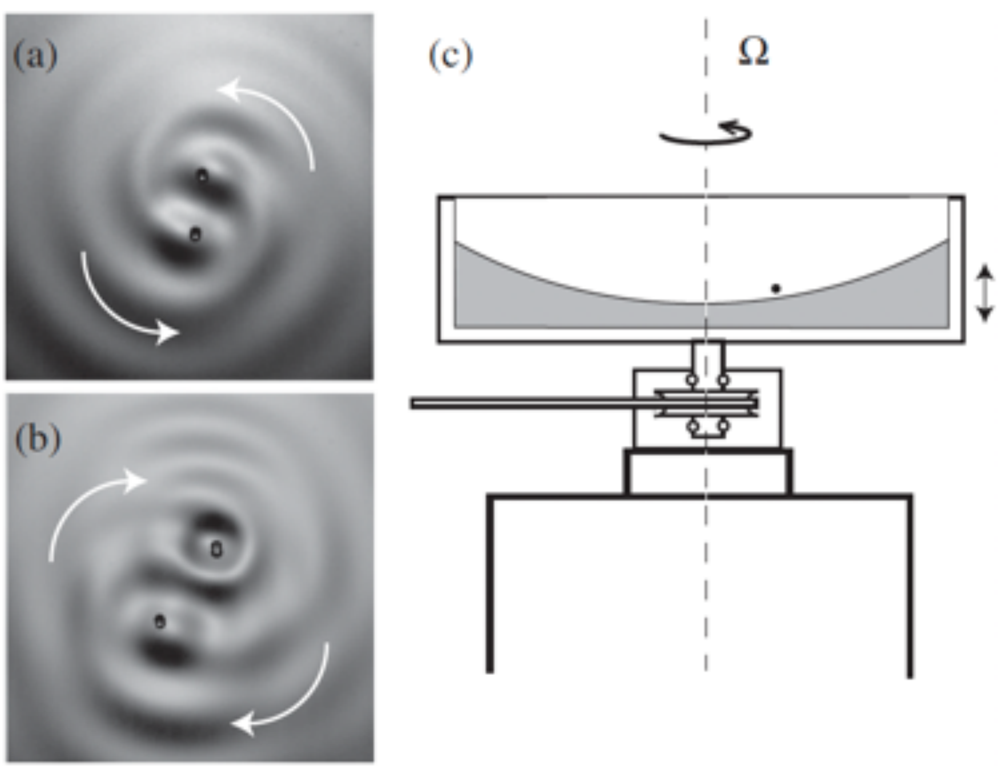

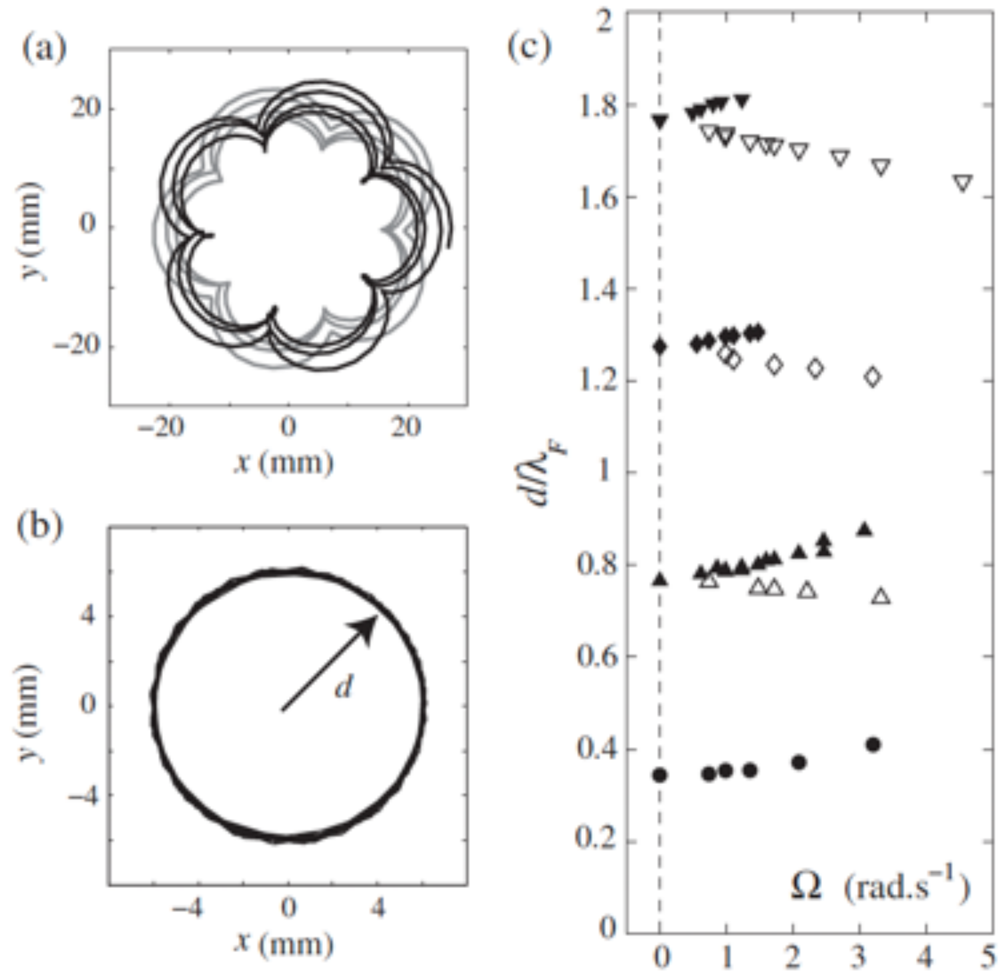

PHYSICAL REVIEW E **94**, 042224 (2016)

Self-attraction into spinning eigenstates of a mobile wave source by its emission back-reaction

Matthieu Labousse,[1,2,*] Stéphane Perrard,[2] Yves Couder,[2] and Emmanuel Fort[1,†]
[1]*Institut Langevin, ESPCI Paris, PSL Research University, CNRS, 1 rue Jussieu, 75005 Paris, France*
[2]*Matière et Systèmes Complexes, Université Paris Diderot, CNRS, Sorbonne Paris Cité, Bâtiment Condorcet, 10 rue Alice Domon et Léonie Duquet, 75013 Paris, France*
(Received 1 June 2016; published 27 October 2016)

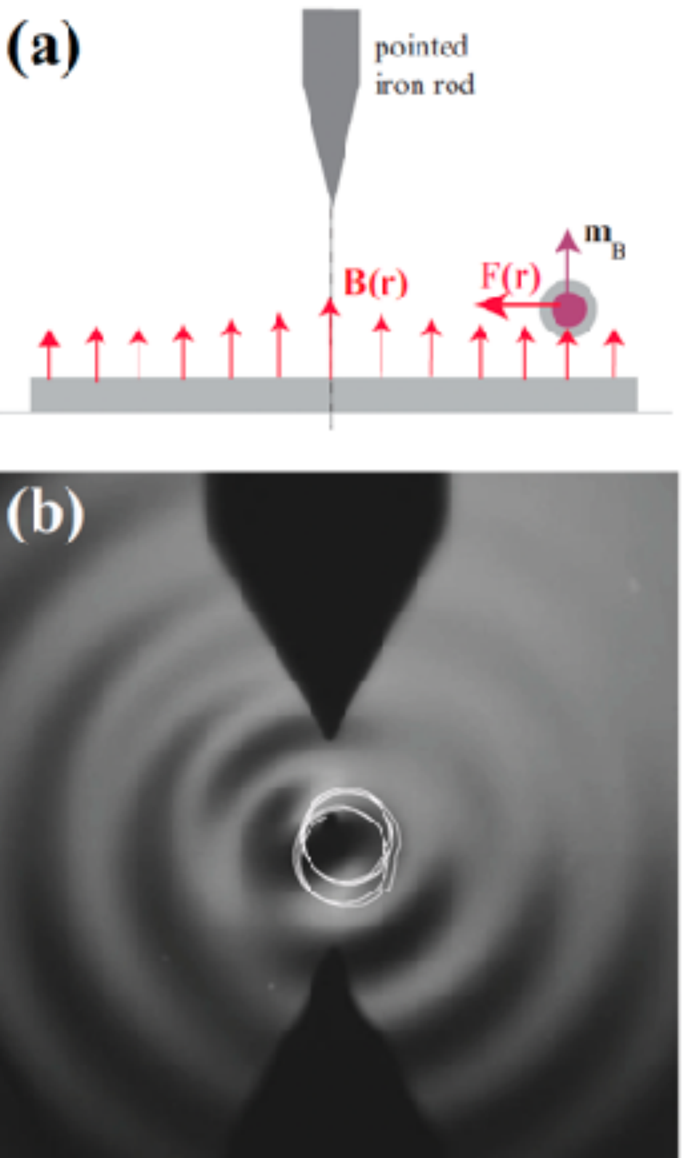

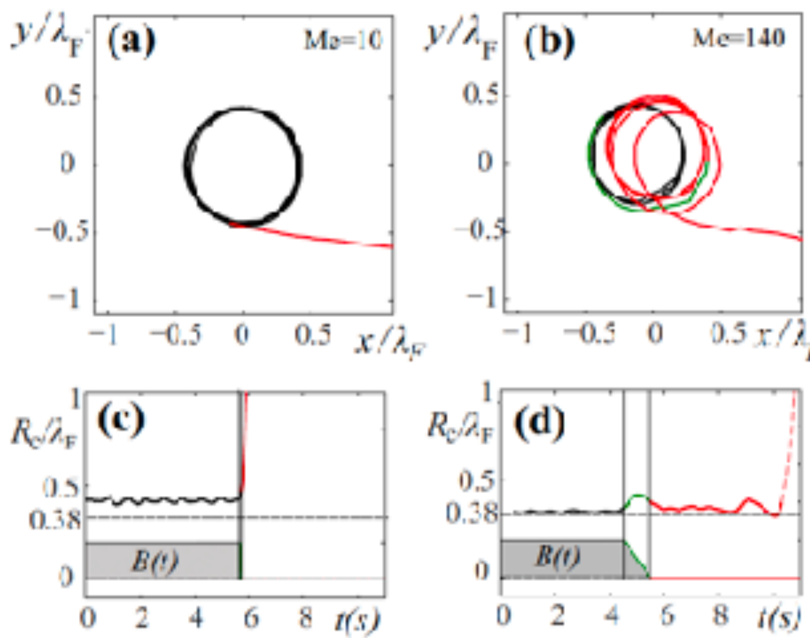

FIG. 2. Typical trajectories observed when the confinement i
turned off for two values of the memory parameters. (a) Short memor
(Me ≈ 10). (b) Long memory (Me ≈ 140) (see Movie S1 [36]). (c,d
Temporal evolution of the normalized trajectory radius R_c/λ_F alon
these two trajectories (black: magnetic field on, green: transition time
and red: no central force.

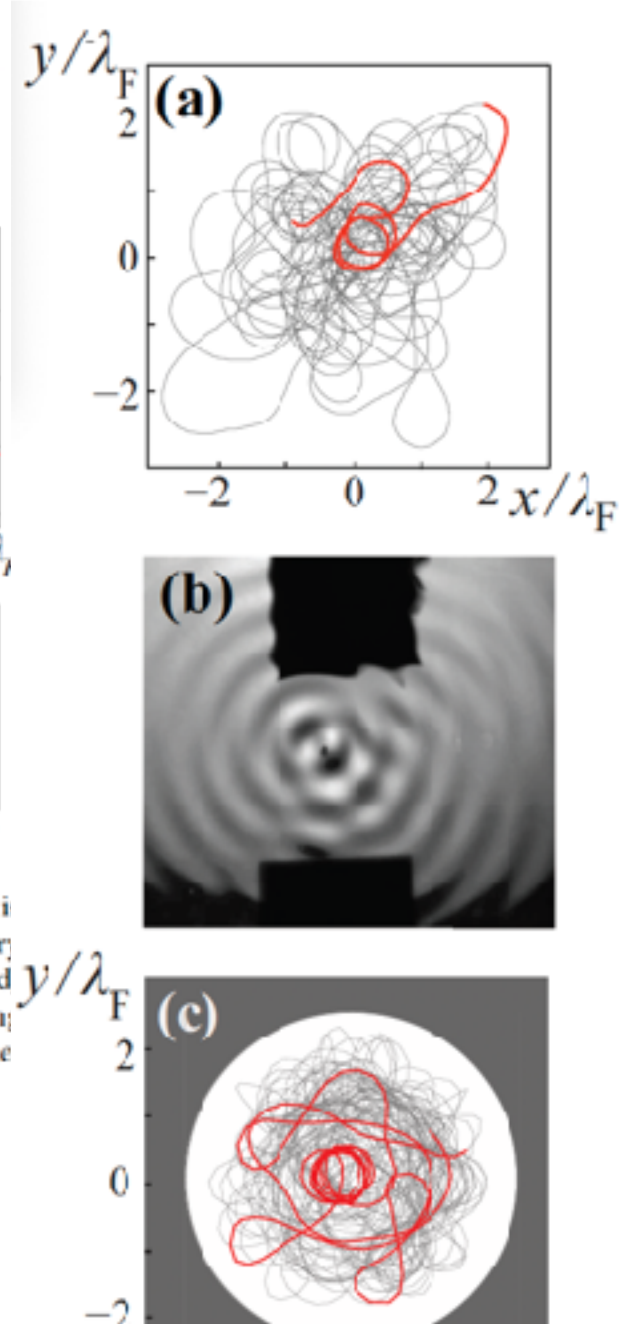

Hydrodynamic spin states

Bernard-Bernardet *et al*. (2023)

- weak topographical confinement enables spin states

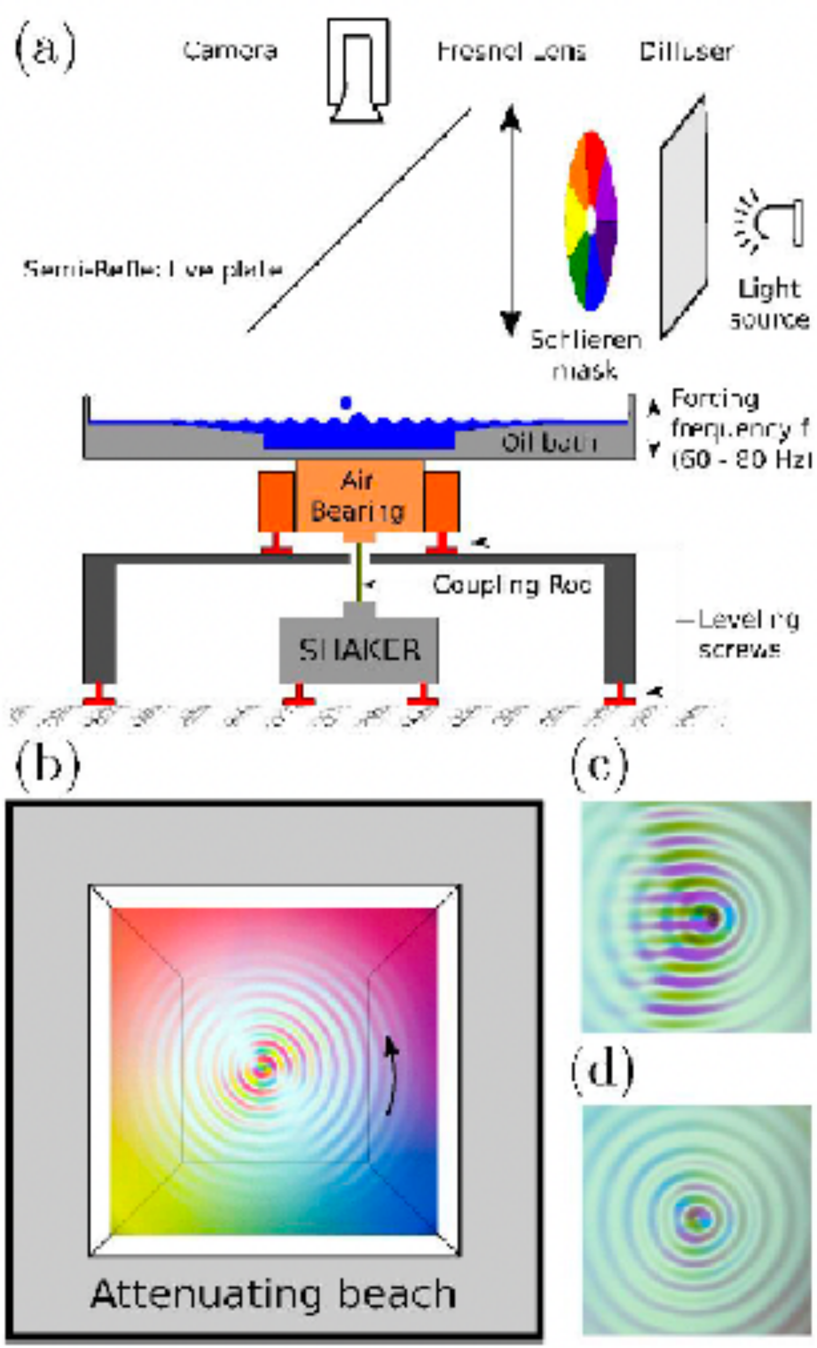

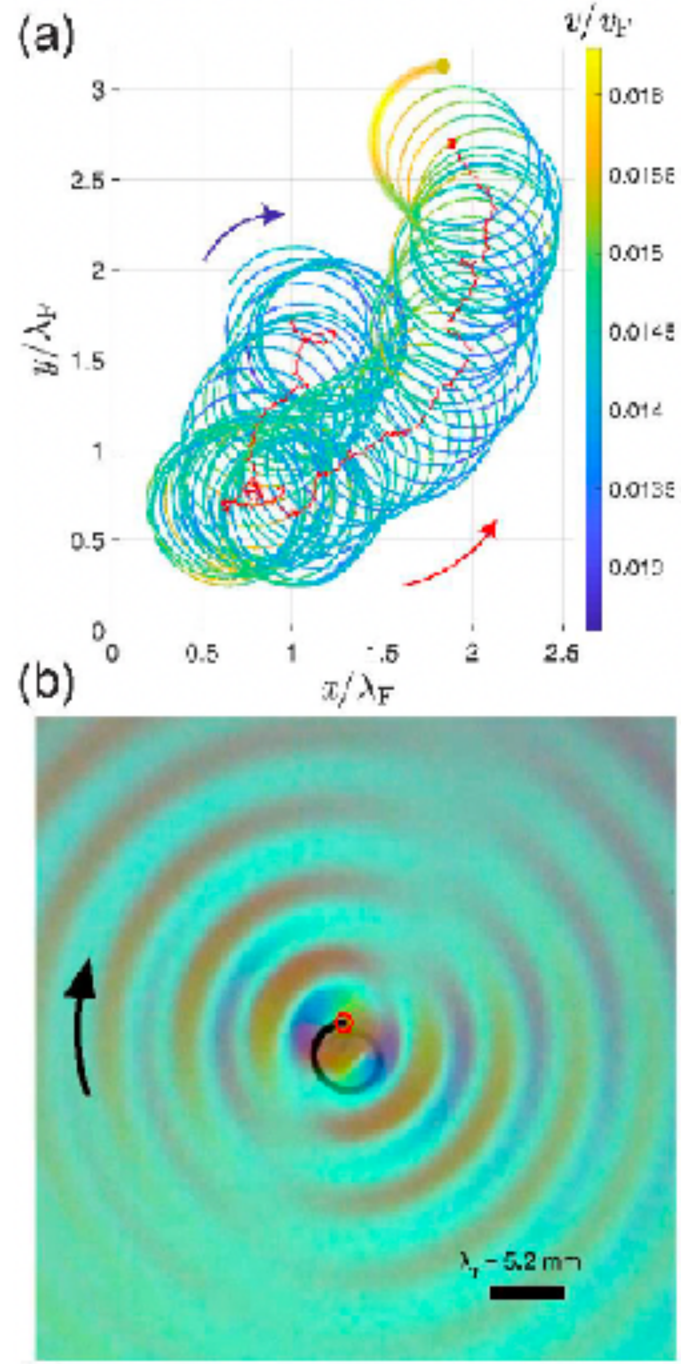

Rotational trapping at very high Ω

Oza *et al*. (2014)

- rotation transforms walkers to bouncers, since orbital radius approaches zero
- trapped states have infinitesimal radius, but finite orbital frequency
- deduced trapping criterion by considering high Ω , small radius limit
- not readily achievable in the lab

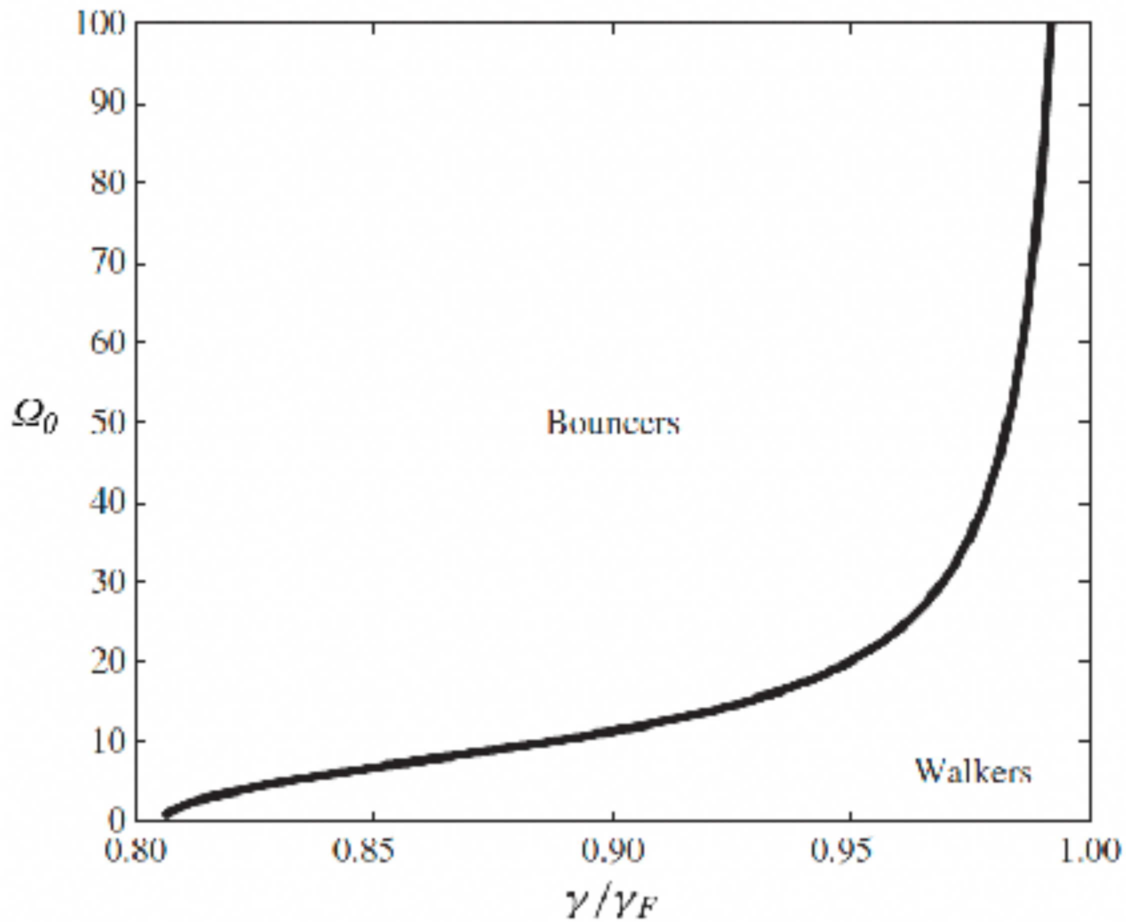

Quantization of inertial orbits in a rotating frame

Fort et al. (2010)
Harris et al. (2014)
Oza et al. (2014)

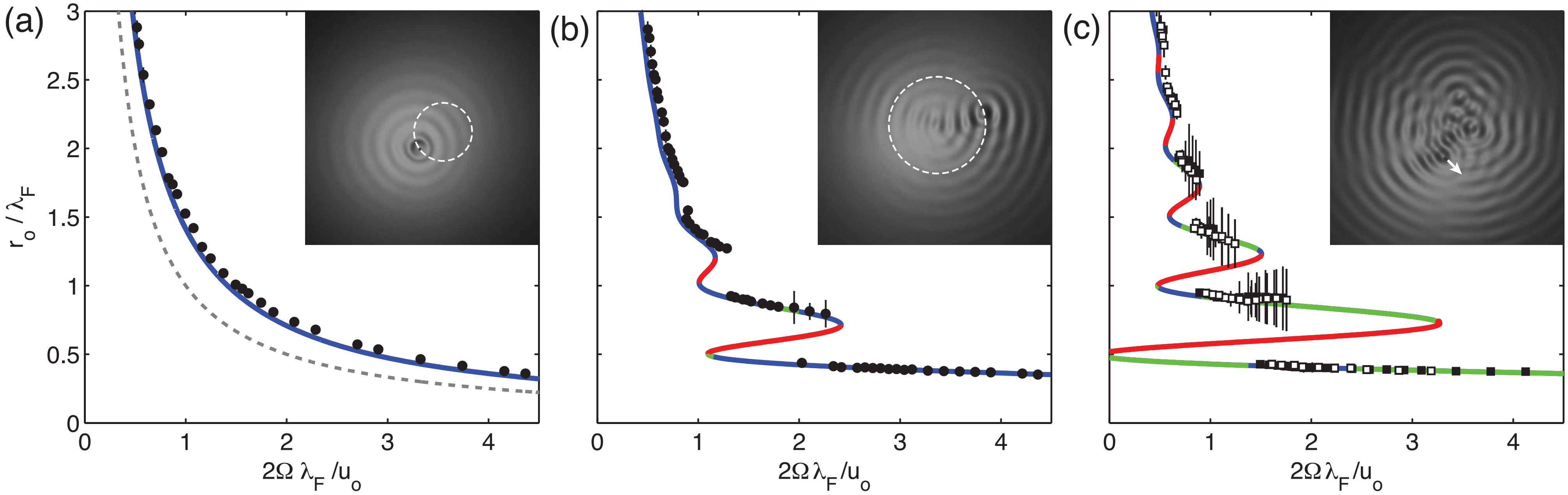

- orbital quantization emerges owing to the walker's interaction with its own wake
- results from the dynamic constraint imposed by its monochromatic self-potential
- orbital quantization is a generic feature of pilot-wave dynamics subject to constraints

The tongue diagrams: stability plots

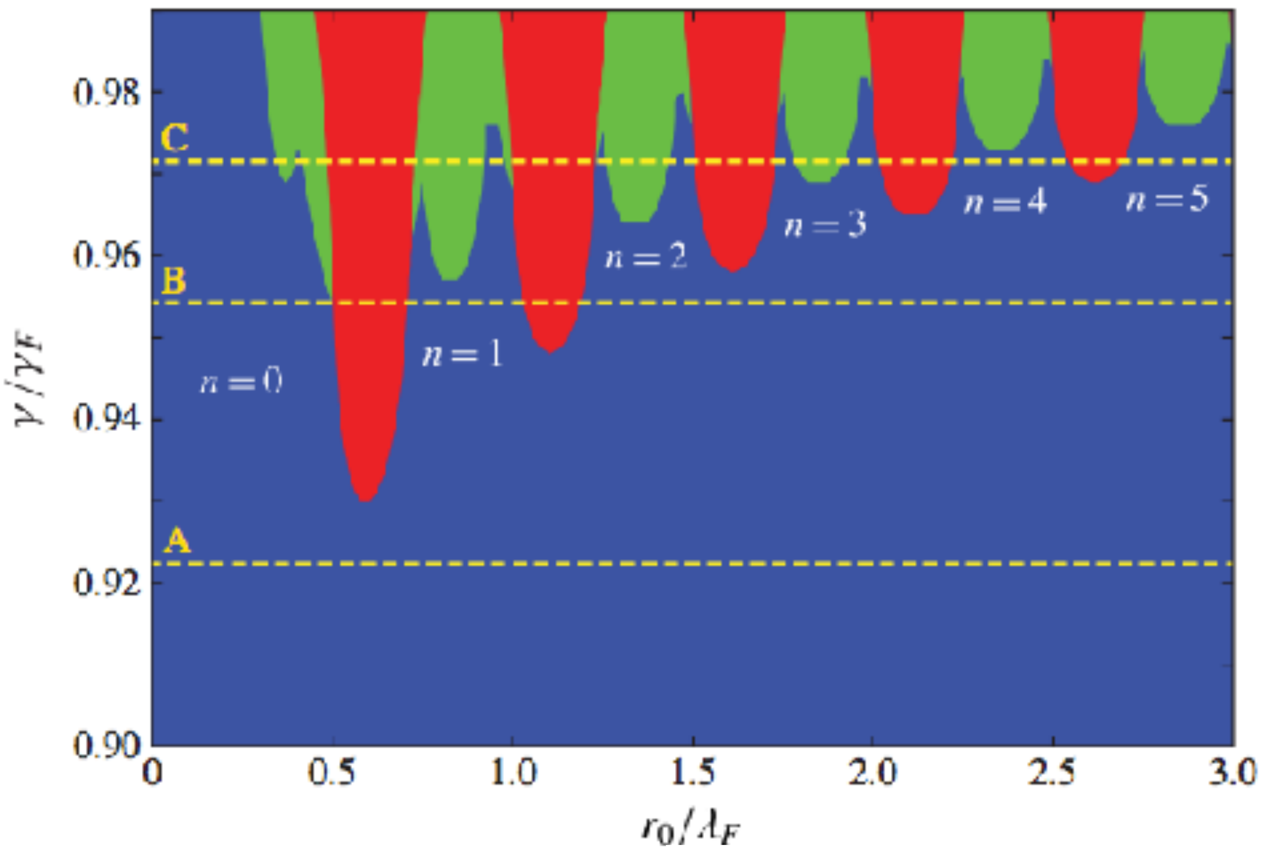

- Blue: Stable orbit
- Red: Unstable orbit (largest eigenvalue real)
- Green: Unstable orbit (largest eigenvalue complex)

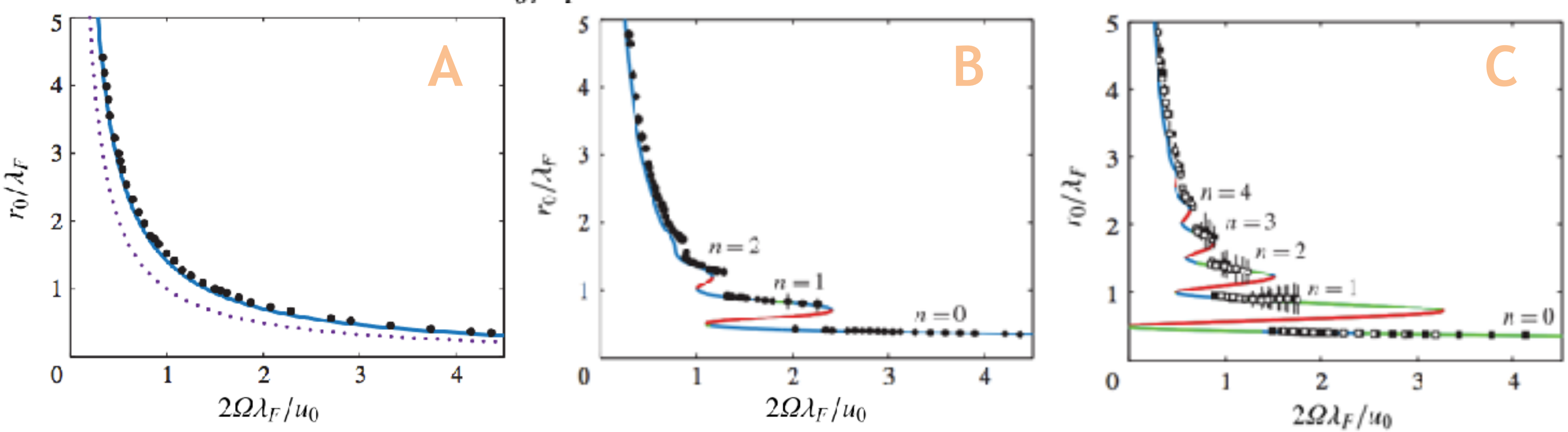

The tongue diagrams: form rationalized by Nicholas Liu

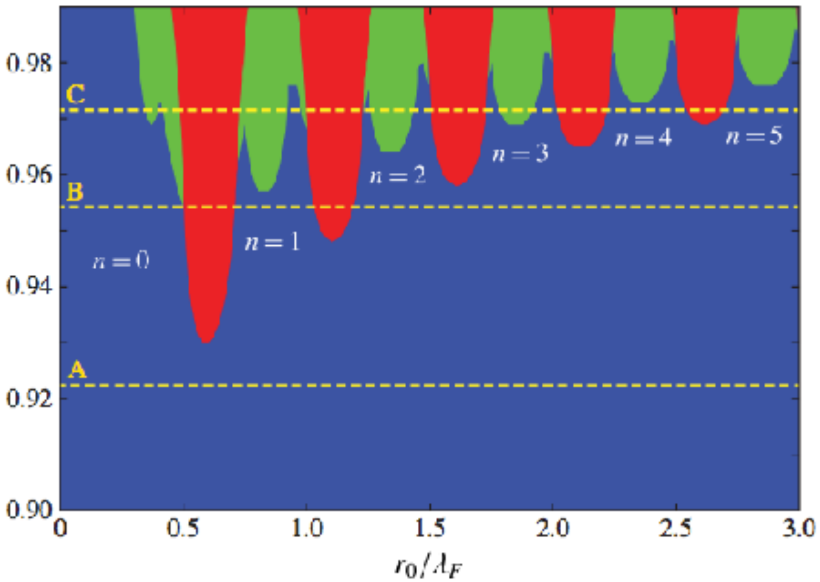

- Blue: Stable orbit
- Red: Unstable orbit (largest eigenvalue real)
- Green: Unstable orbit (largest eigenvalue complex)

Half-orbit wave damping factor

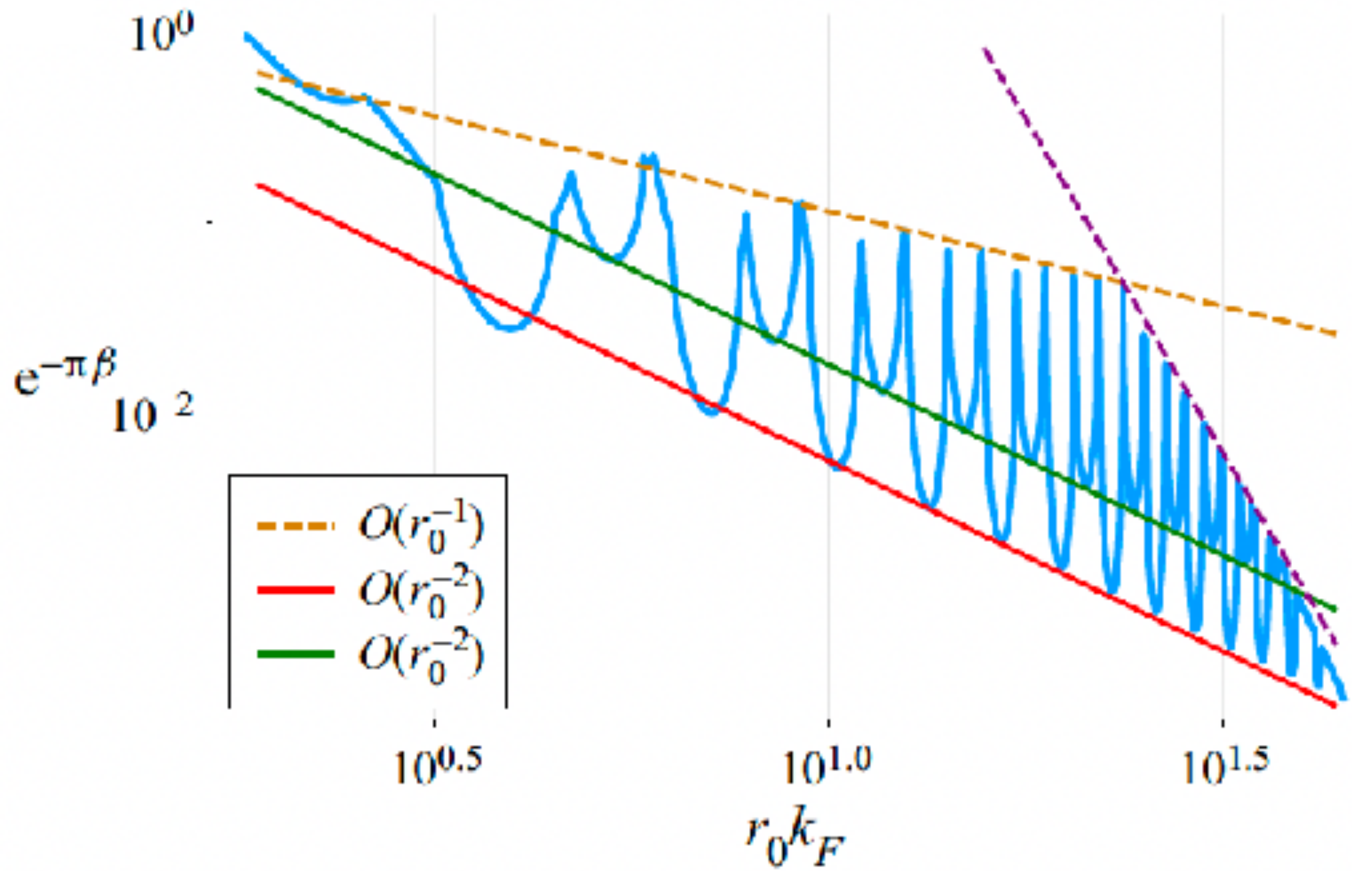

Non-linear behavior - Simulations

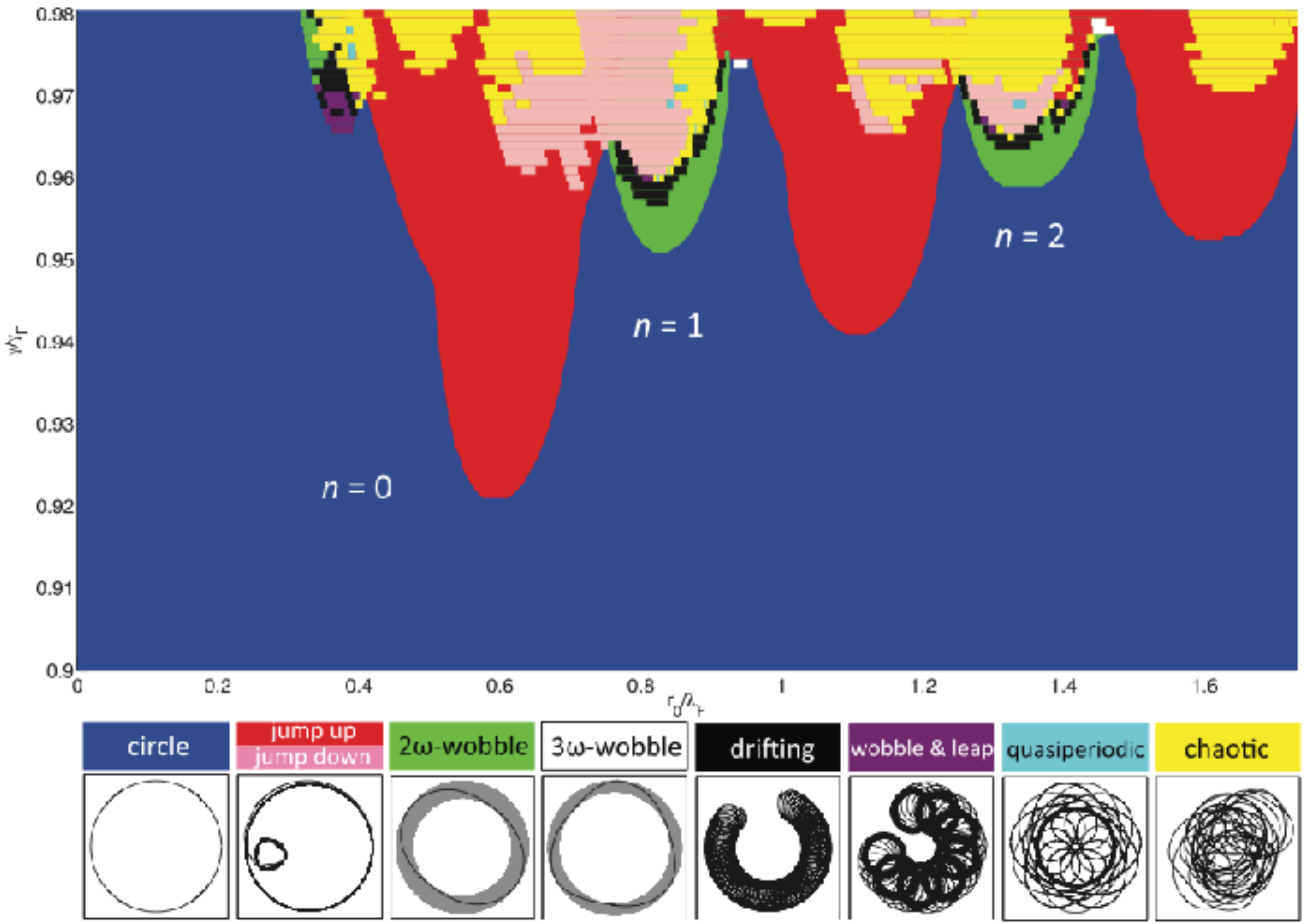

Oza, Wind-Willassen, Harris, Rosales & Bush, *PHF* (2014)

Weakly non-linear behavior - Simulations

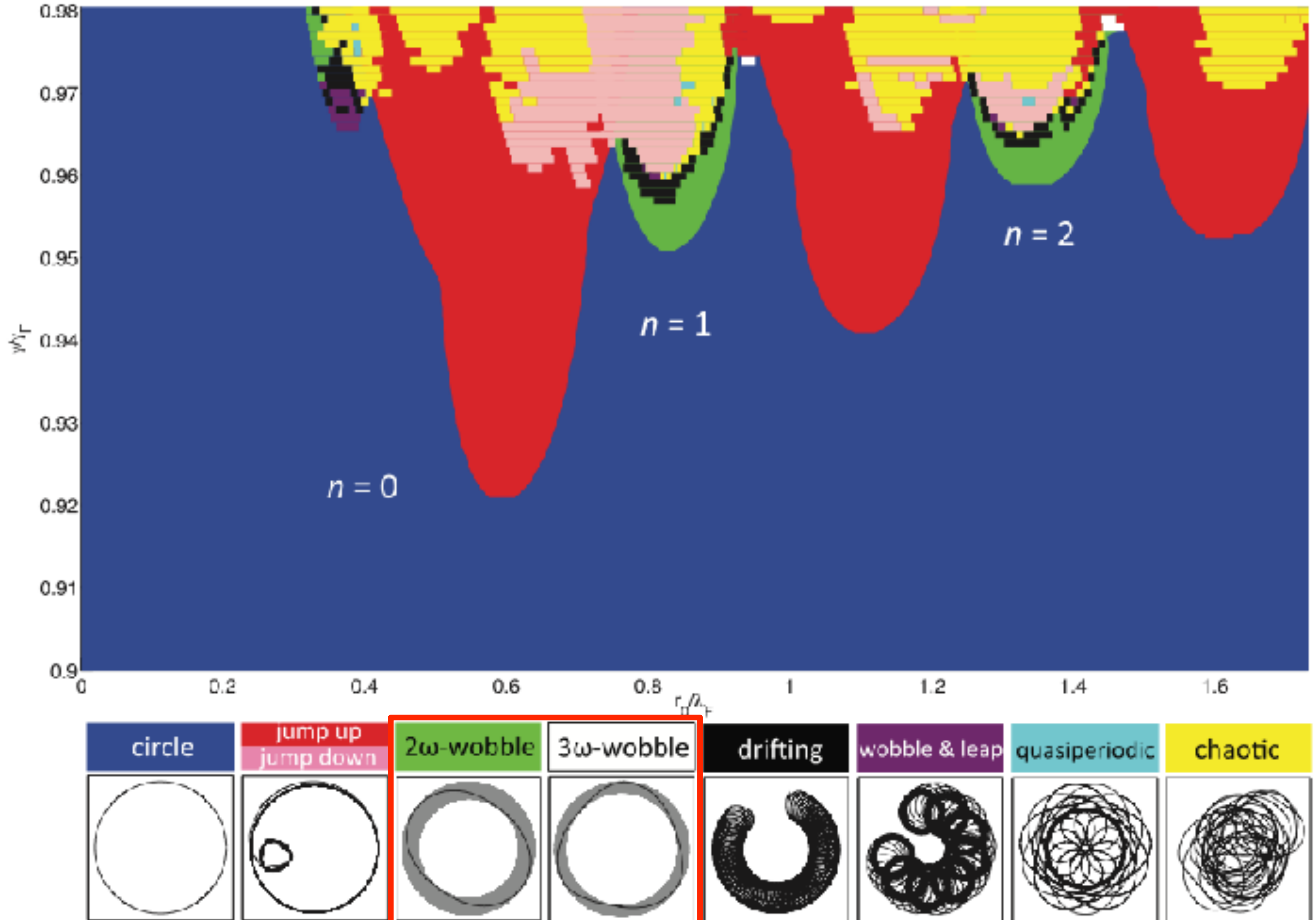

Oza, Wind-Willassen, Harris, Rosales & Bush, *PHF* (2014)

Wobbling orbits

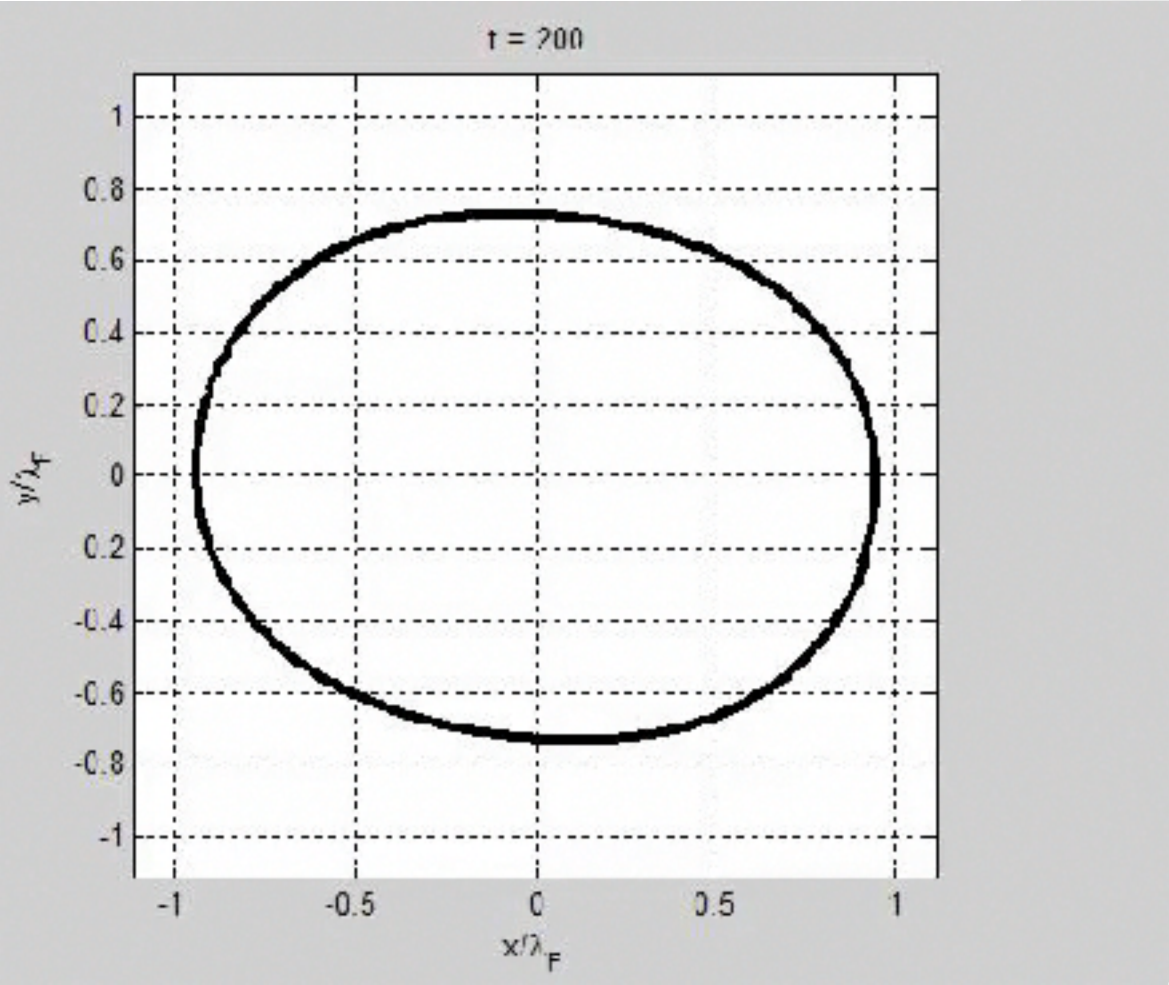

wobbling frequency ≈ 2ω

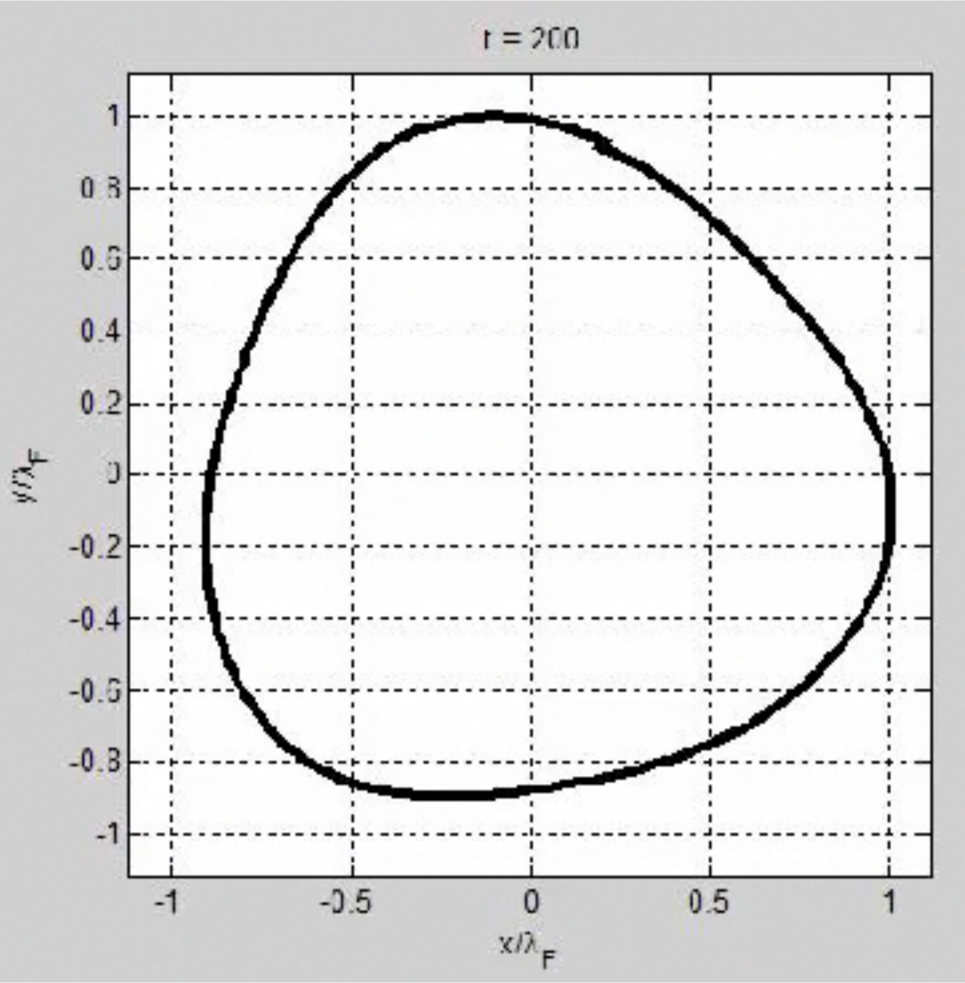

wobbling frequency ≈ 3ω

Wobbling orbits

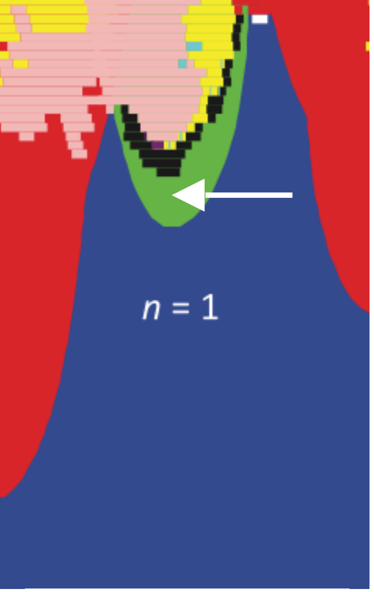

2ω-wobble

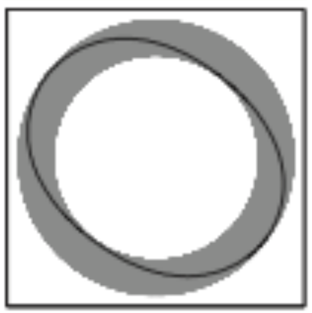

Simulation

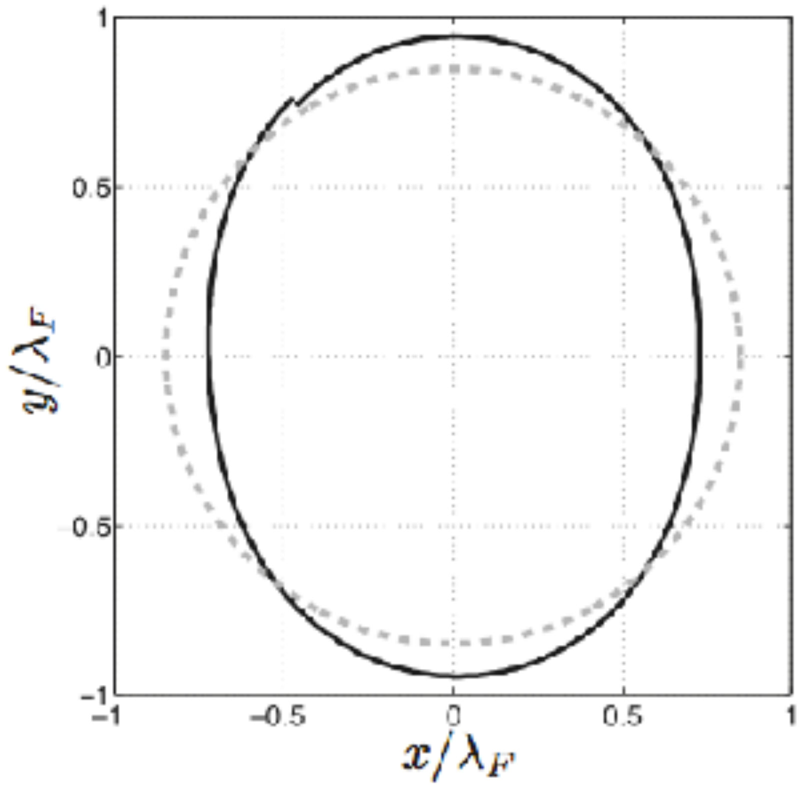

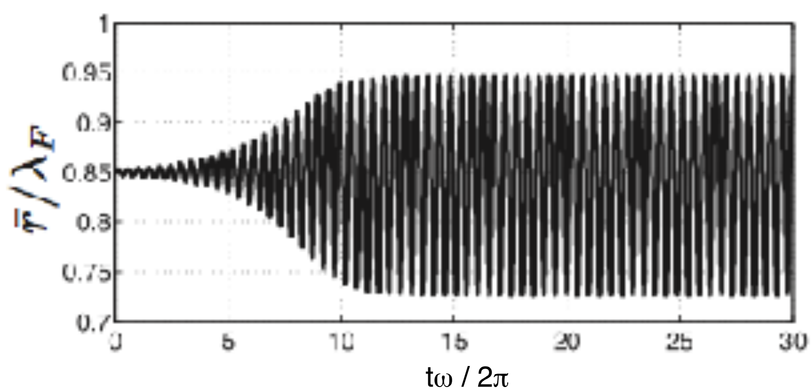

Experiment

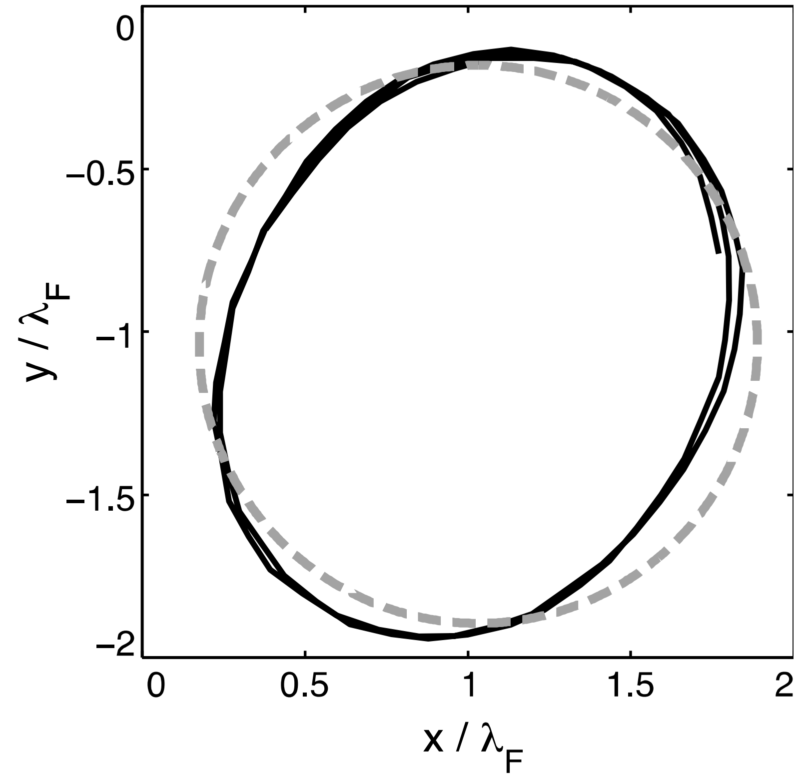

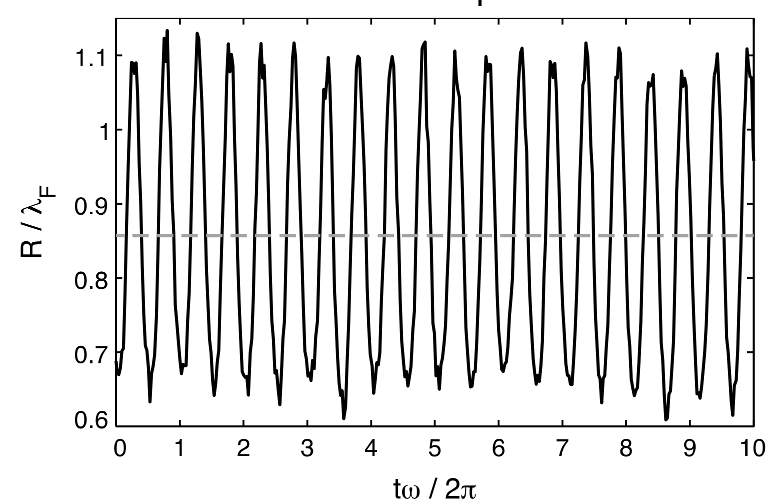

Wobbling orbits

Numerical simulation

Experiments

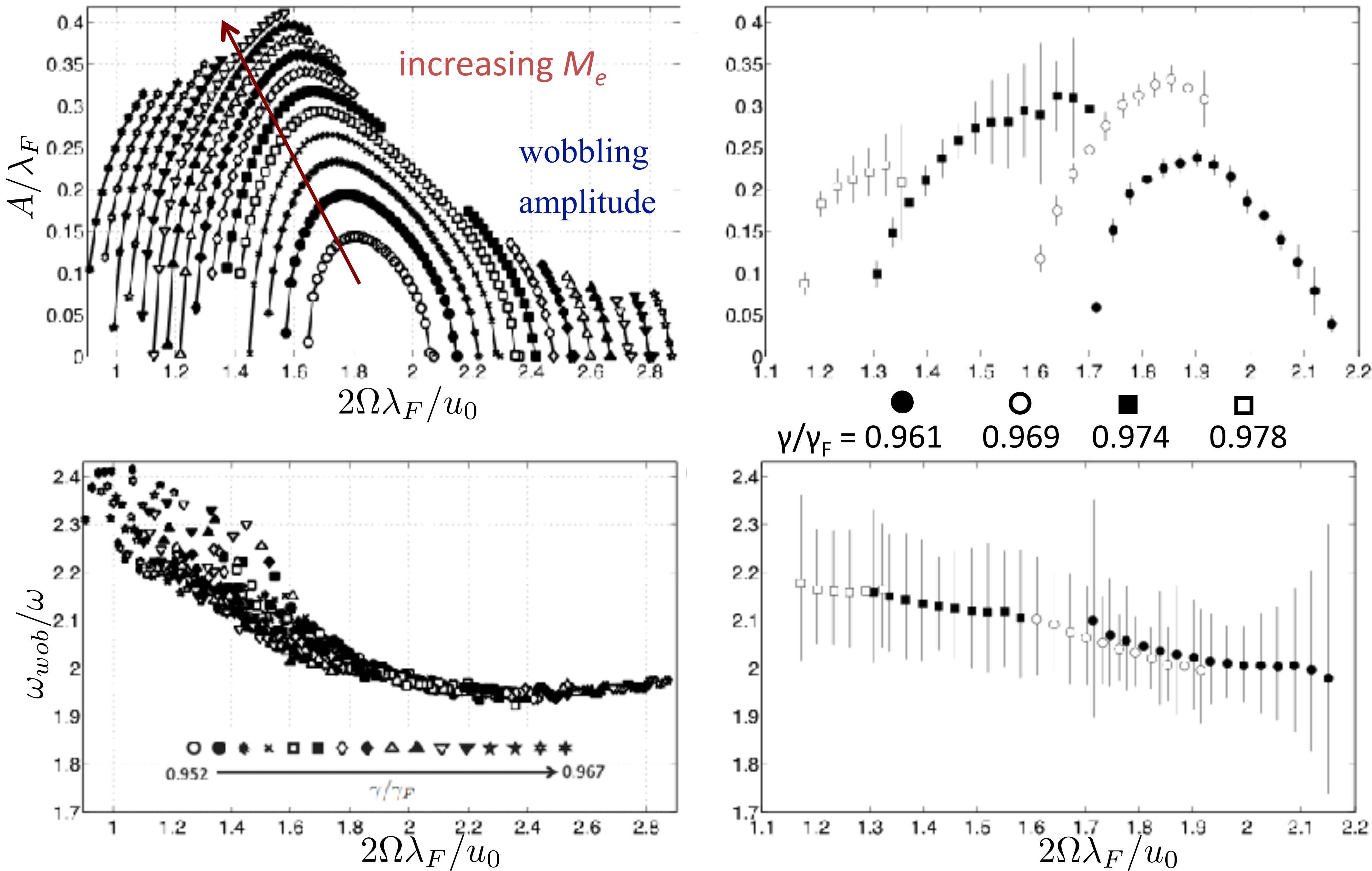

Wobbling frequency: experiments vs theory

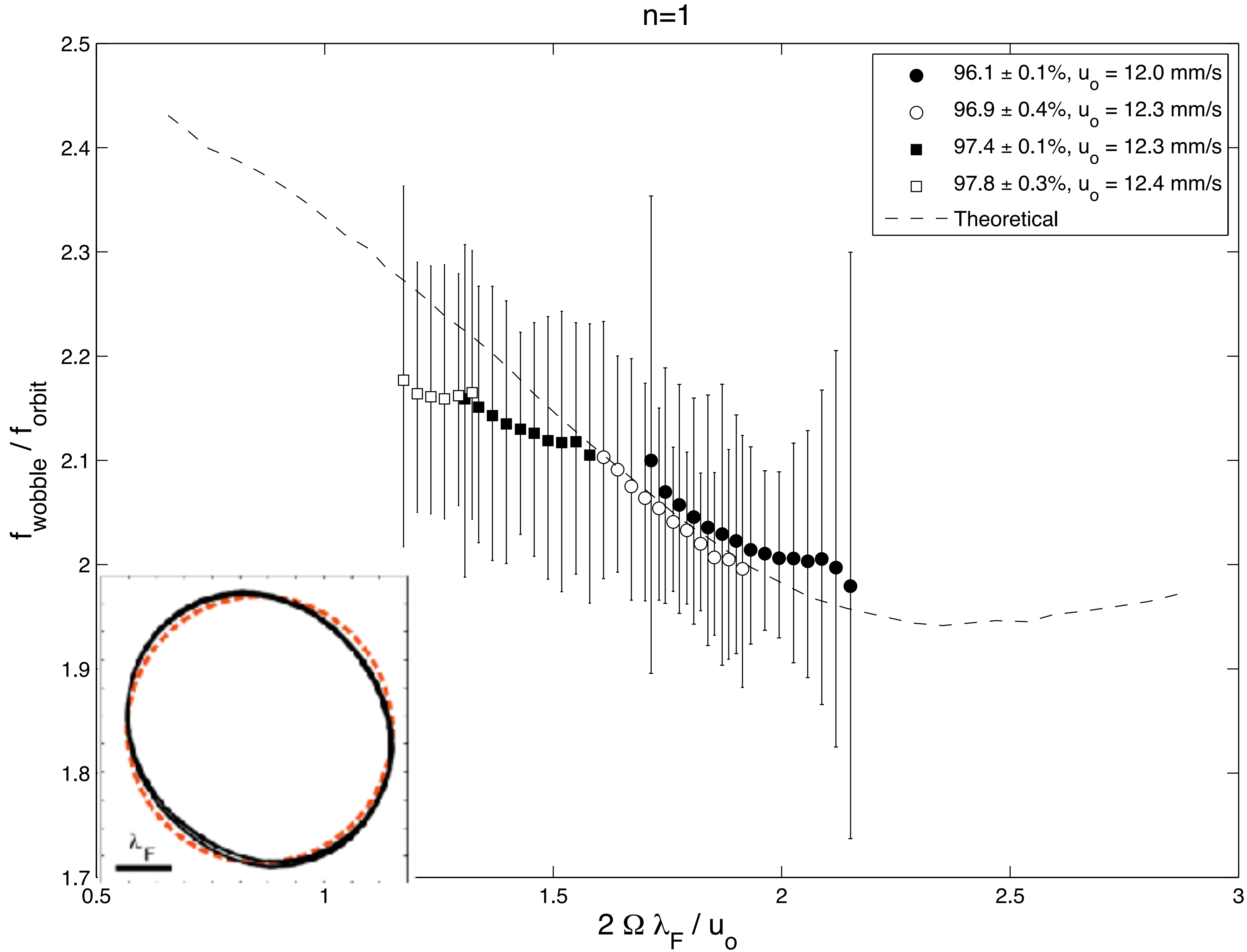

Liu *et al*., *JFM* (2023)

Non-linear behavior - Simulations

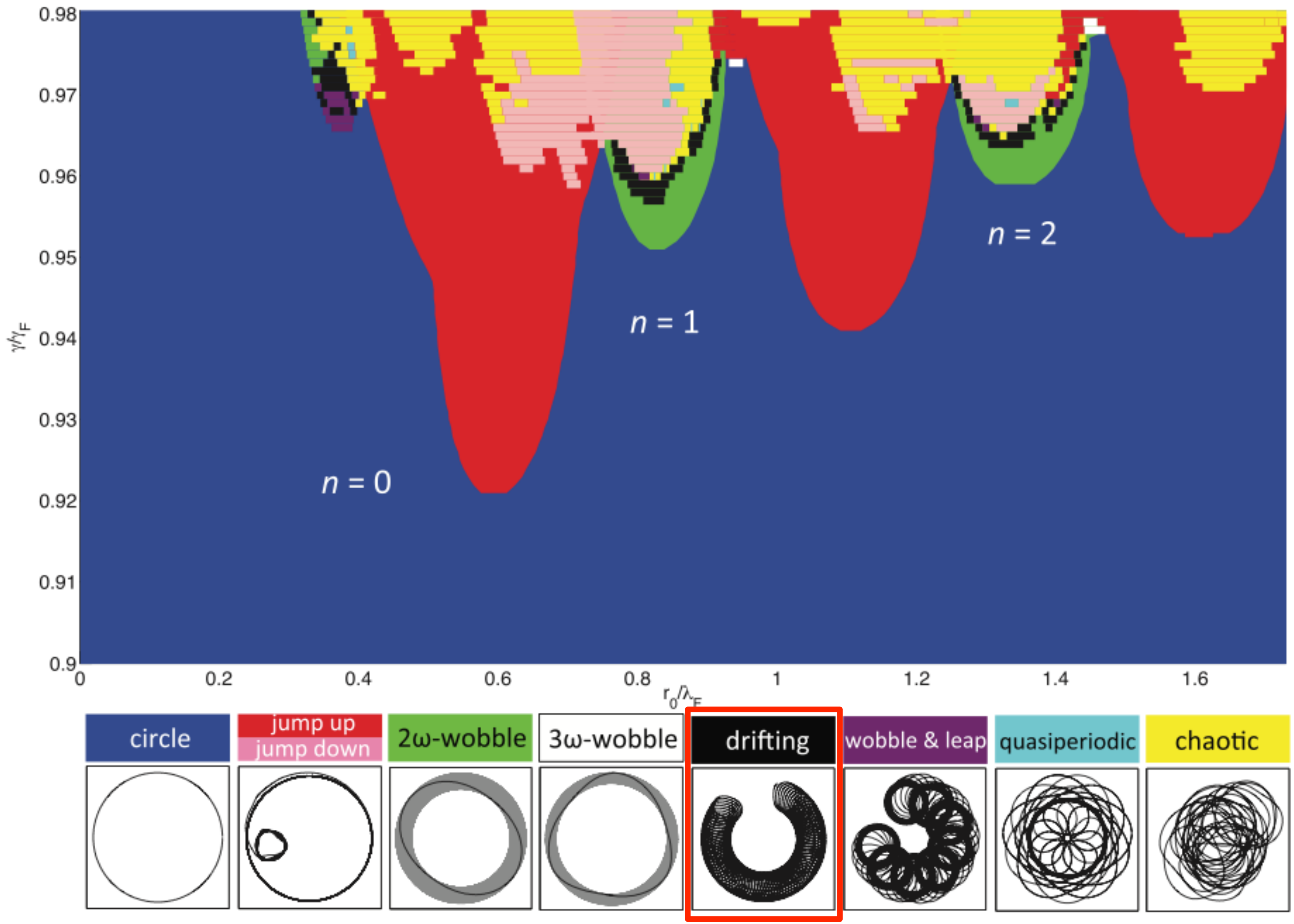

Oza, Wind-Willassen, Harris, Rosales & Bush, *PHF* (2014)

Wobble and drift

- windows of periodicity in a predominantly chaotic regime

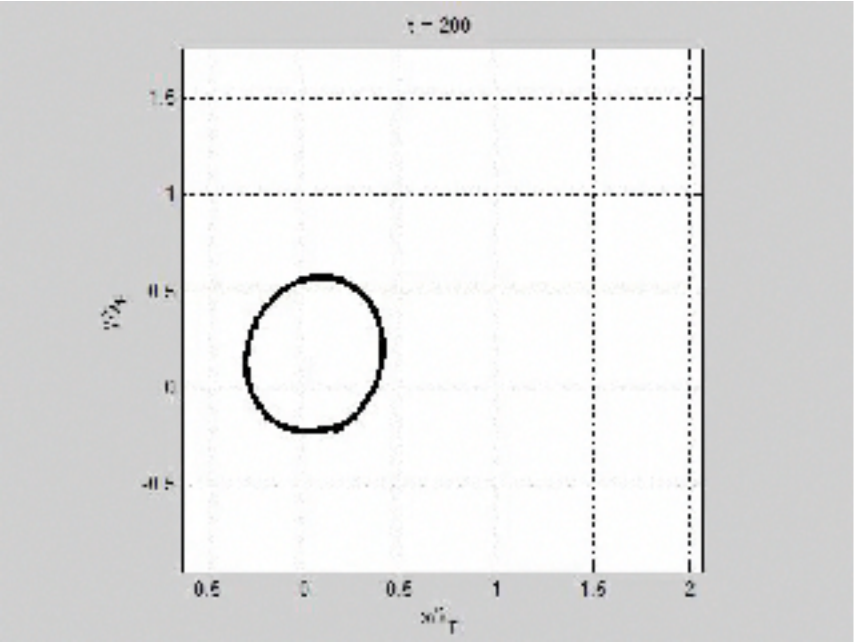

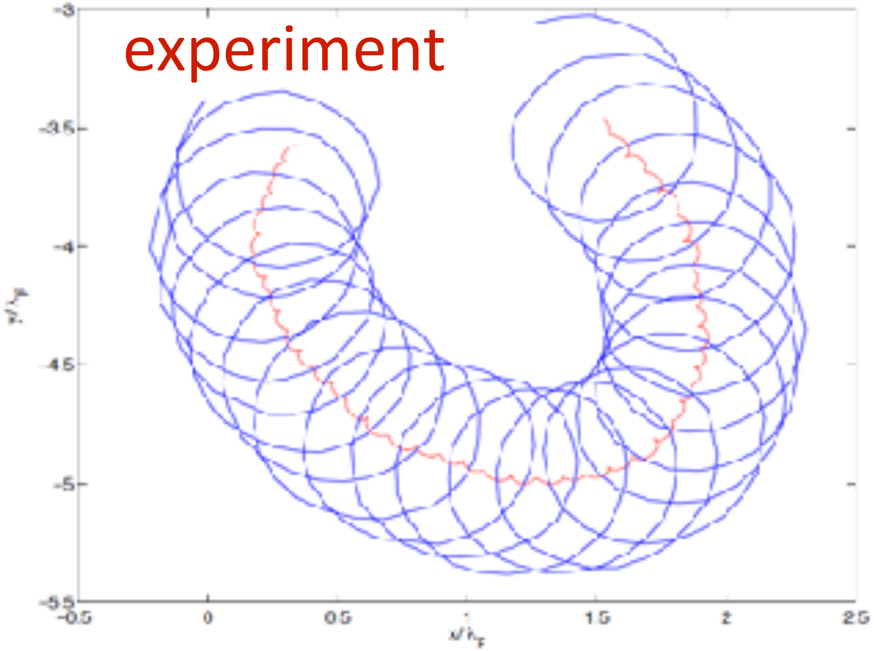

- note spontaneous multiple scale dynamics: drop vibration, spin, drift

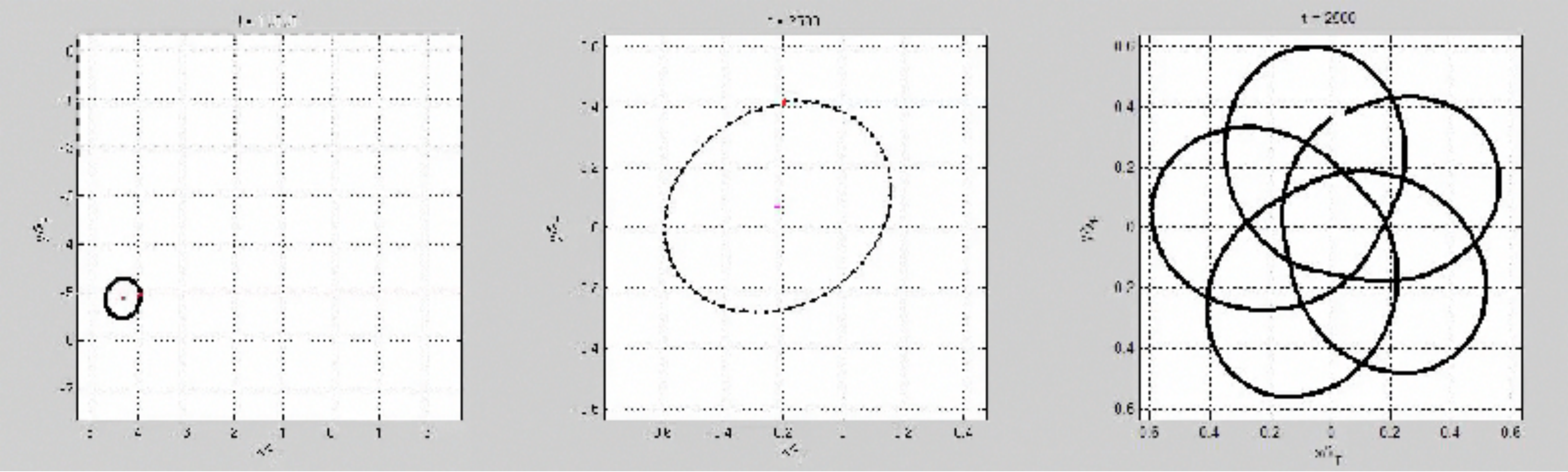

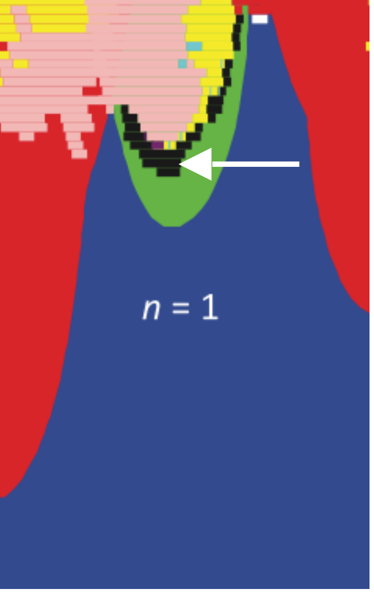

Wobbling and drifting orbits

Multiscale orbits

Simulation

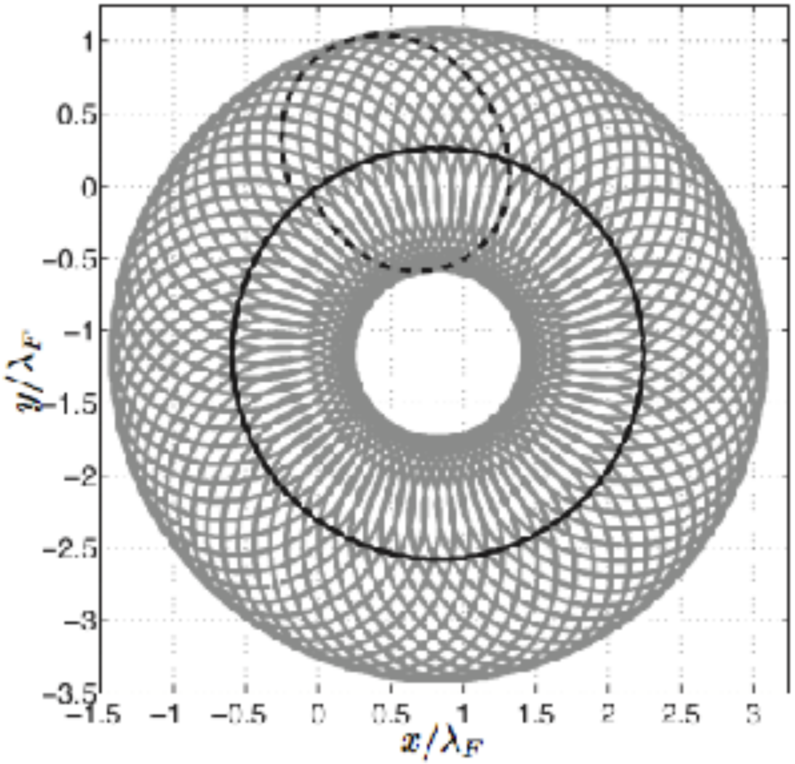

Experiment

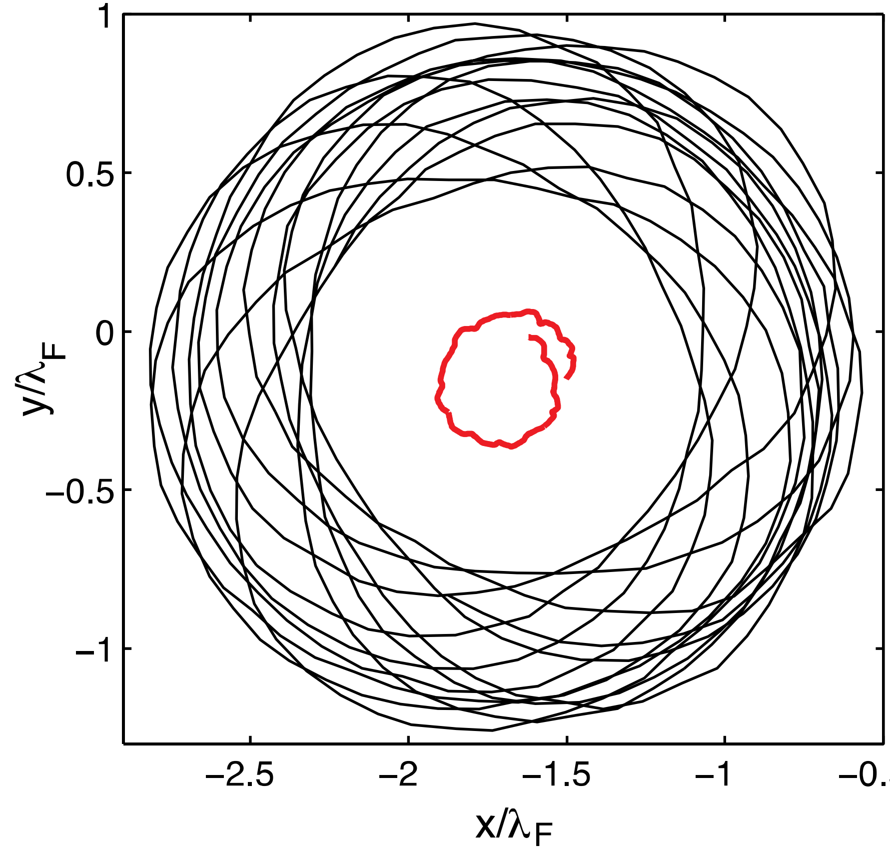

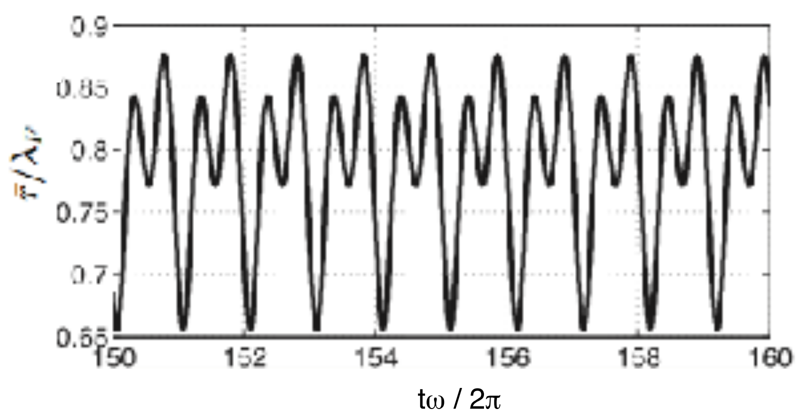

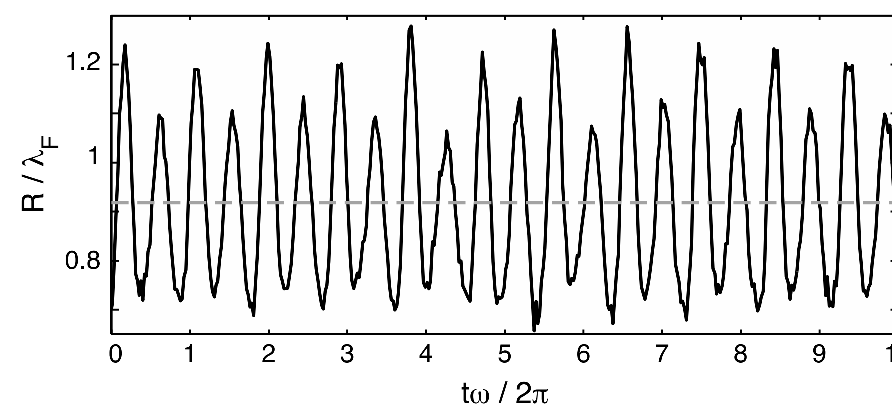

Wobbling orbits ($n = 1$)

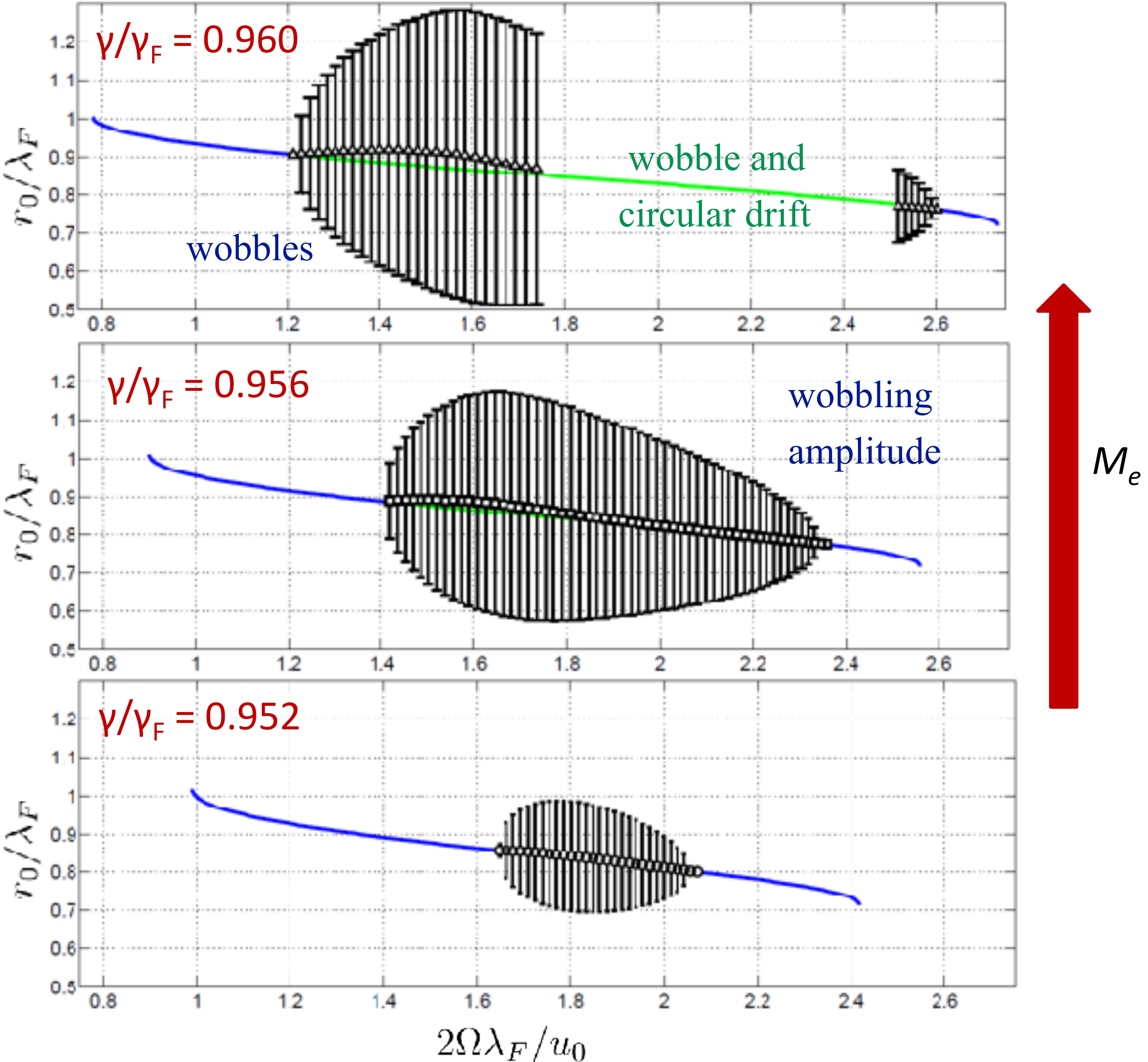

Drift amplitude and frequency

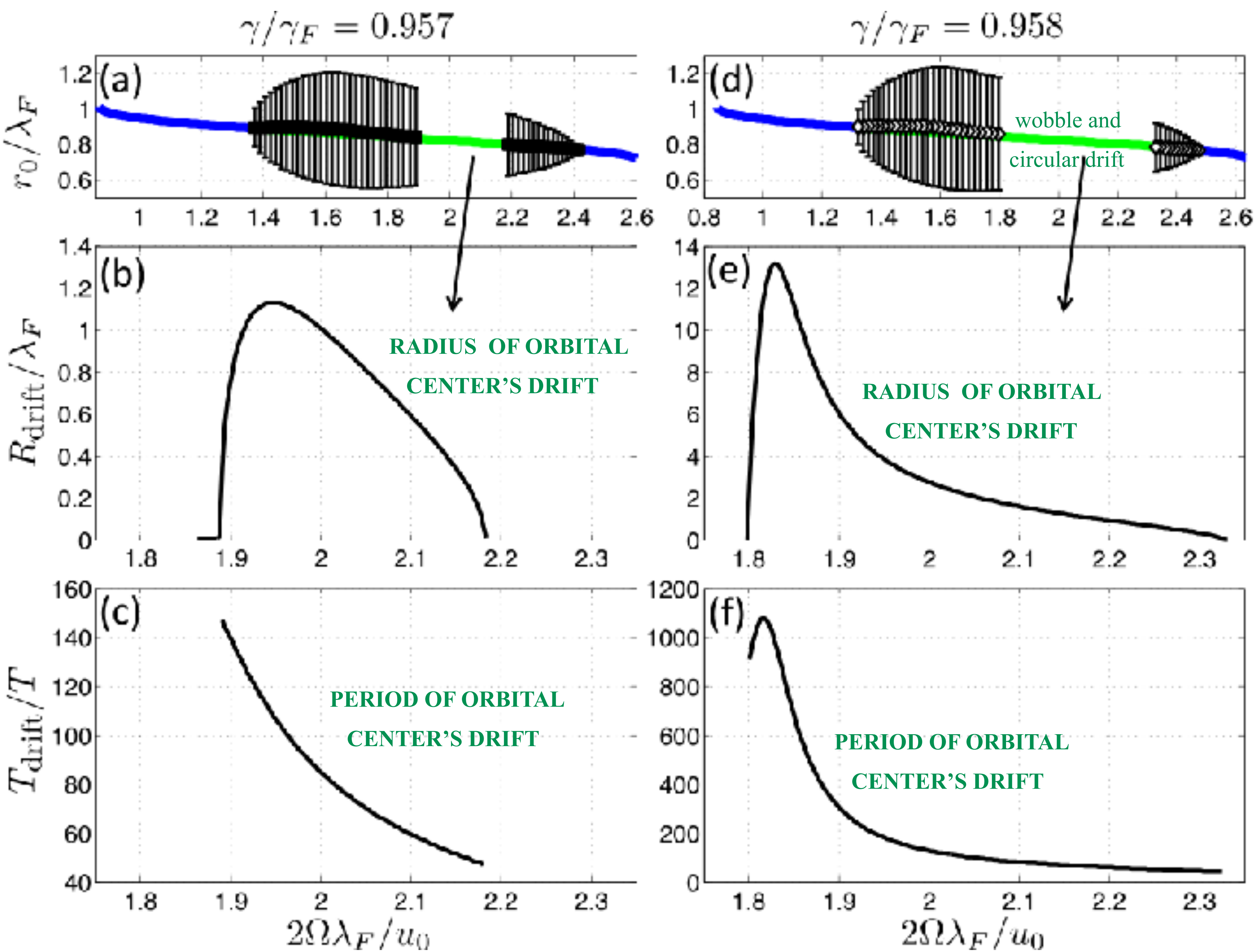

Wobble and leap

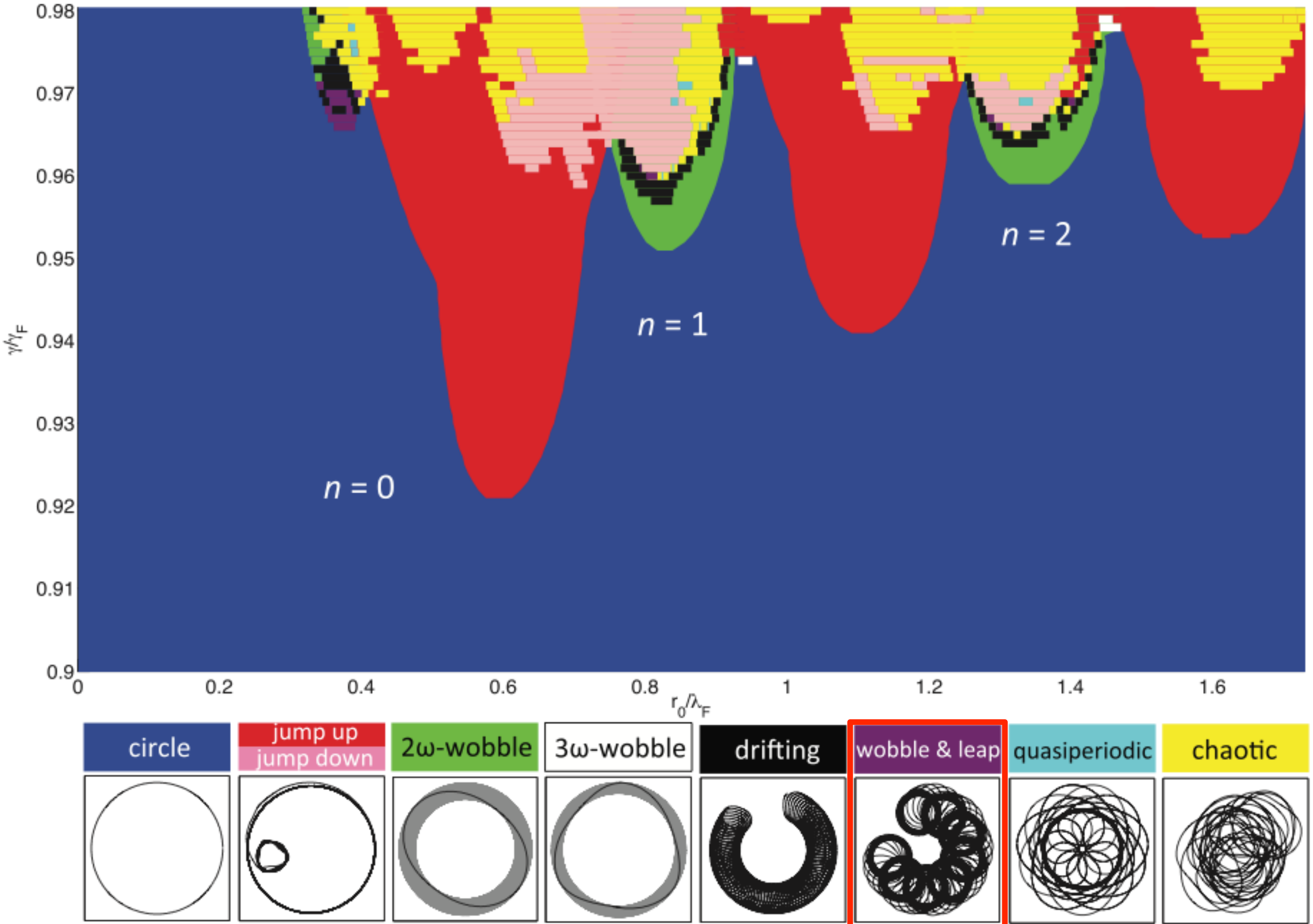

Oza, Wind-Willassen, Harris, Rosales & Bush, *PHF* (2014)

Wobble & leap dynamics

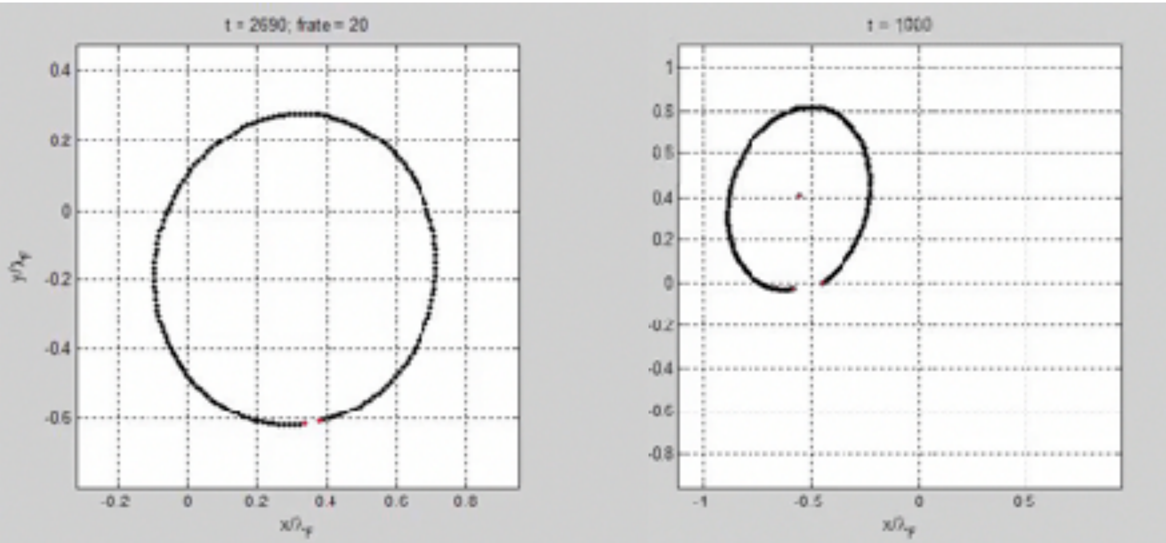

Experiment

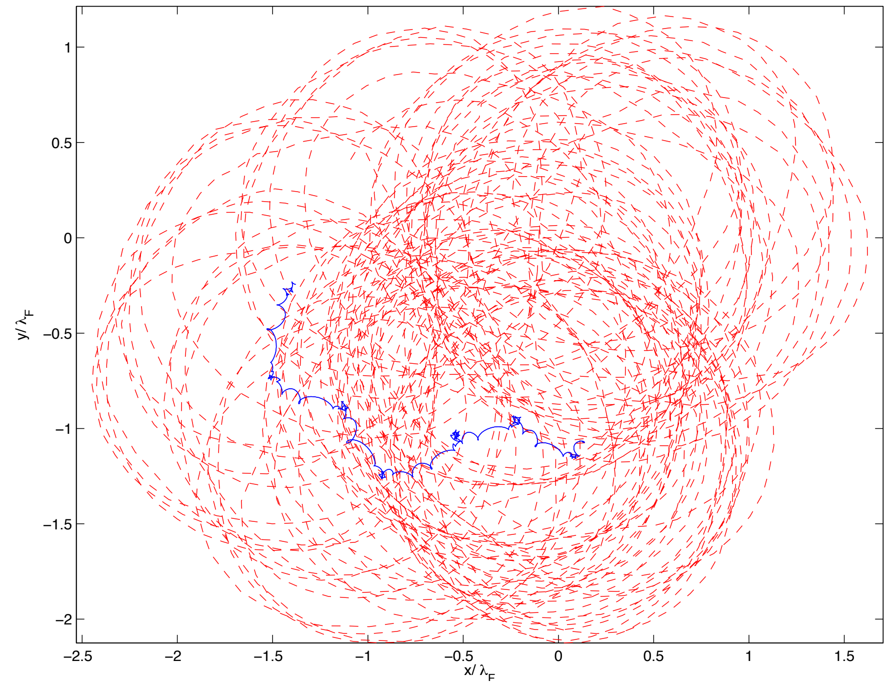

Simulations

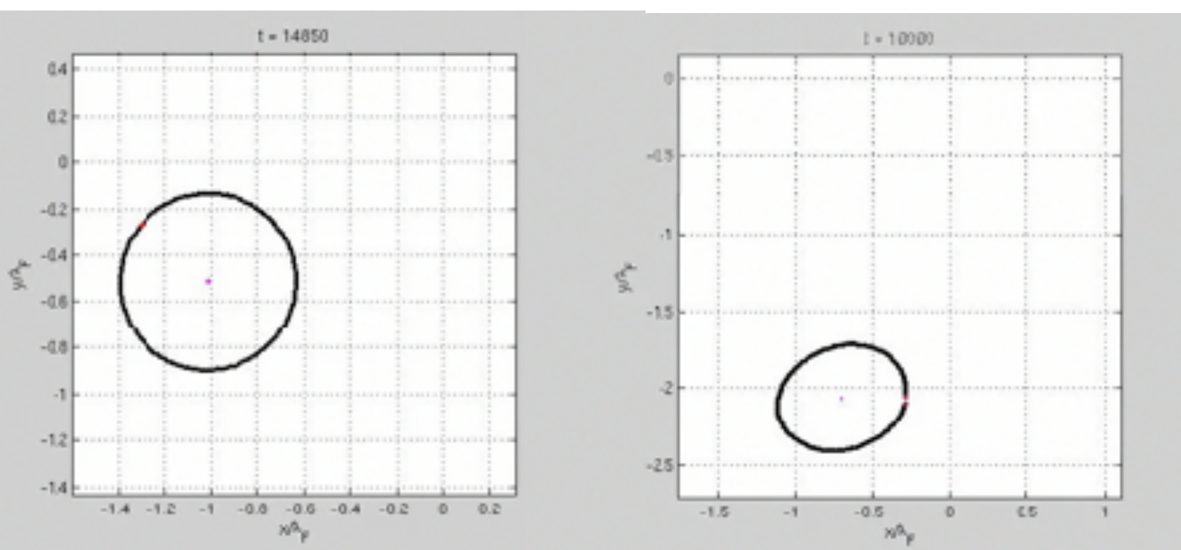

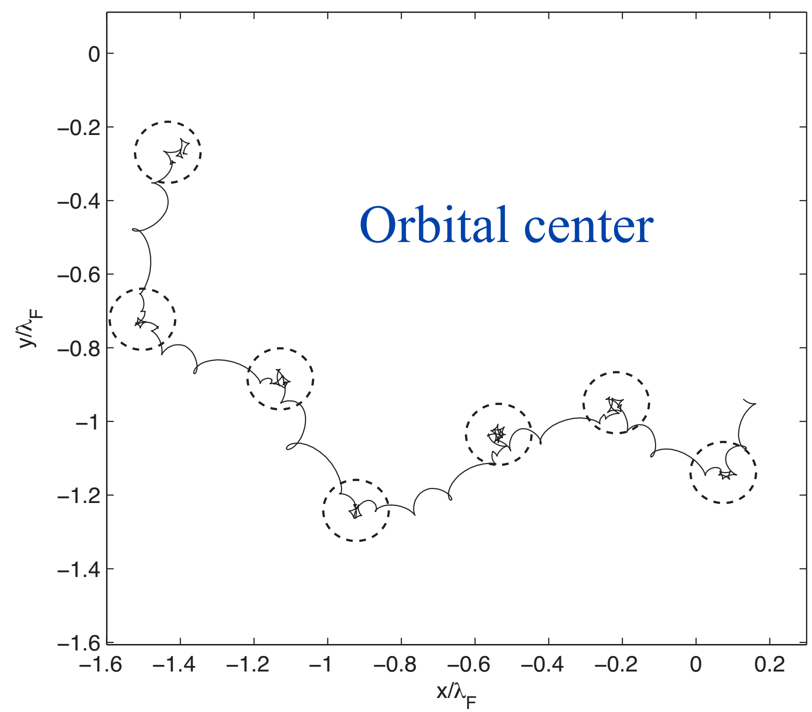

Wobble & leap

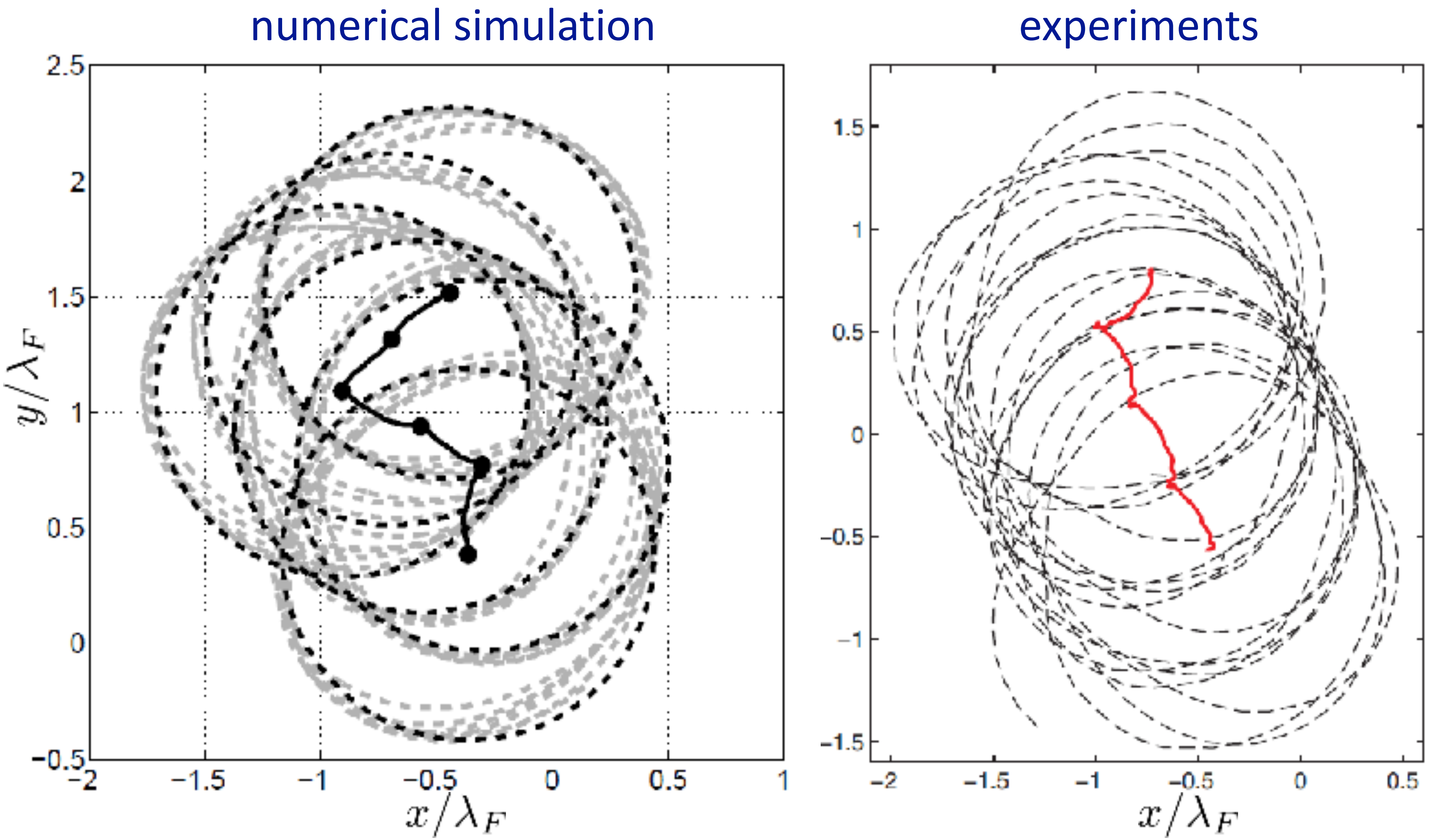
numerical simulation
experiments
2.5
2
1.5
1
0.5
0
−0.5
y/λ_F
−2
−1.5
−1
−0.5
0
0.5
1
x/λ_F
1.5
1
0.5
0
−0.5
−1
−1.5
−2
−1.5
−1
−0.5
0
0.5
x/λ_F

Quasi-periodic trajectories

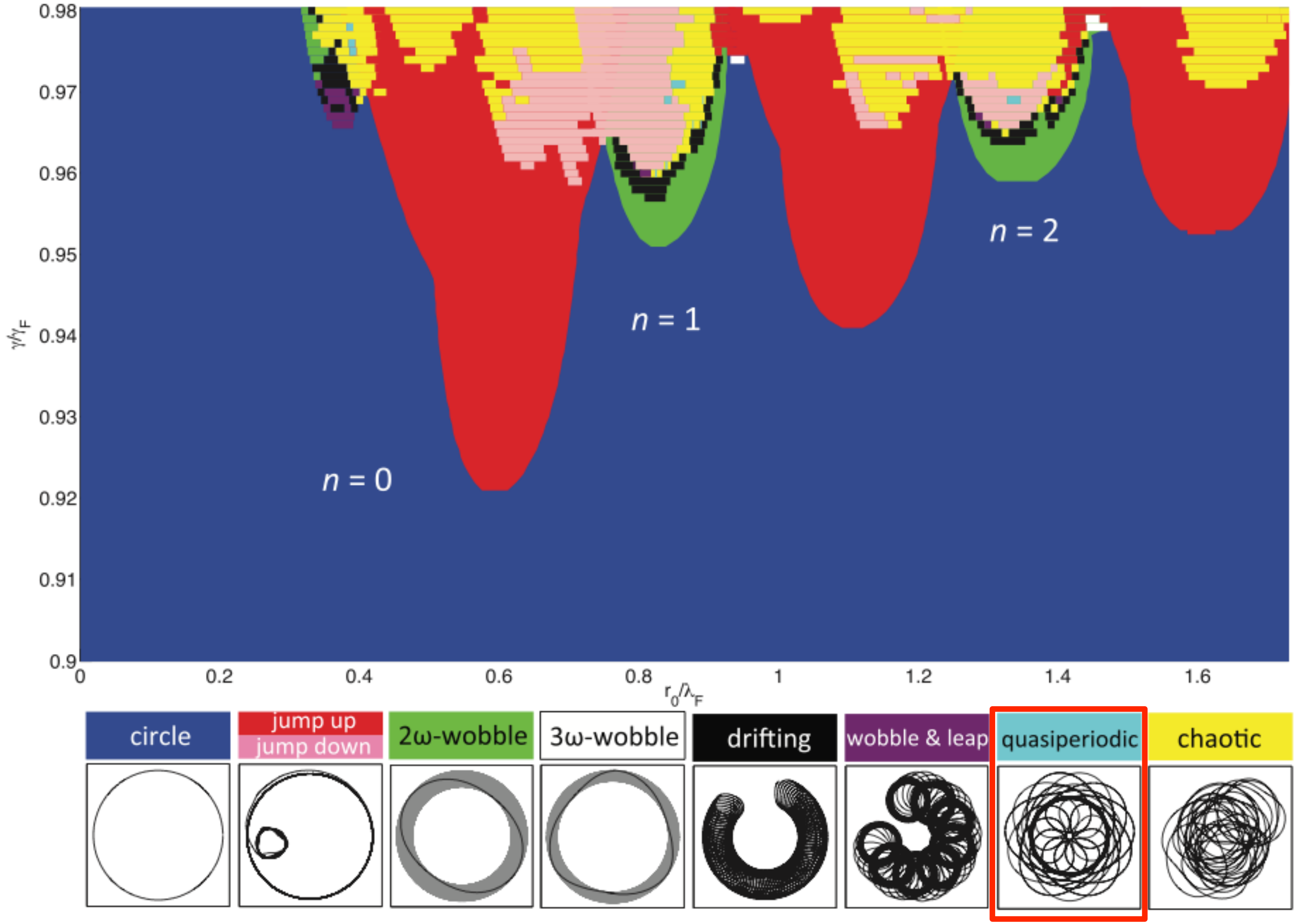

Oza, Wind-Willassen, Harris, Rosales & Bush, *PHF* (2014)

Periodic or quasi-periodic drifting of orbital centers

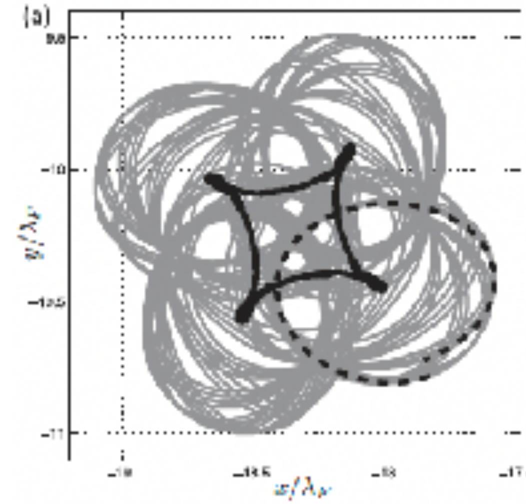

$n = 0$

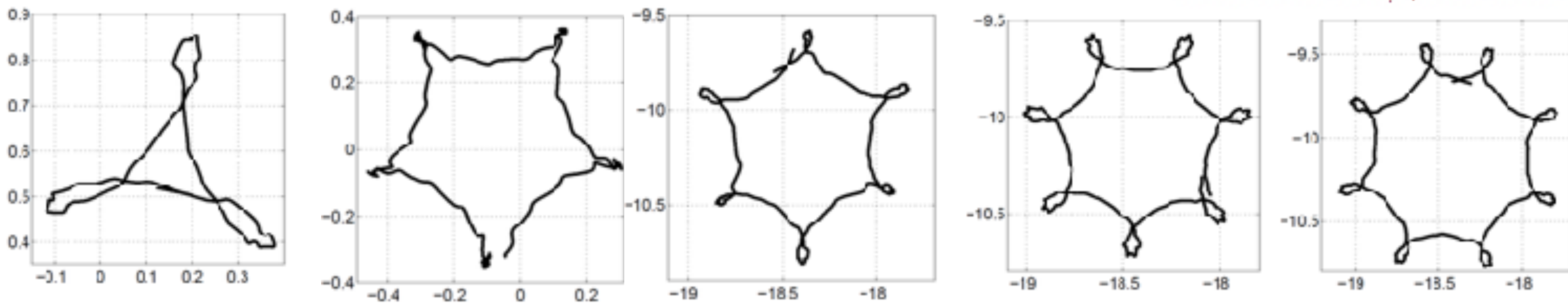

$n = 1$

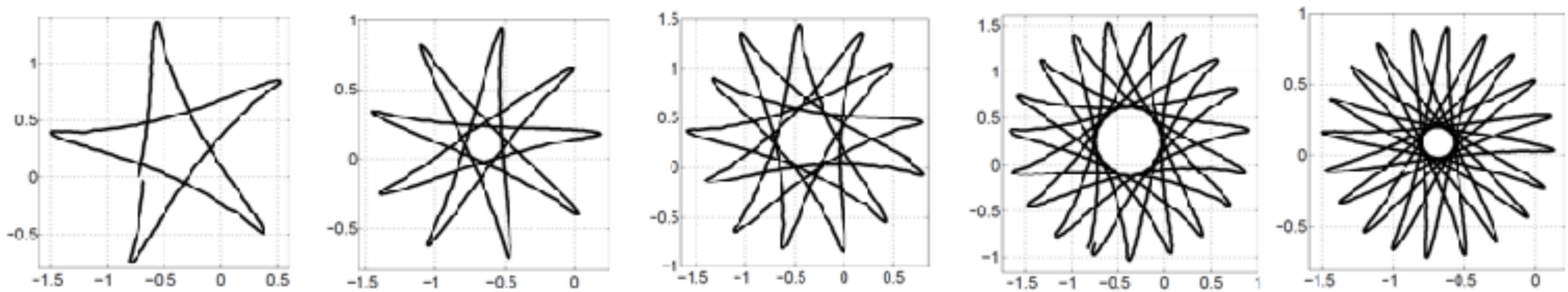

- note spontaneous multiple scale dynamics: drop vibration, spin, drift

Wobble & leap centers

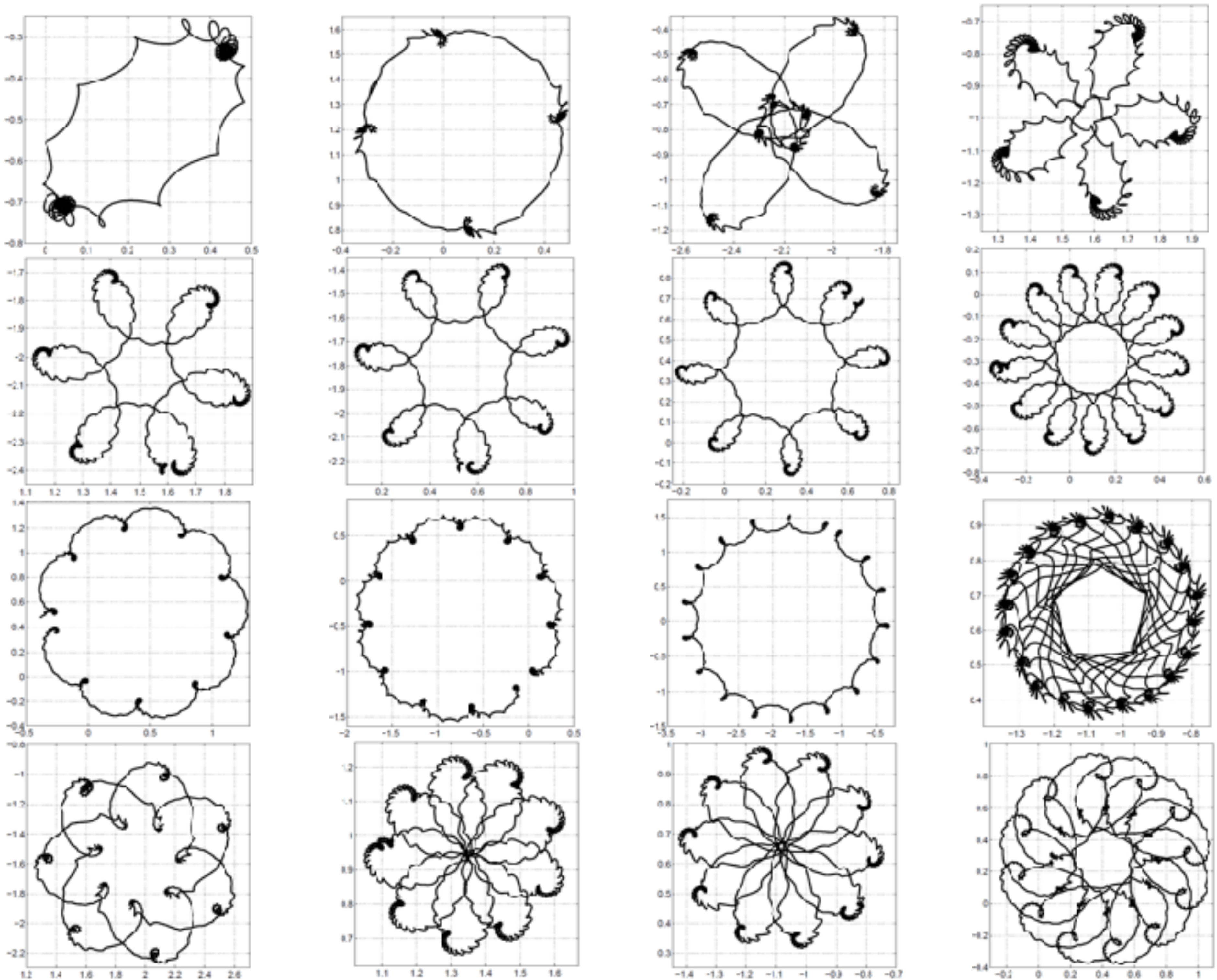

Quasi-periodic motion

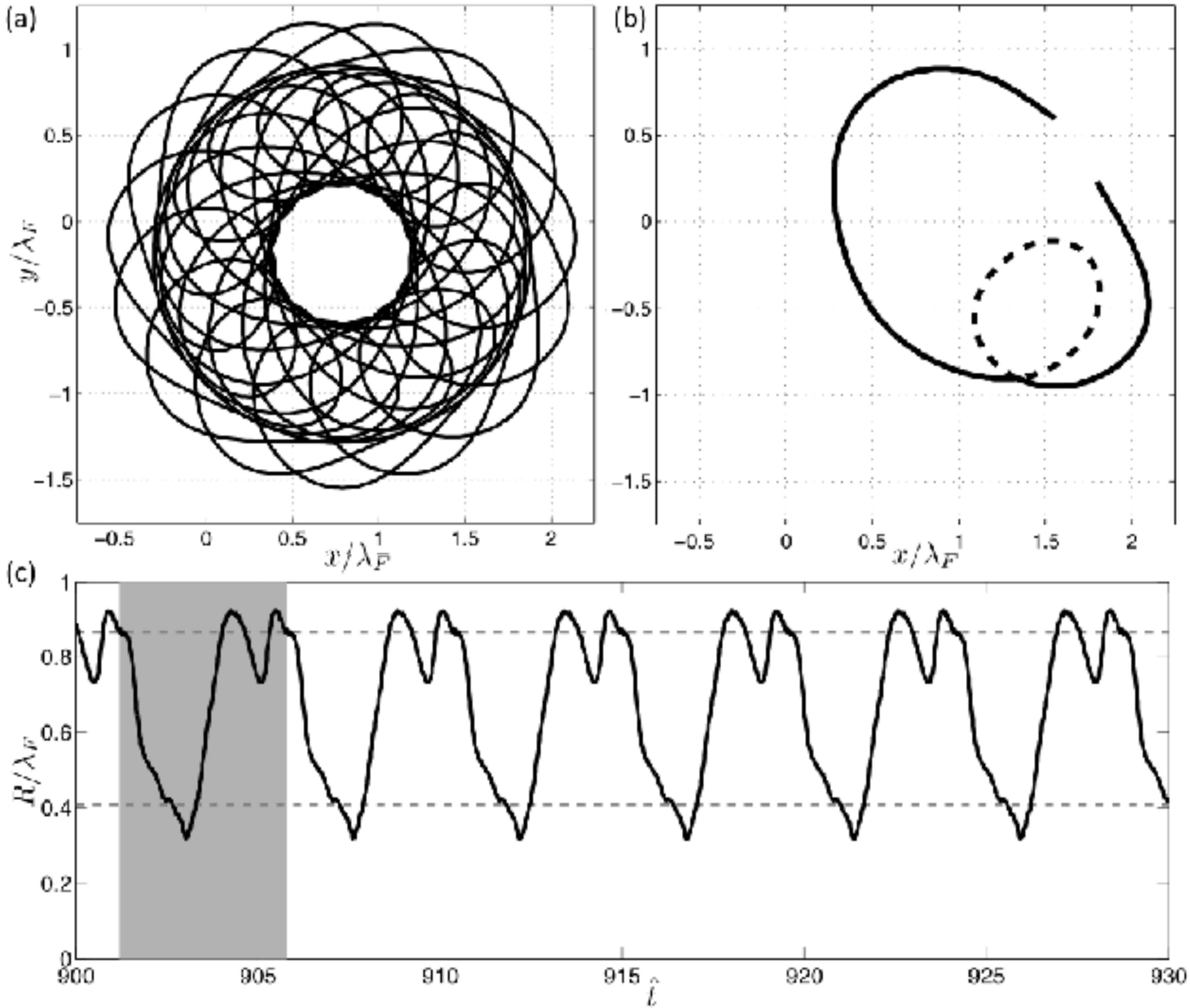

Other complex, quasi periodic orbitals

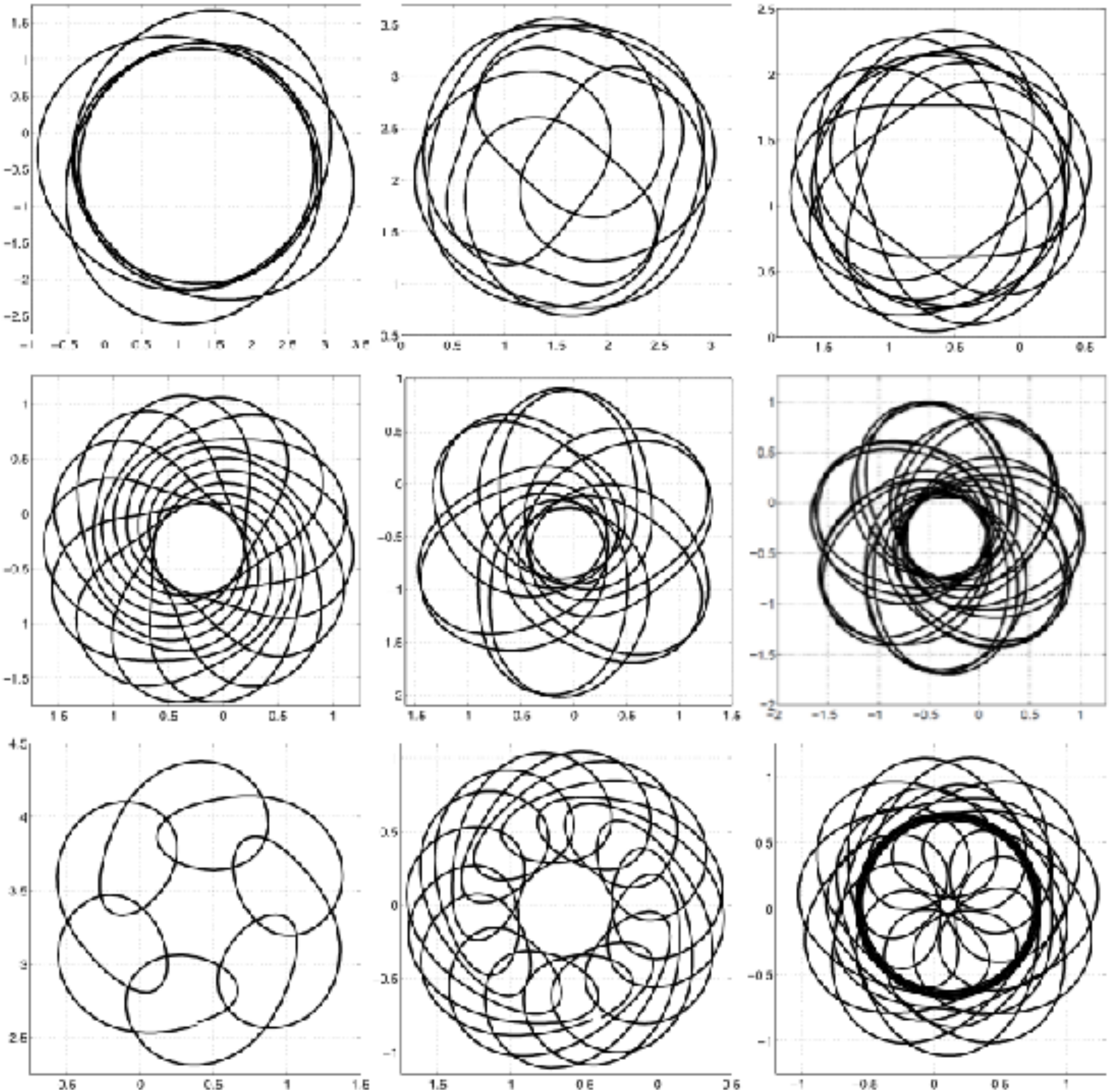

Transition to chaos

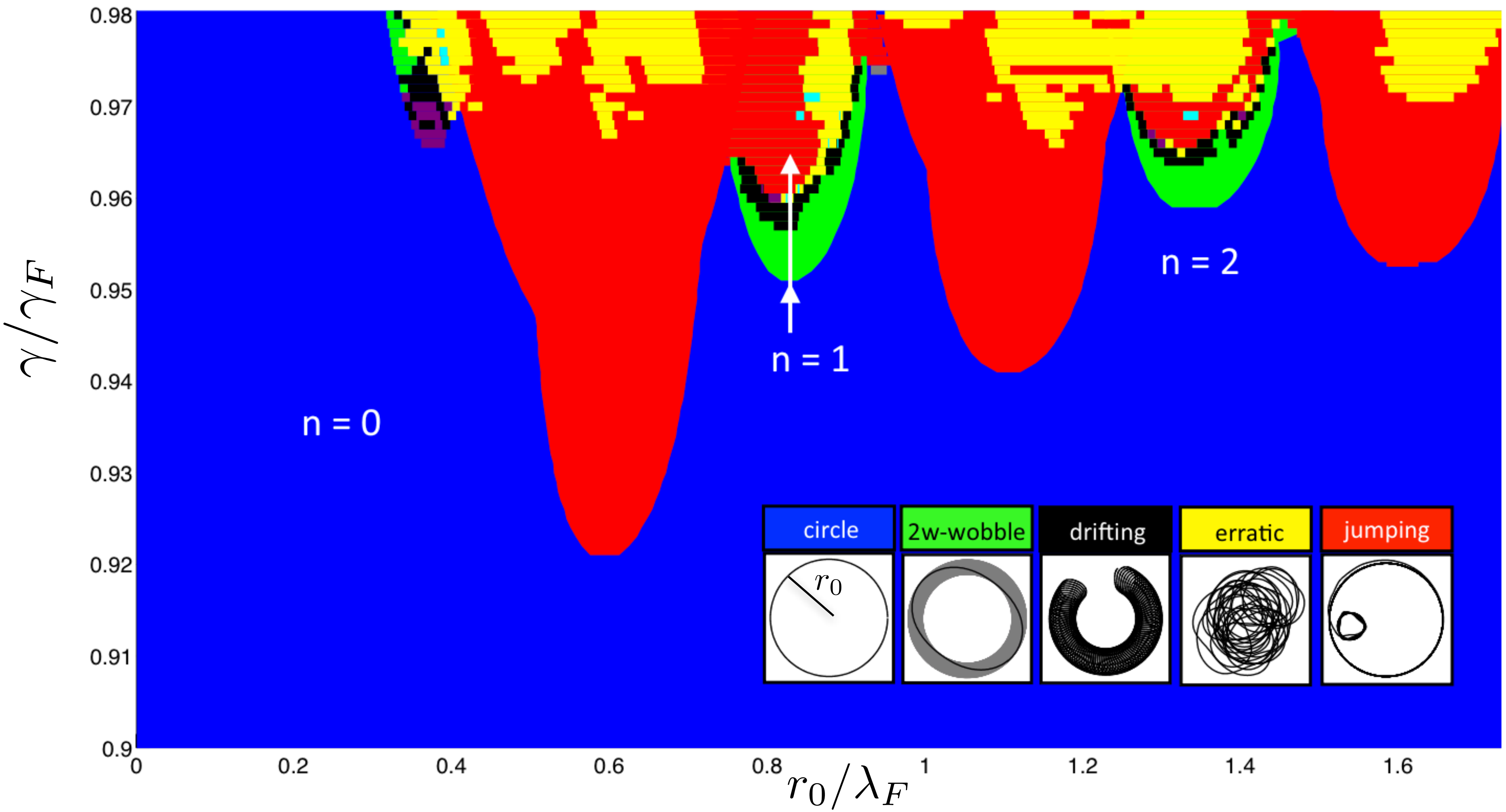

Transition to chaos

Tambasco et al. (2017)

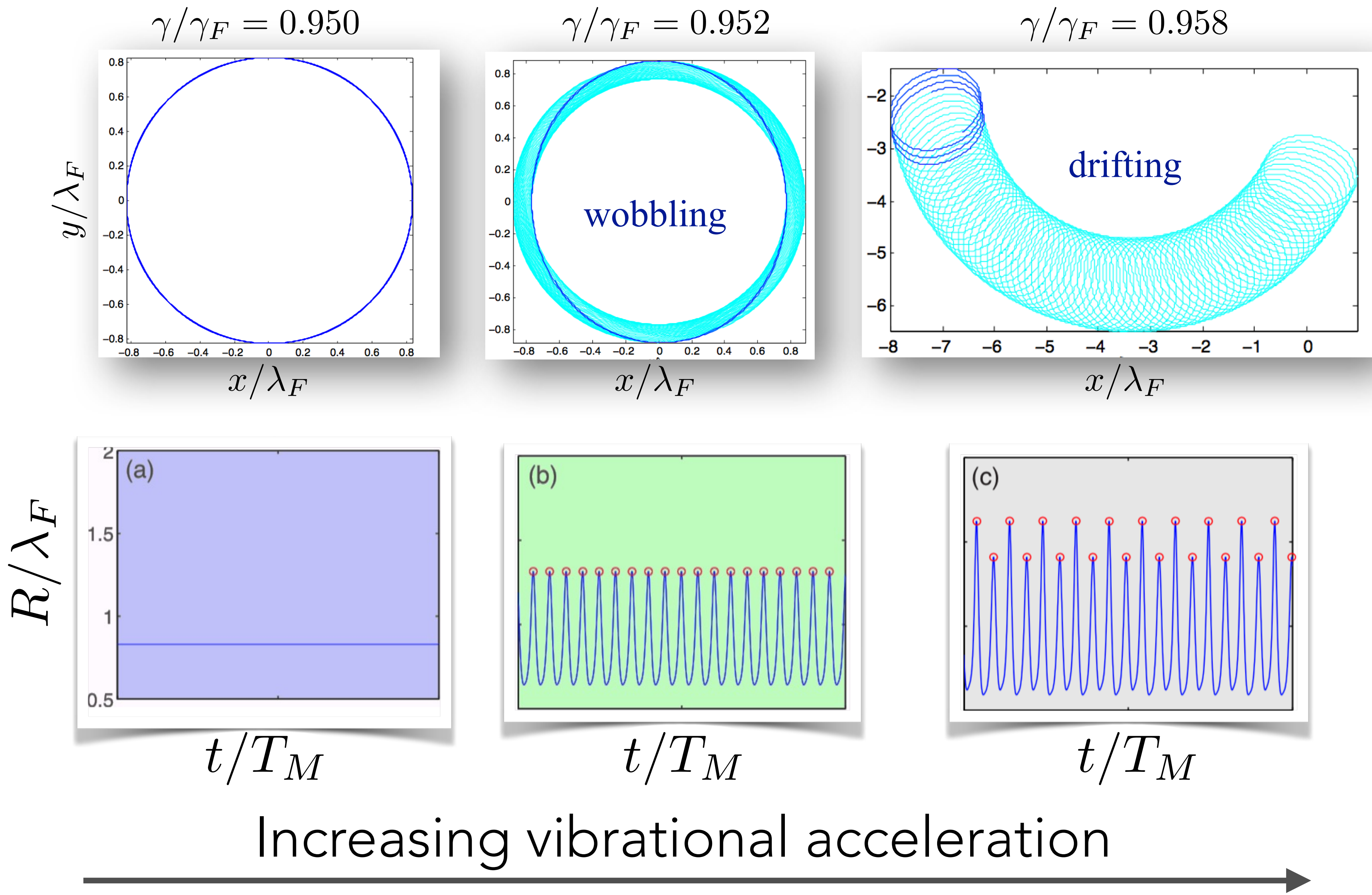

Tambasco et al. (2017)

Transition to chaos

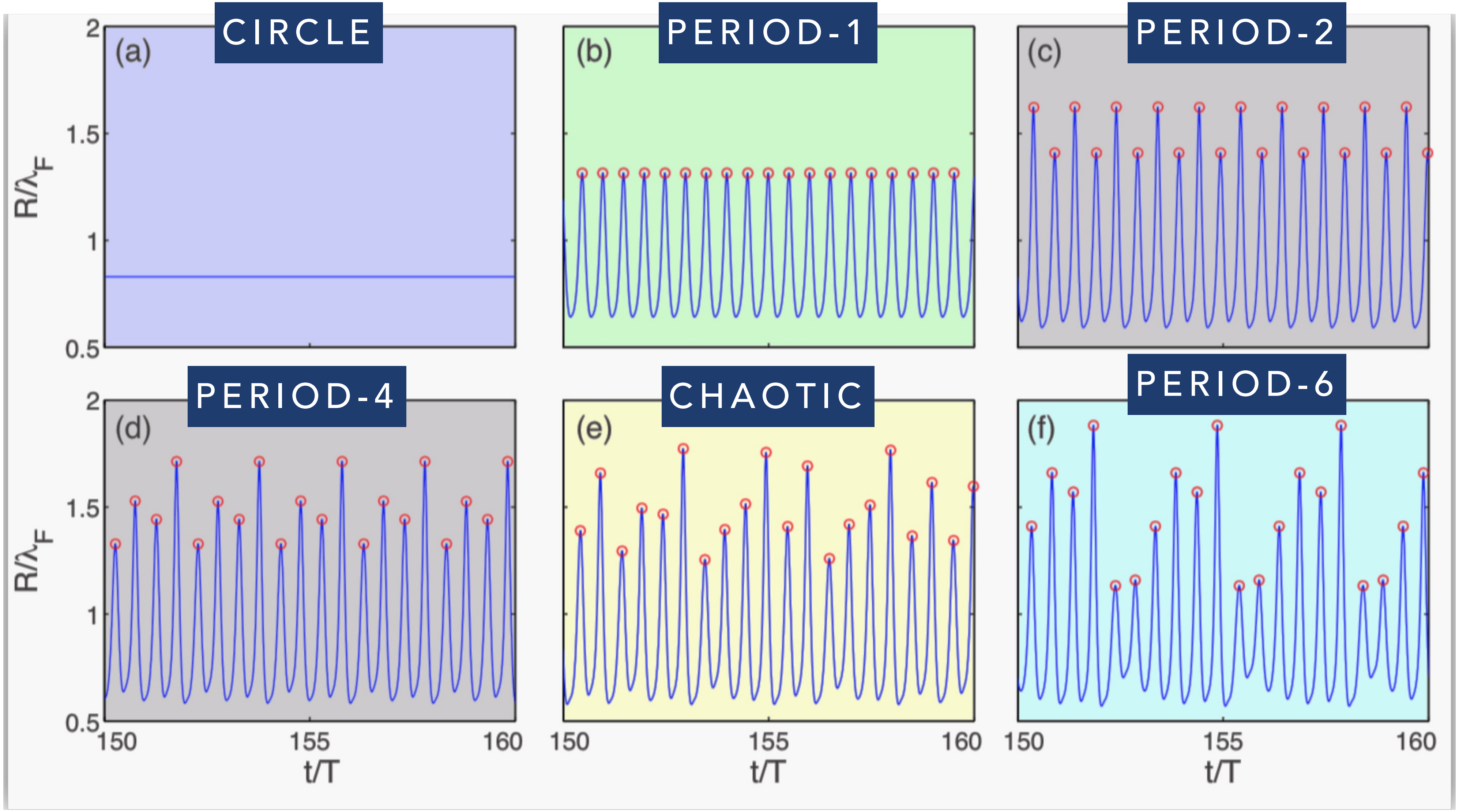

Period-doubling transition to chaos

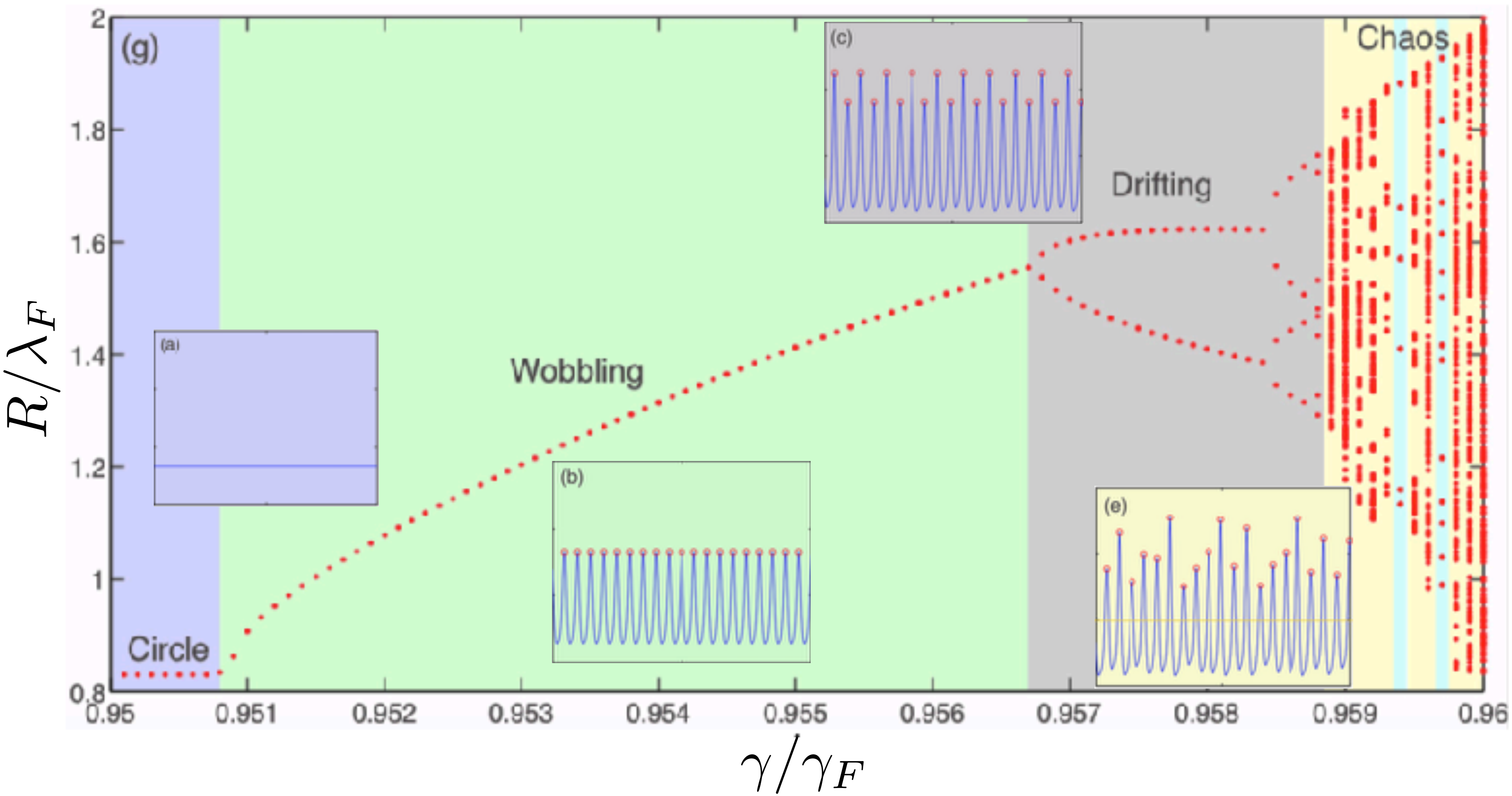

Tambasco et al. (2017)

Chaotic, high-memory regime

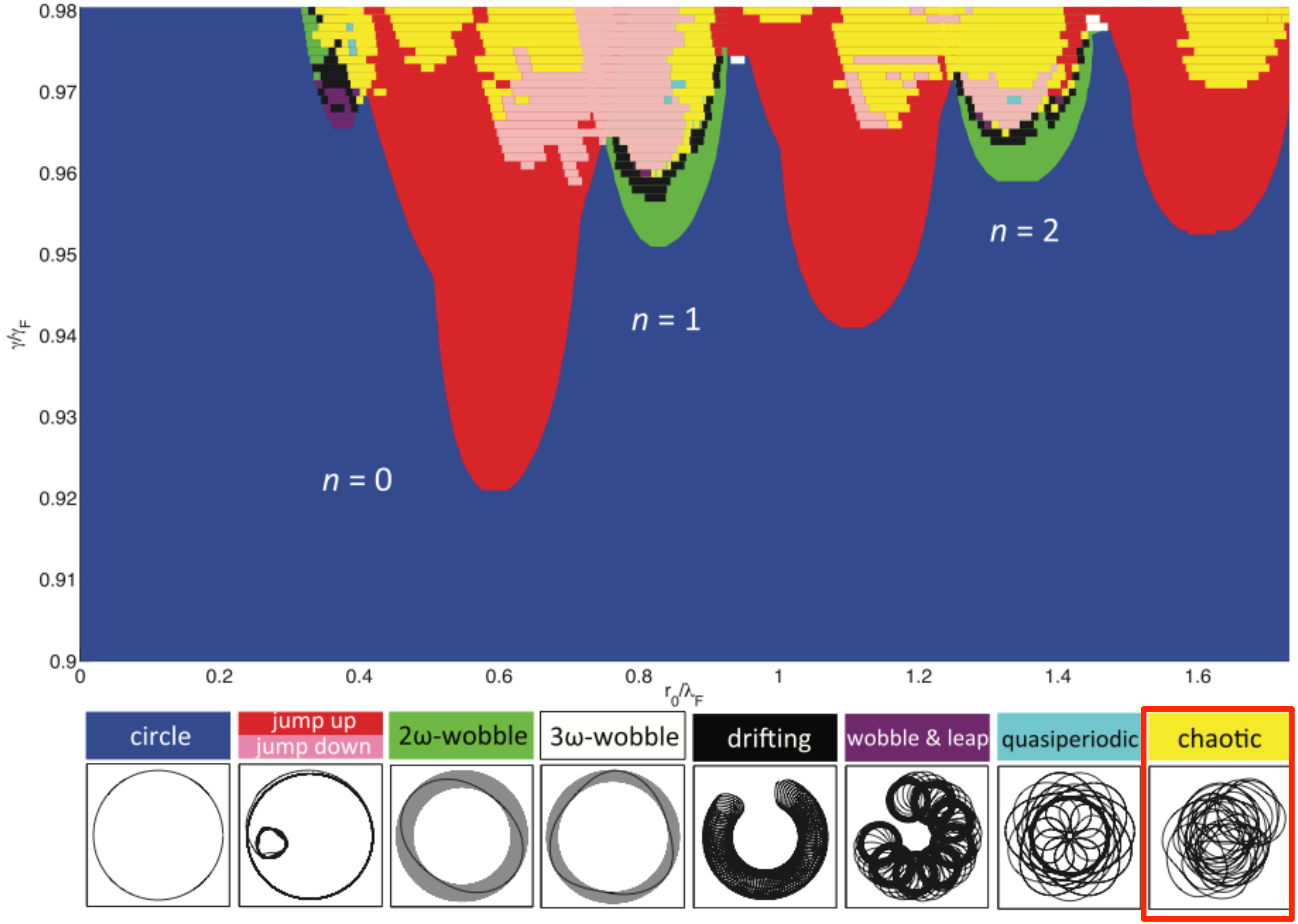

Oza, Wind-Willassen, Harris, Rosales & Bush, *PHF* (2014)

Transition to Chaotic Trajectories

$\gamma/\gamma_F = 0.975 \pm 0.002$

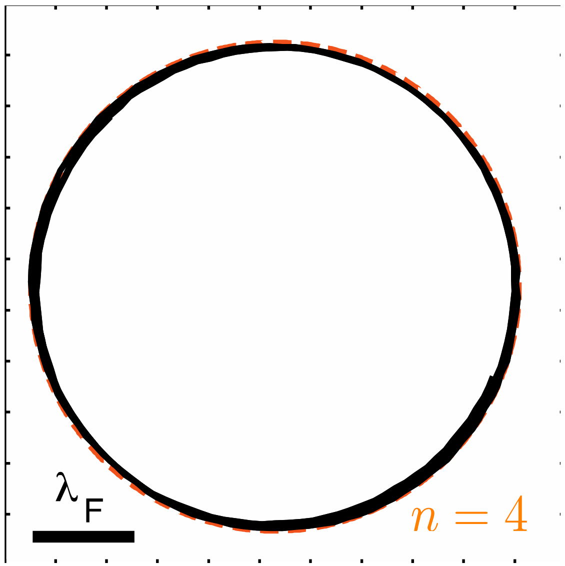

$\gamma/\gamma_F = 0.980 \pm 0.002$

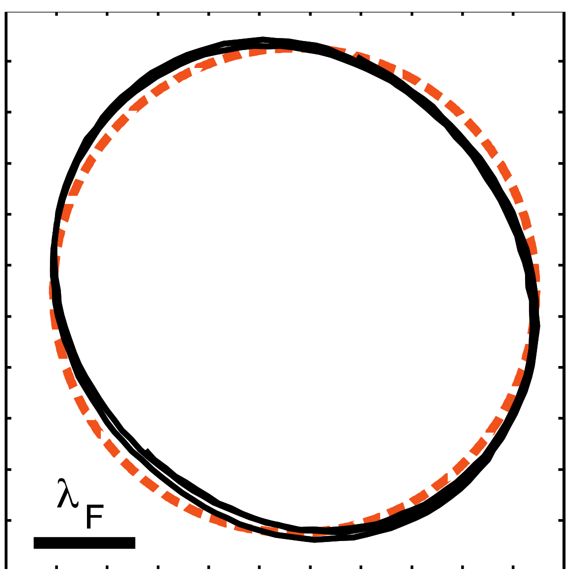

$\gamma/\gamma_F = 0.990 \pm 0.002$

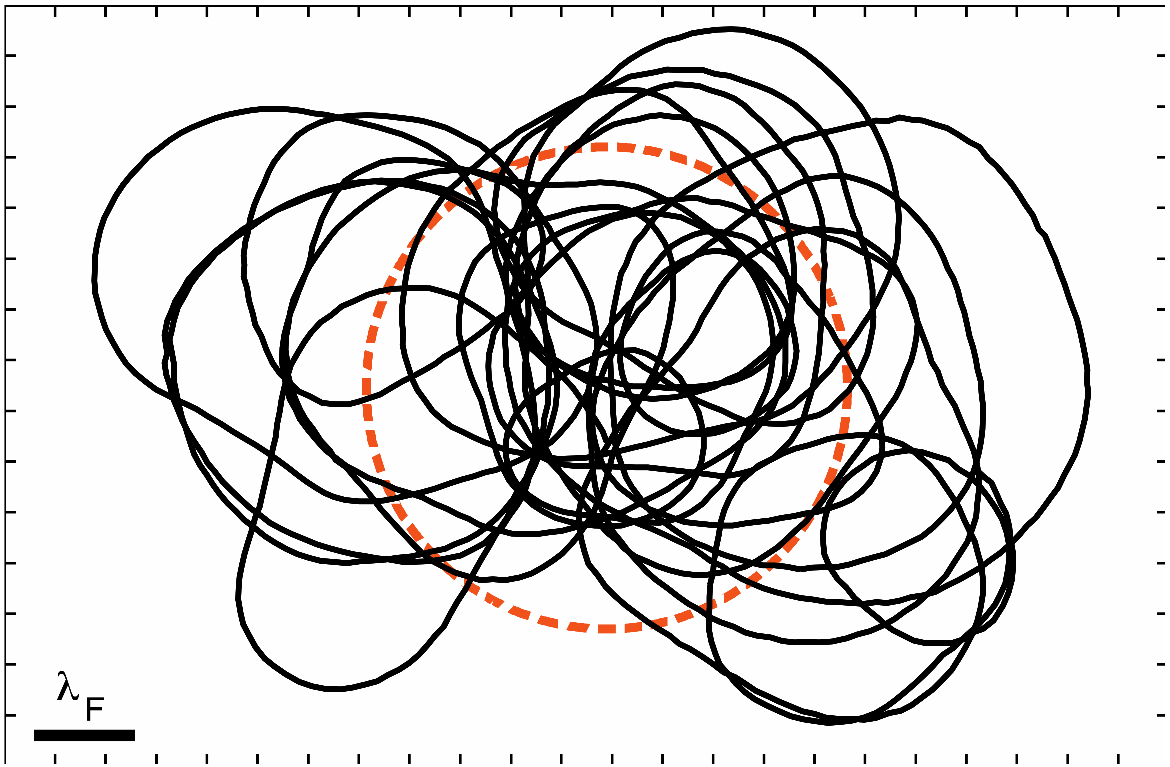

Can we recover anything from this complex trajectory?

Chaotic trajectories

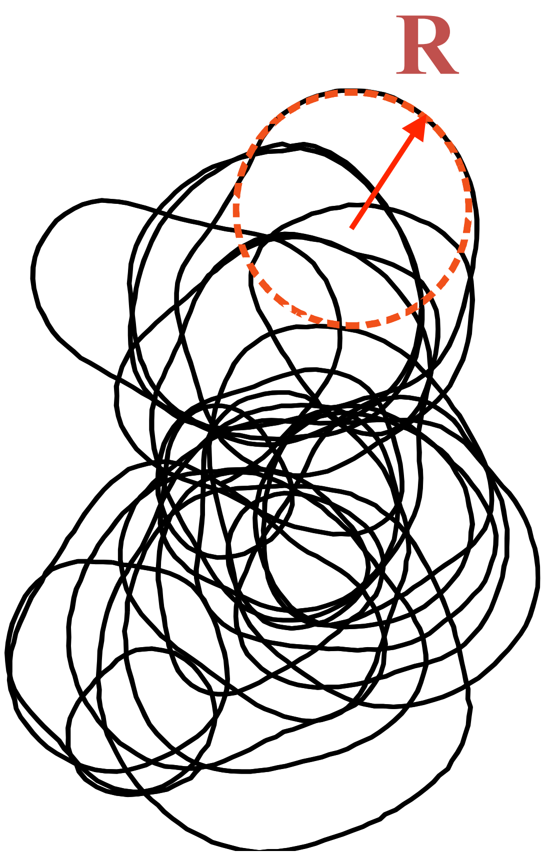

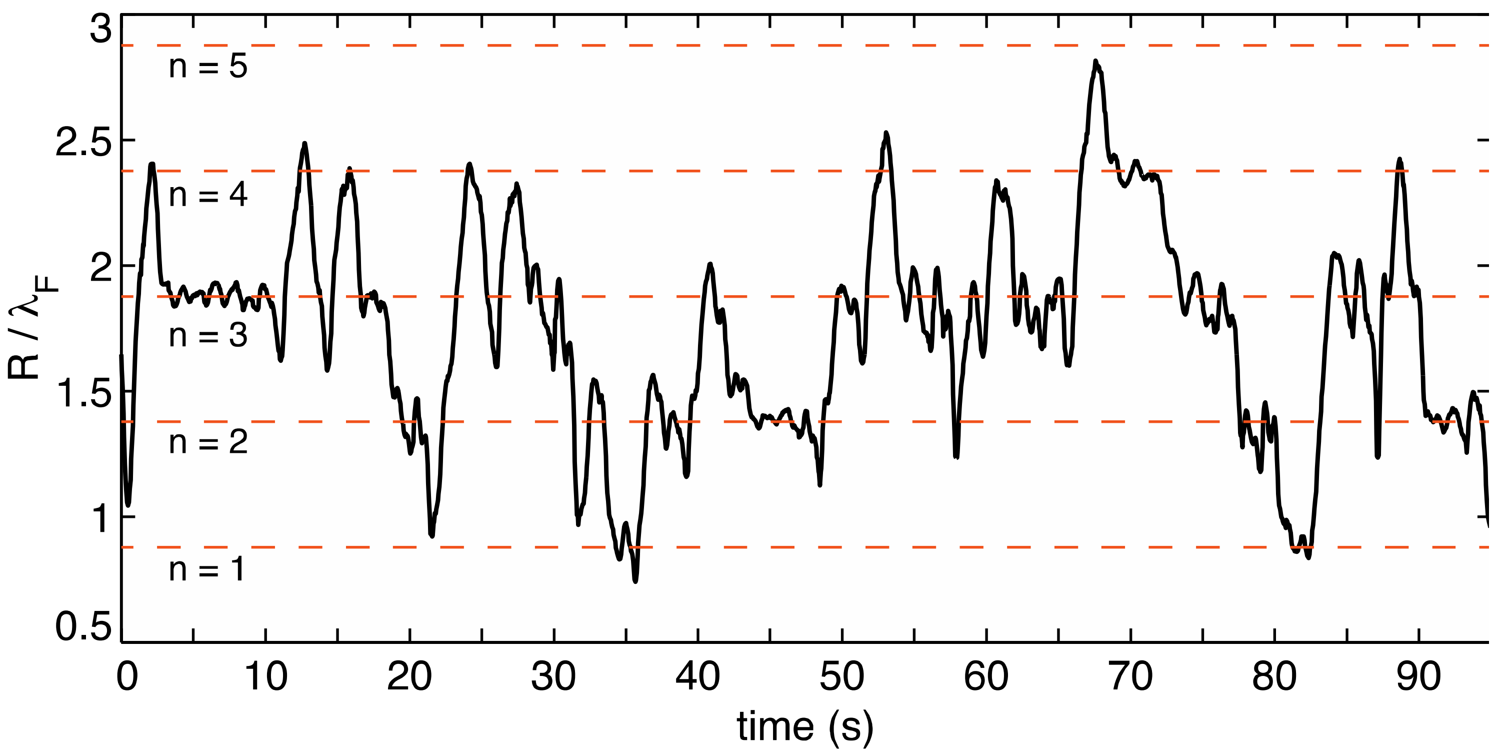

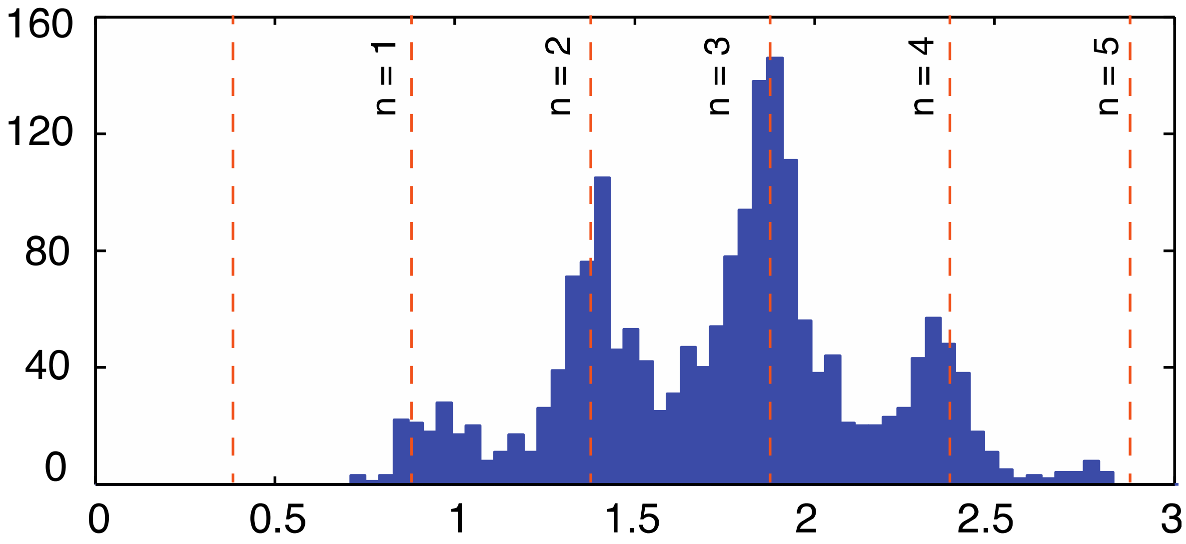

Walker switches between arcs with radii corresponding to the unstable quantized orbits.

Evolution of statistical behavior at fixed Ω

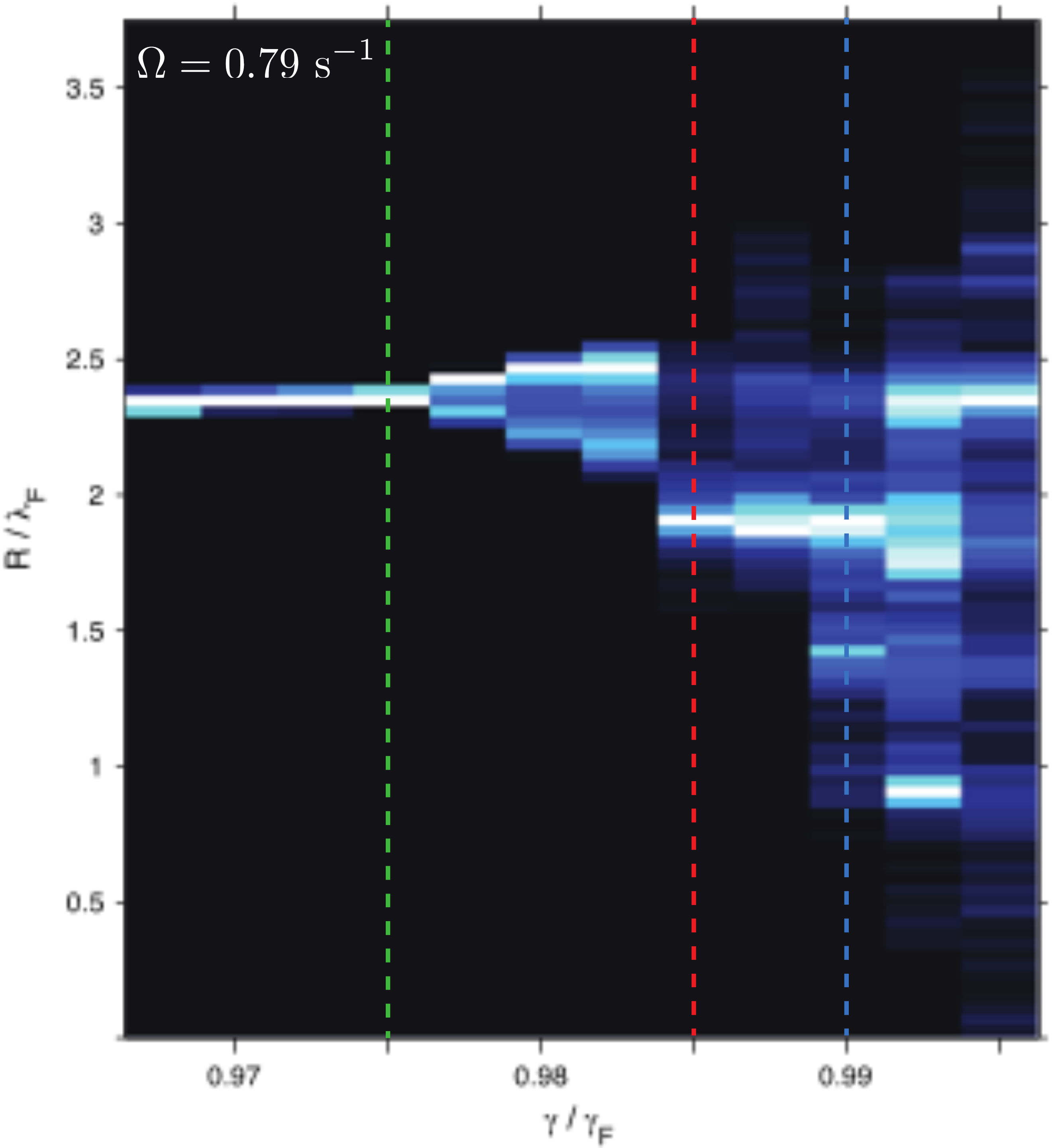

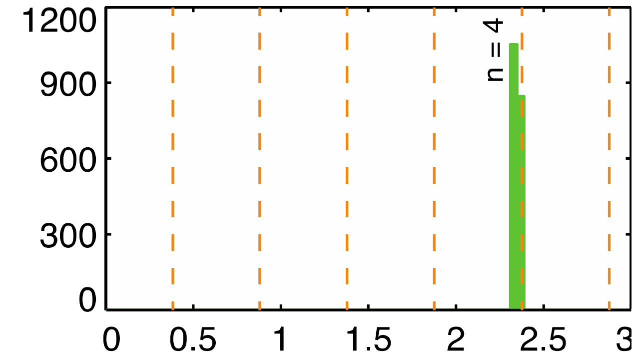

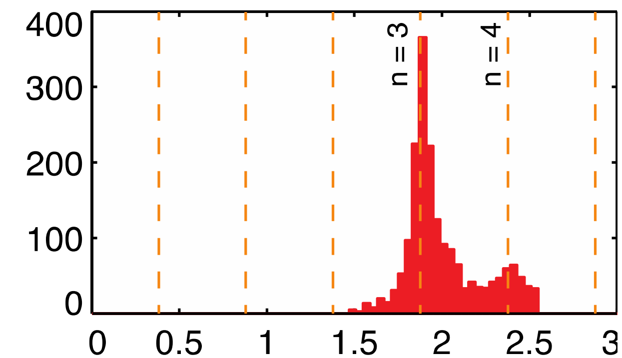

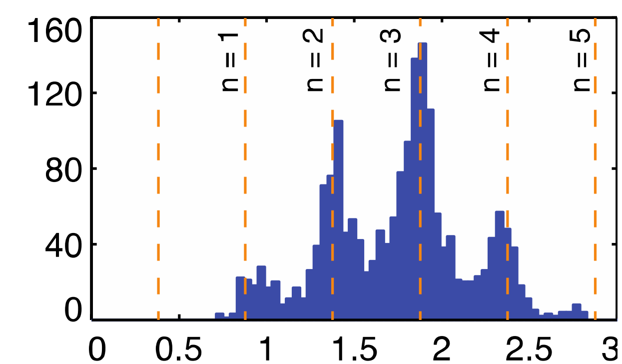

Evolution of statistical behavior with memory

Experiment

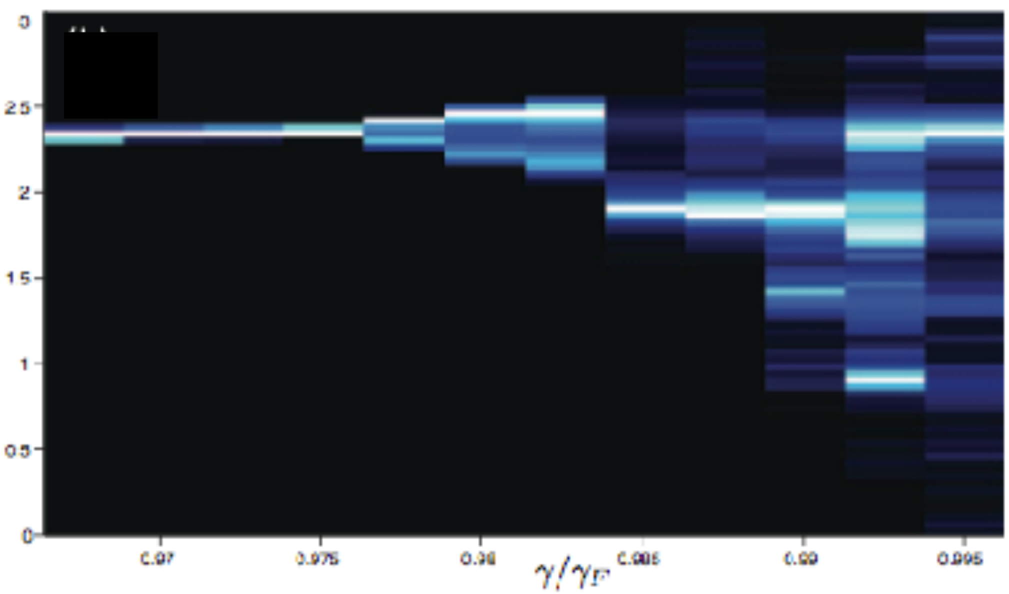

Simulation

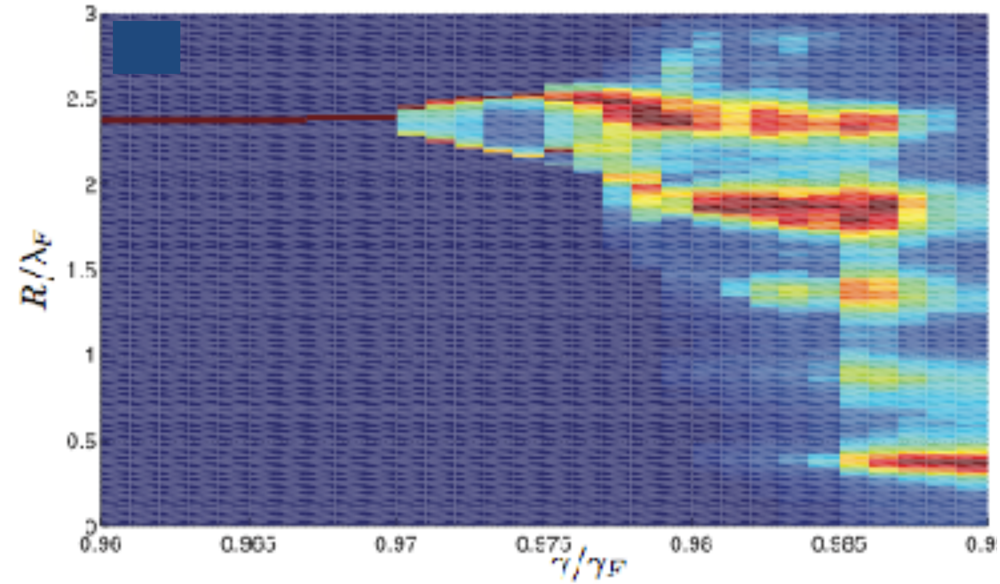

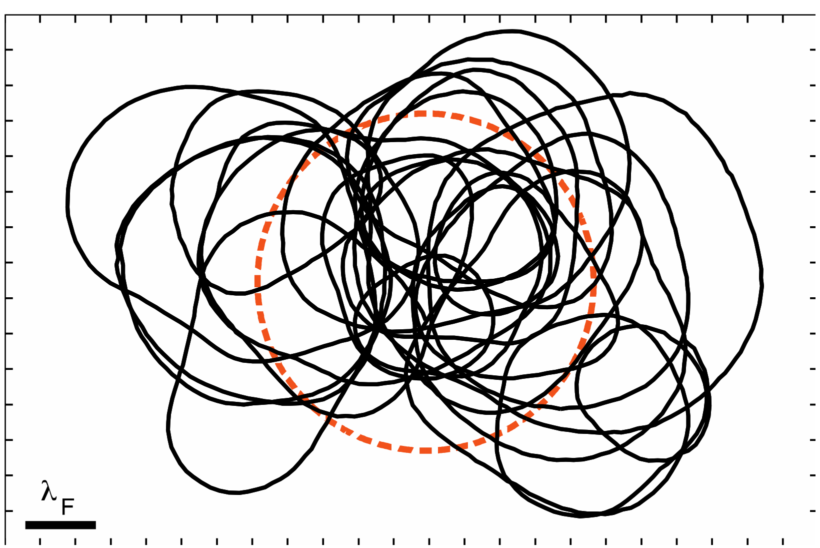

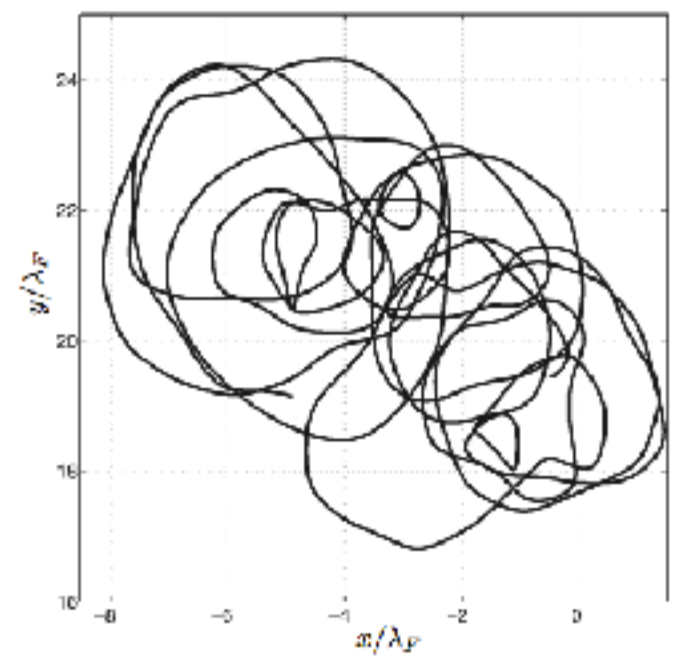

- as the memory is increased, an increasing number of orbital levels become accessible

Statistical behavior at high memory

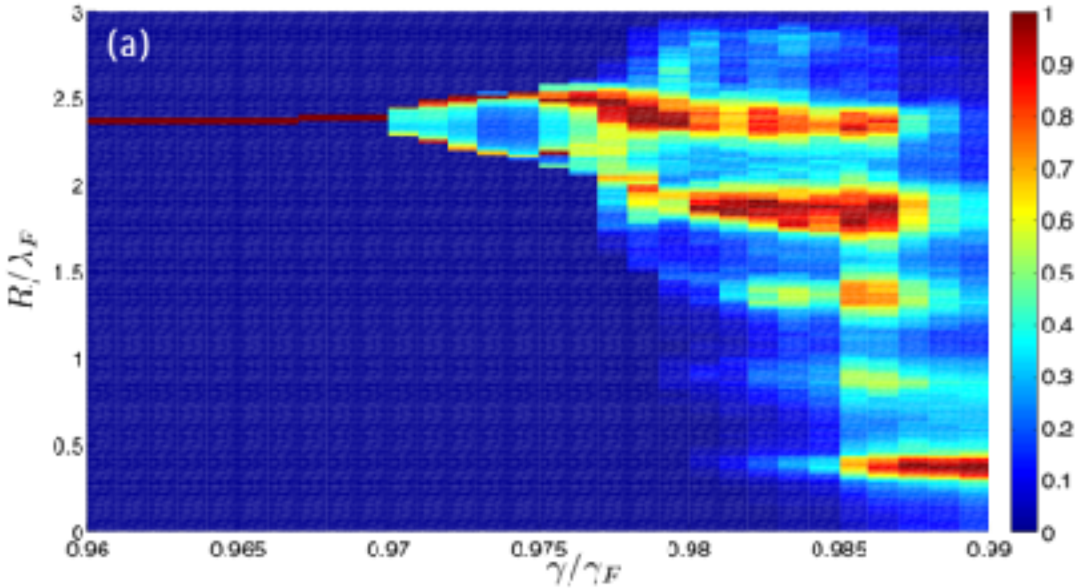

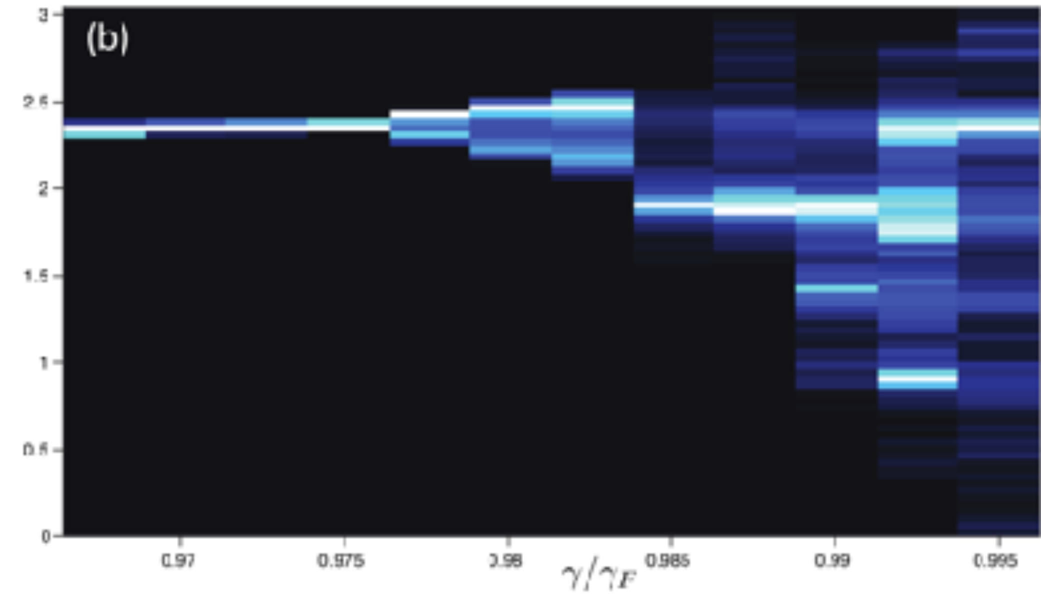

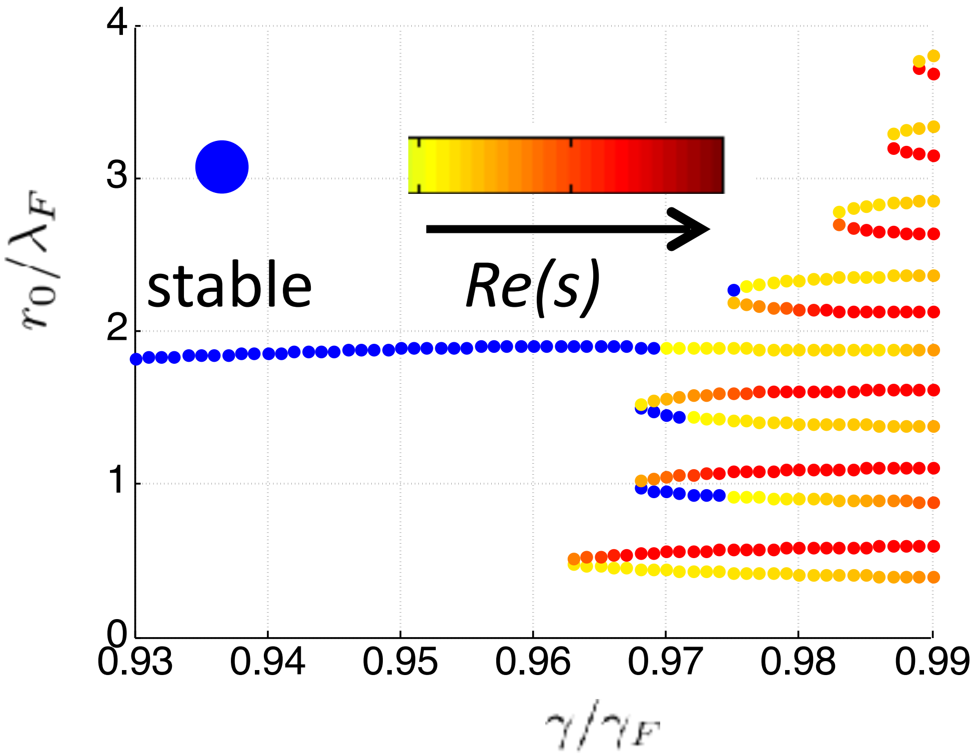

Influence of unstable circular orbits reflected in statistics

Evolution of statistical behavior at fixed memory

Experiment

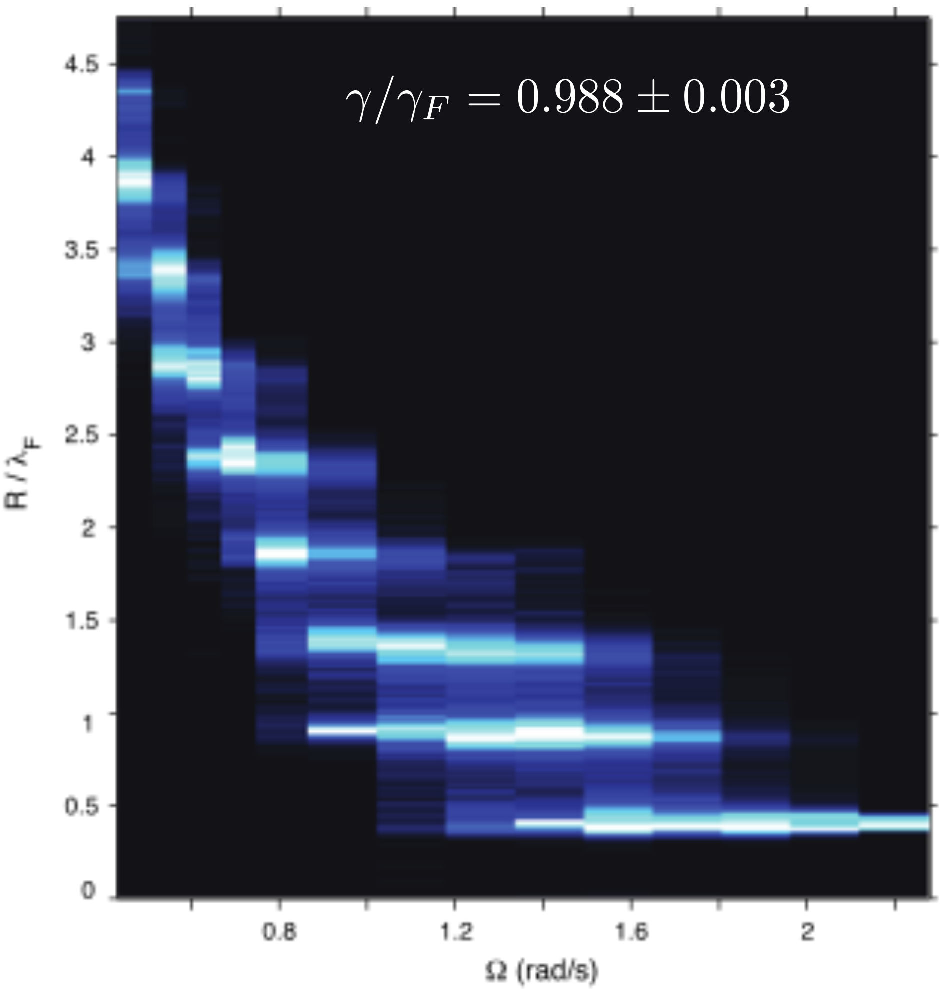

Simulation

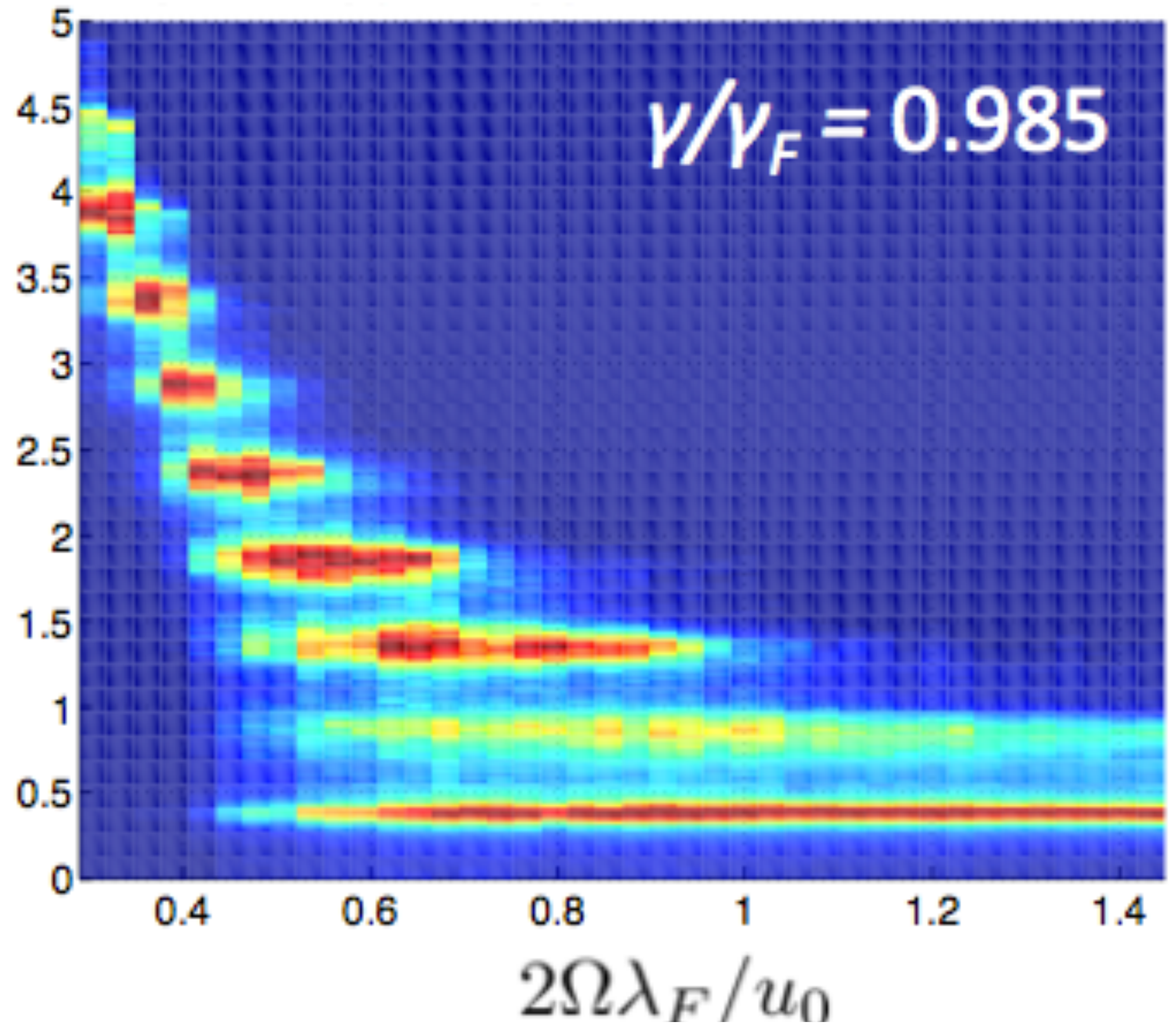

- the rotation rate defines the mean orbital radius
- the memory defines the number of accessible levels

Evolution of statistical behavior at fixed memory

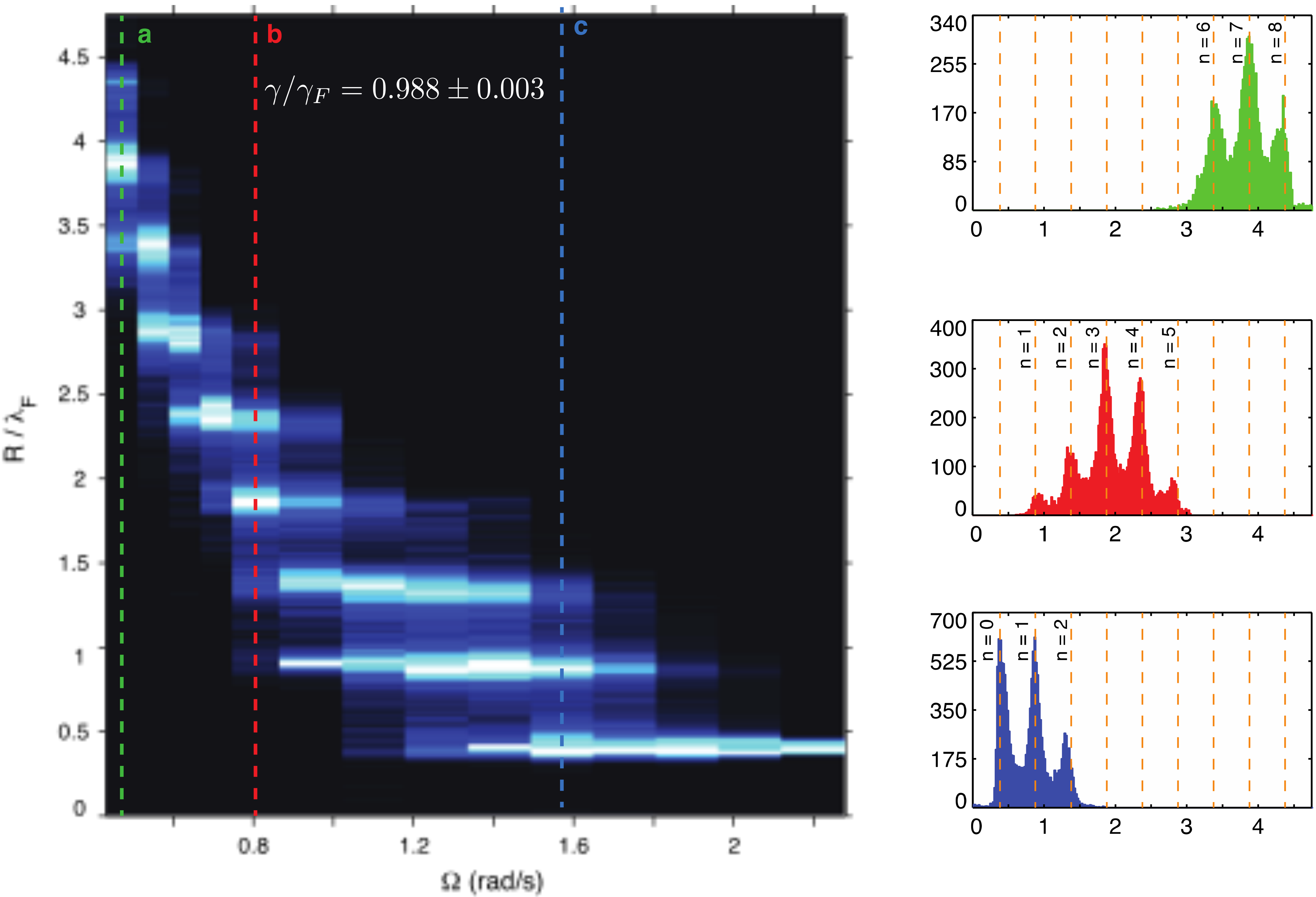

Multimodal statistics in orbital dynamics

Harris et al. (2014)
Oza et al. (2014)

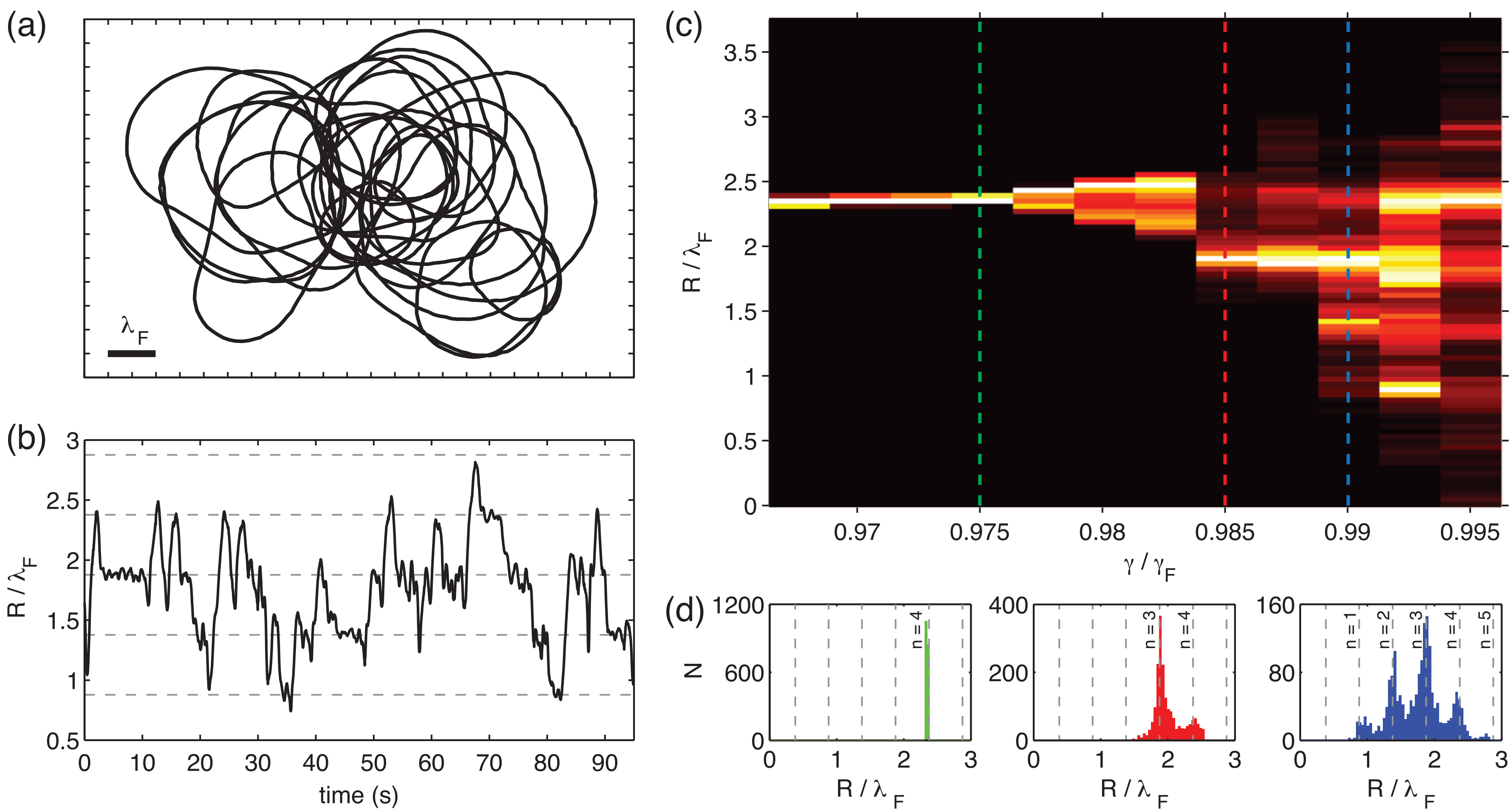

- at high memory, quantized orbits destabilize, chaotic trajectories emerge
- unstable eigenstates represent attractors, leave an imprint on the statistics
- multimodal statistics reflect superposition of unstable dynamical states

High-memory limit:
chaotic pilot-wave dynamics

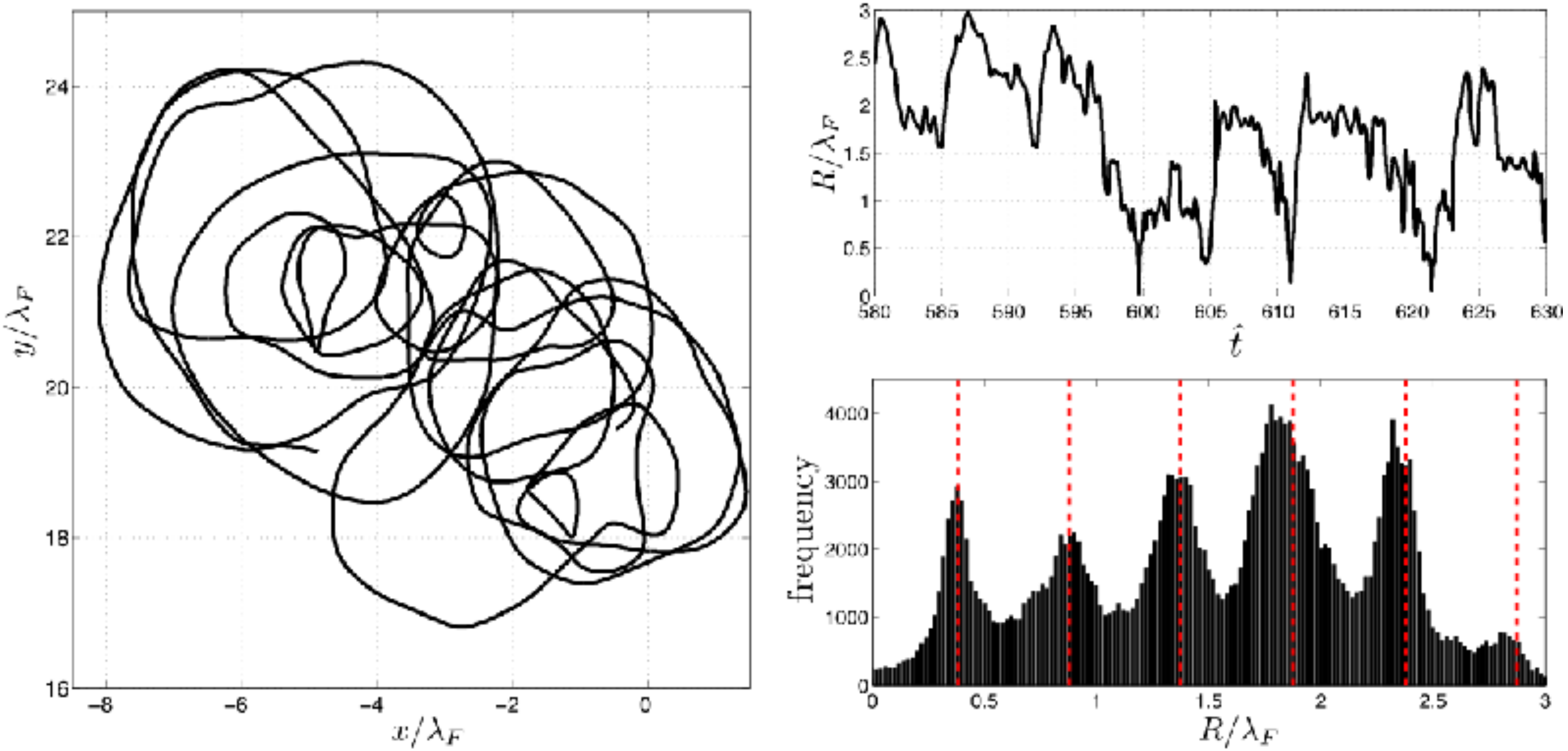

Peaks at the zeros of $J_0(k_F r)$

Walking at ultra-high memory: Simulations with strobe model

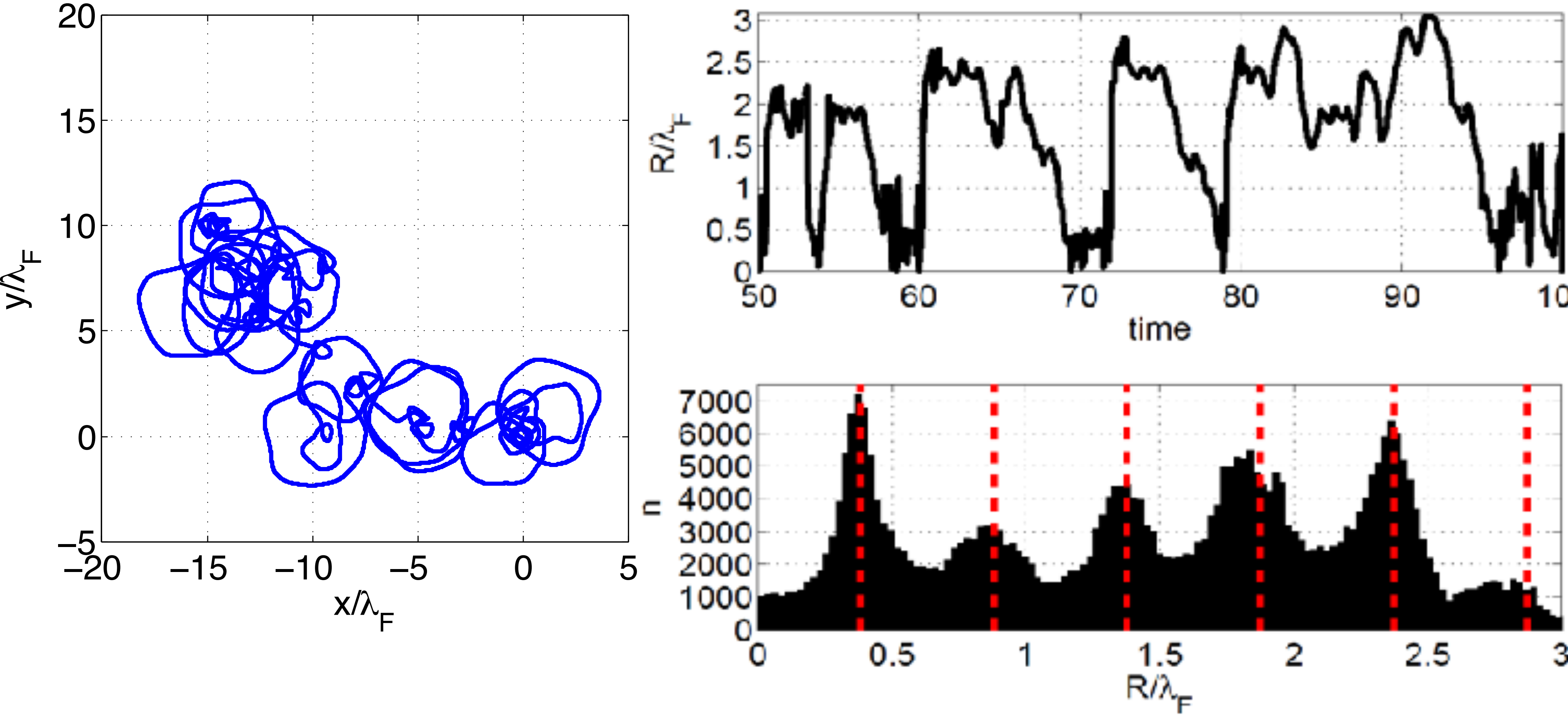

- coherent, wave-like statistics emerge from chaotic pilot-wave dynamics
- wave-like statistics reflect imprint of unstable eigenstates

A heuristic for orbital stability

Liu *et al.*, *JFM* (2023)

Pilot wave field

$$\hat{h}(\boldsymbol{x}, t) = \int_{-\infty}^{t} \mathrm{J}_0(|\boldsymbol{x} - \boldsymbol{x}_p(s)|)\, \mathrm{e}^{-\mu(t-s)}\, \mathrm{d}s$$

Mean wave field

$$\bar{h}(r) = \frac{1}{\mu} \mathrm{J}_0(r_0)\, \mathrm{J}_0(r)$$

Force imparted by mean wave field

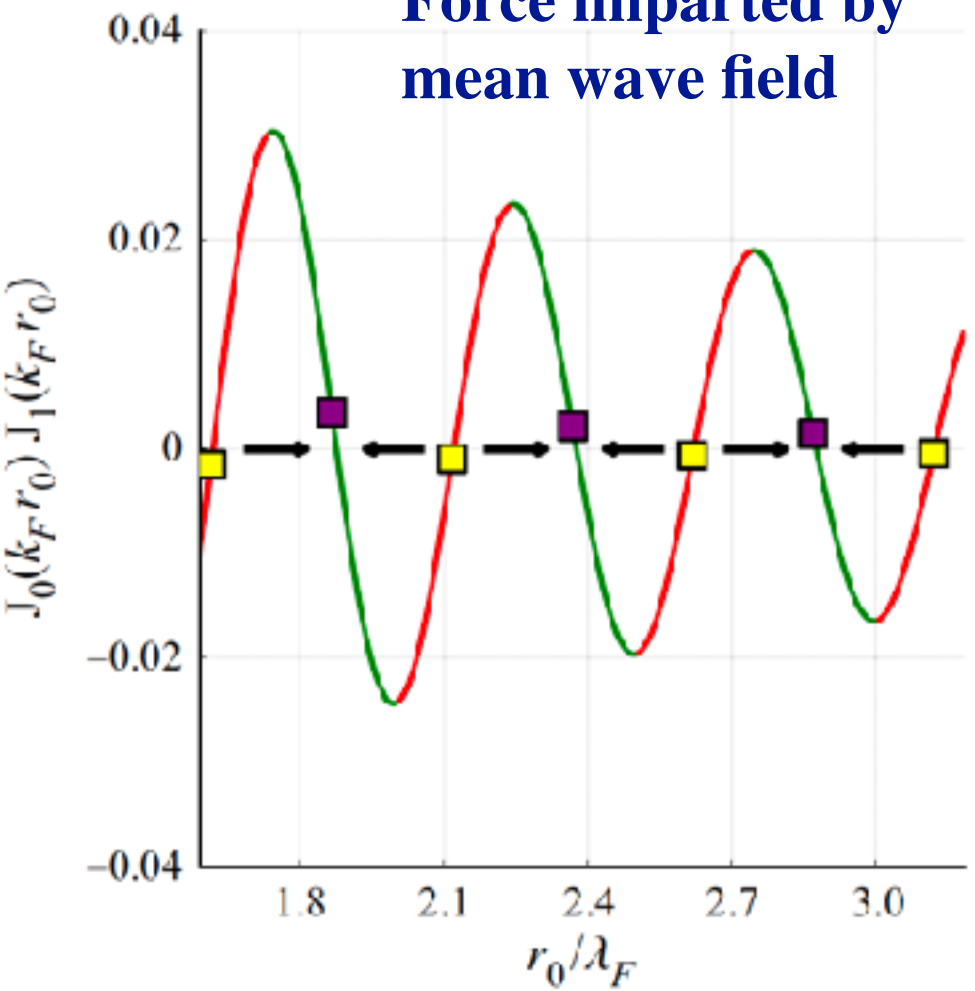

- orbits along zeros in $J_0(r)$ should minimize the global wave energy
- orbits along maxima in mean wave field destabilize via monotonic instability
- orbits along minima in mean wave field destabilize via wobbling

Energetics

Liu *et al.*, *JFM* (2023)

Wave energy: $$E = \lim_{R\to\infty} \frac{1}{R}\left[\int_{|x|\le R} \frac{1}{2}\rho g h^2\,\mathrm{d}x + \int_{|x|\le R} \sigma\left(\sqrt{1+|\nabla h|^2}-1\right)\mathrm{d}x\right]$$

Linear waves: $$E = (\rho g + \sigma k_F^2) \lim_{R\to\infty} \frac{1}{2R}\int_{|x|\le R} h^2(\boldsymbol{x},t)\,\mathrm{d}\boldsymbol{x}$$

Nondimensionalize: $$\Gamma = (\gamma - \gamma_W)/(\gamma_F - \gamma_W) = 1-\mu$$

$\hat{h} = h/h_0$ and $\hat{E} = E/E_0$, where $h_0 = AT_W/T_F$ and $E_0 = h_0^2 k_F^{-1}(\rho g + \sigma k_F^2)$

$$\hat{E} = \frac{1}{\mu}\,\mathrm{H} \quad \text{and} \quad \hat{E} = \frac{1}{\mu^2}\left(1 - \frac{U^2}{2}\right)$$

where $U = r_0\omega$ is the orbital speed.

Redimensionalize:

$$E_p = \frac{1}{2}m|\dot{\boldsymbol{x}}_p|^2 + V(\boldsymbol{x}_p) + mgH_B\gamma_D(|\dot{\boldsymbol{x}}_p|) \quad \text{and} \quad \boxed{\frac{H}{H_B} = \frac{E}{E_B} = \gamma_D(v) = 1 - \frac{v^2}{c^2}}$$

- prompted the general result deduced for stroboscopic energetics

Motion in a central force field

nature COMMUNICATIONS

ARTICLE

Received 3 Jul 2013 | Accepted 7 Jan 2014 | Published 30 Jan 2014

DOI: 10.1038/ncomms4219

Self-organization into quantized eigenstates of a classical wave-driven particle

Stéphane Perrard[1], Matthieu Labousse[2], Marc Miskin[1,2,†], Emmanuel Fort[2] & Yves Couder[1]

PHYSICAL REVIEW FLUIDS 2, 113602 (2017)

Simulations of pilot-wave dynamics in a simple harmonic potential

Kristin M. Kurianski,[1] Anand U. Oza,[2] and John W. M. Bush[1,*]

[1]*Department of Mathematics, Massachusetts Institute of Technology, Cambridge, Massachusetts 02139, USA*

[2]*Courant Institute of Mathematical Sciences, New York University, New York, New York 10012, USA*

(Received 22 April 2017; published 14 November 2017)

Motion in a central force field

- encapsulate ferrofluid: apply external forces to walker via magnetic field
- experimental modeling of a particle in a simple harmonic oscillator

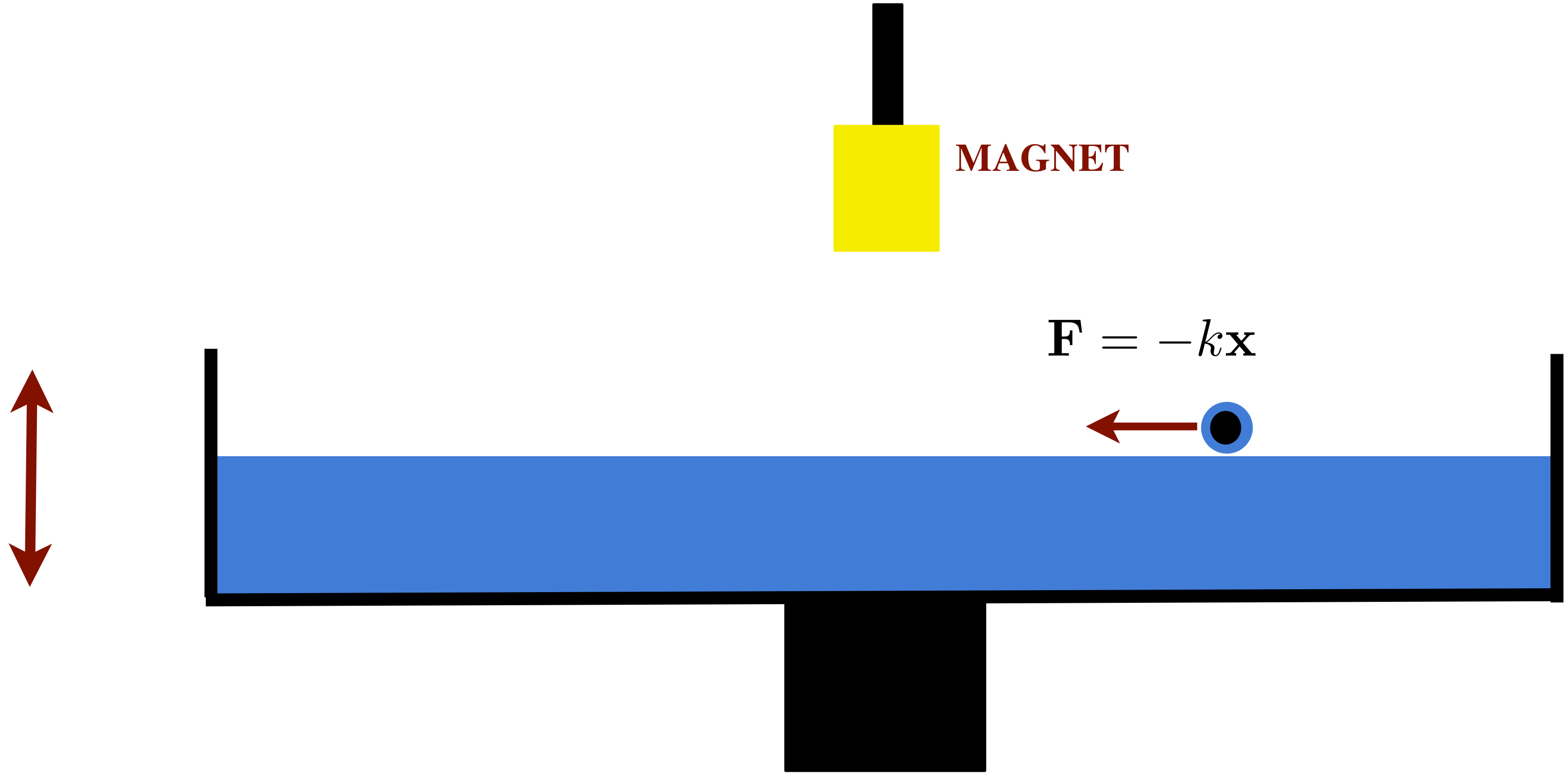

Perrard et al. (2014), Labousse et al. (2015)

Double quantization

- orbits quantized in both mean radius (energy) and angular momentum
- orbits characterized in terms of states (n, m) reflecting R, L

Rule: $m \in \{-n, -n+2, \ldots, n-2, n\}$

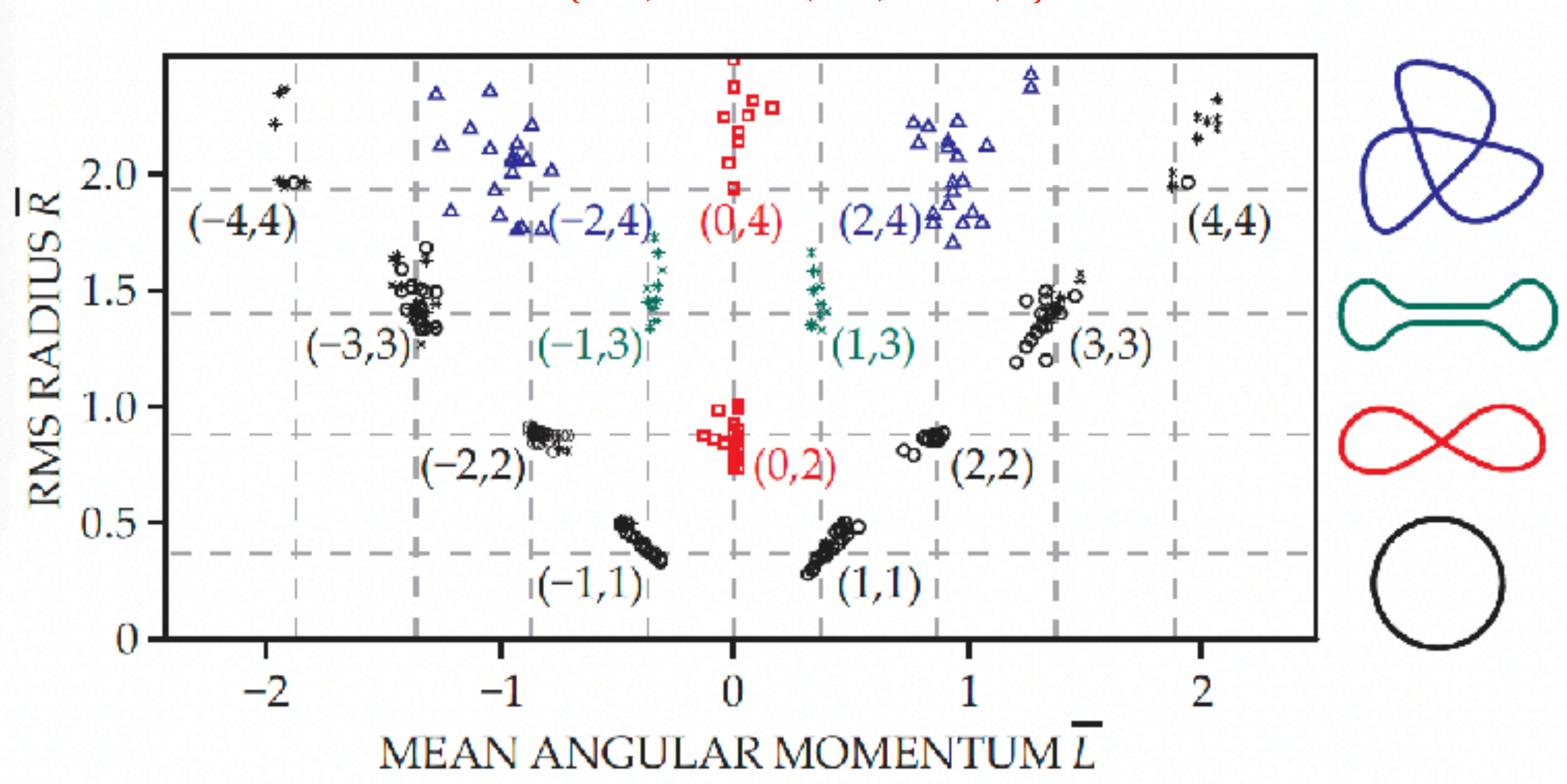

S. Perrard, M. Labousse, M. Miskin E. Fort, Y. Couder, Nature Communication, 5, 3219 (2014)

The chaotic regime at high memory

- droplet switches intermittently between a small number of accessible periodic states

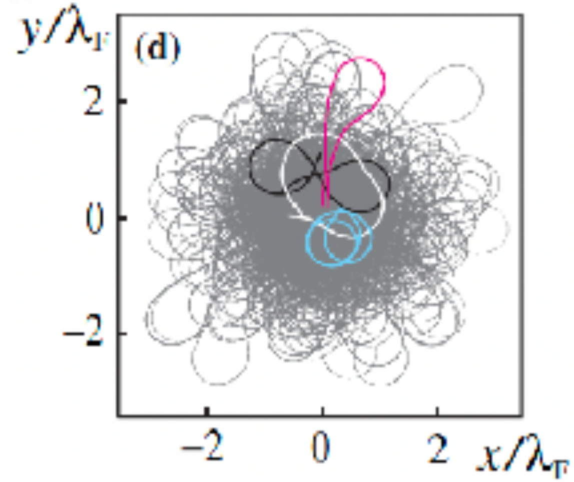

"The detuned trajectory is thus formed from a succession of sequences of pure eigenstates with intermittent transitions between them."

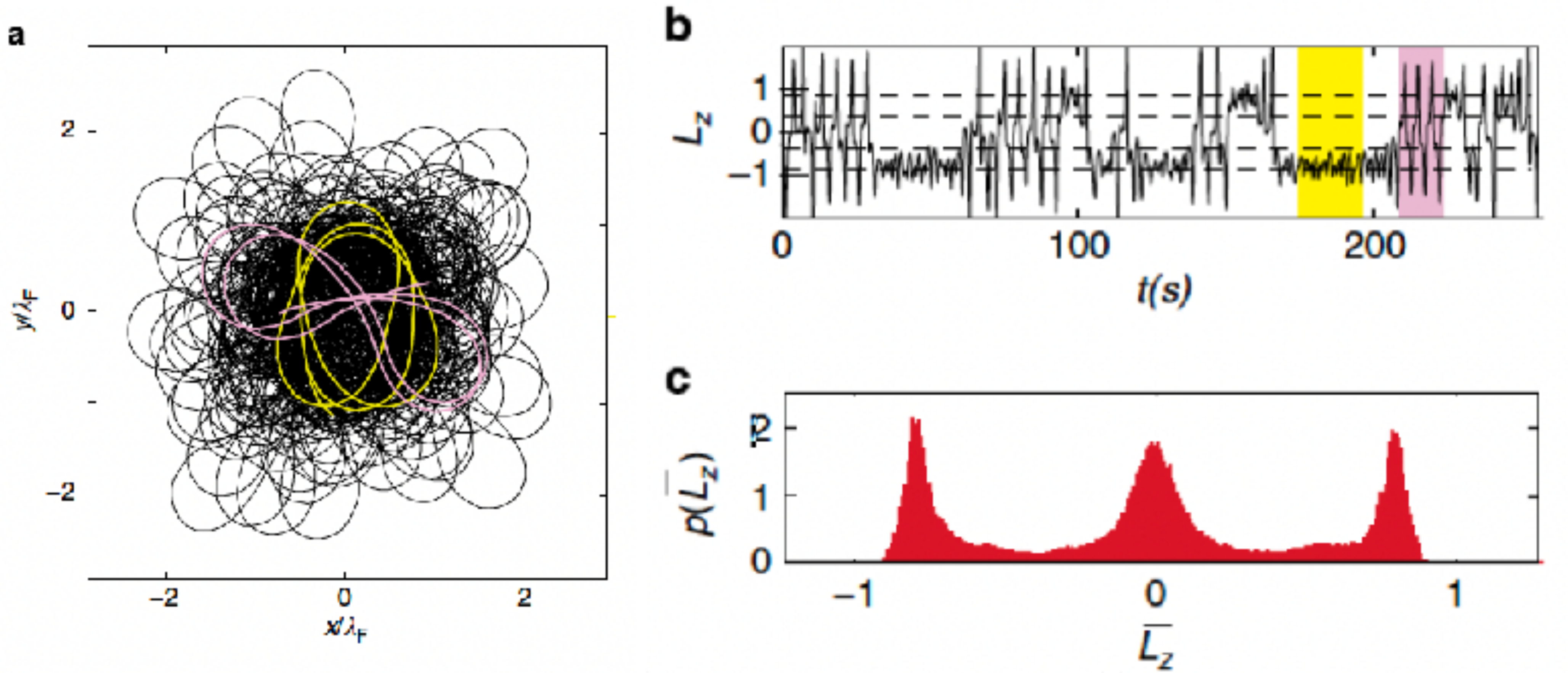

The SHO with the stroboscopic model

Dettmers, Oza & Bush (2017)

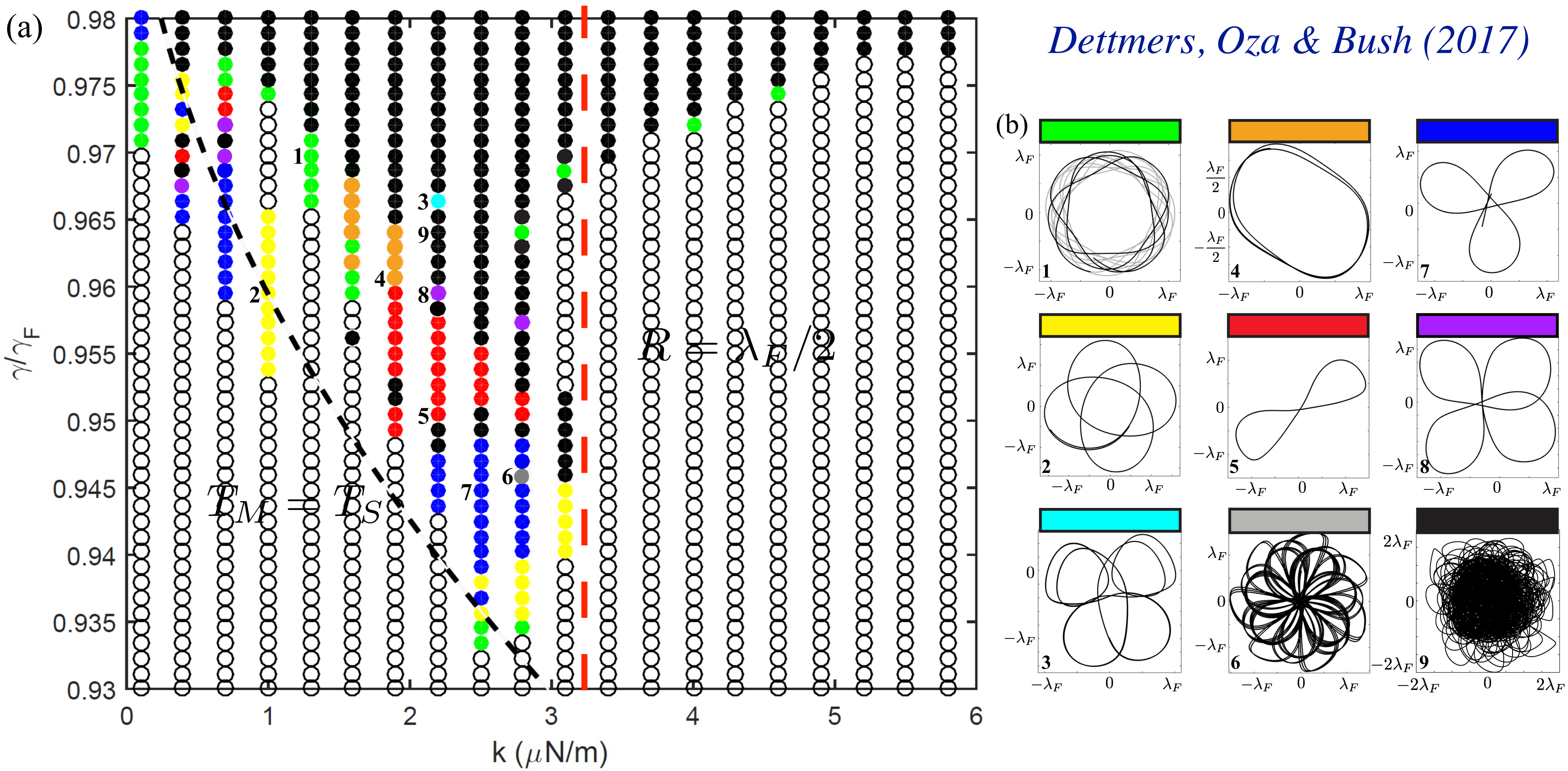

MEMORY TIME **SPRING TIME** **RANGE**

$$T_M \sim (2\nu k_F^2)^{-1}/(1-\gamma/\gamma_F) \qquad T_s = \sqrt{m/k} \qquad R = u_0\sqrt{m/k}$$

- double-quantization emerges when system is effectively `closed'

Periodic orbits

Dettmers et al. (2017)

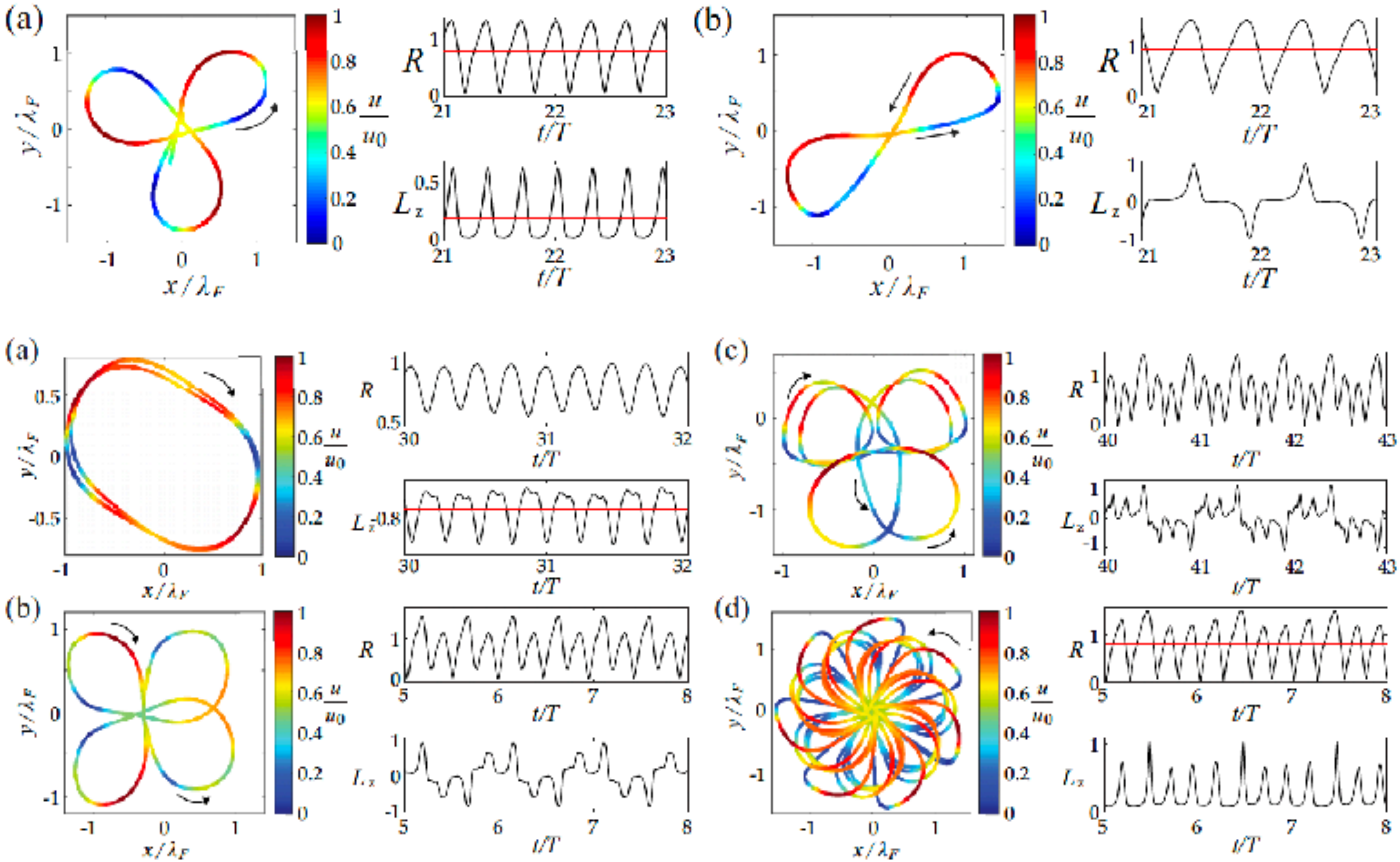

Quantization of periodic orbits

Dettmers et al. (2017)

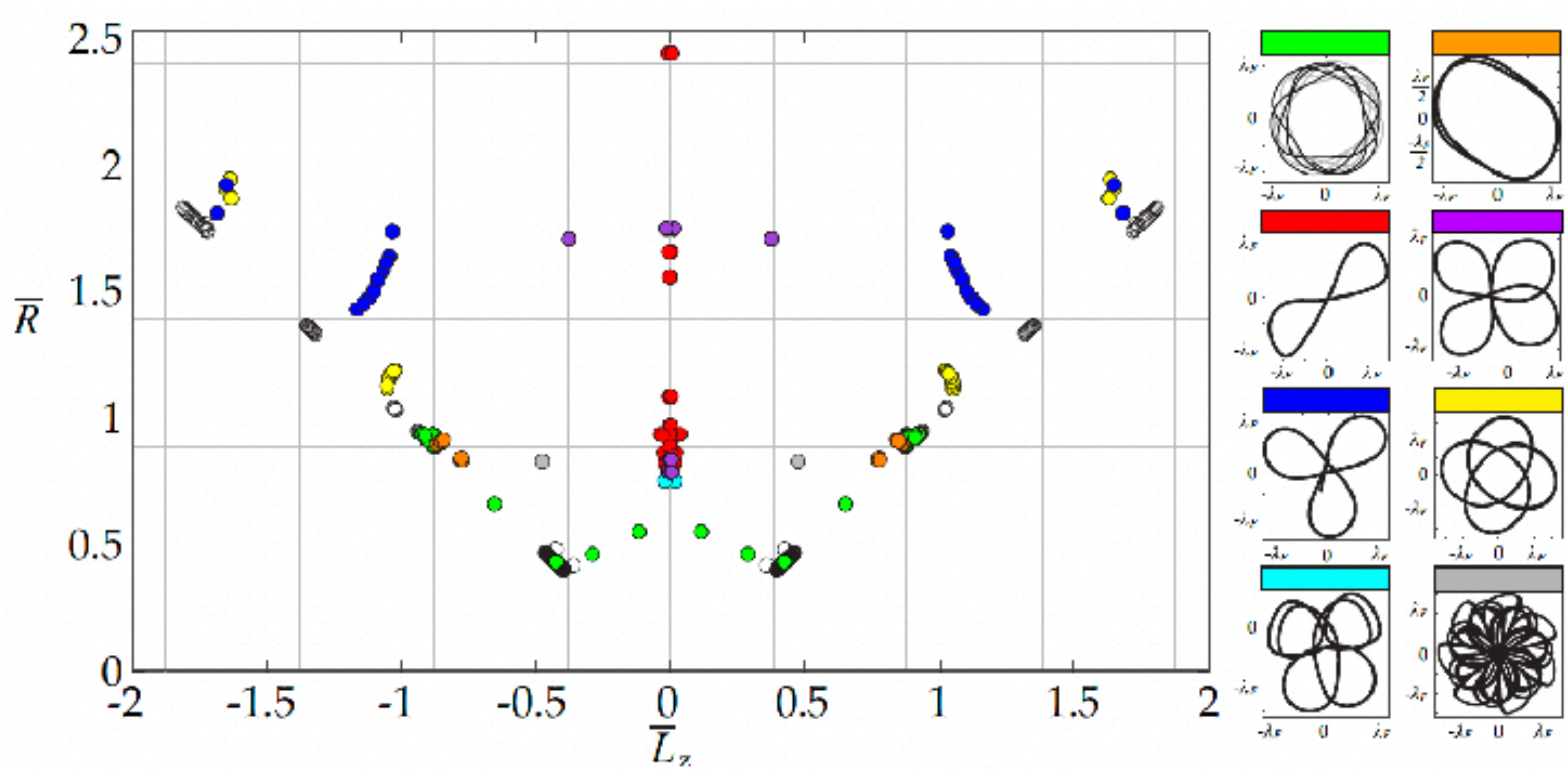

FIG. 4. Dimensionless mean radius $\overline{R}$ and mean angular momentum $\overline{L}_z$ for the periodic and quasiperiodic trajectories observed for $\gamma/\gamma_F > 0.95$.

Chaotic trajectories

Dettmers et al. (2017)

- can be decomposed into quasi periodic subcomponents

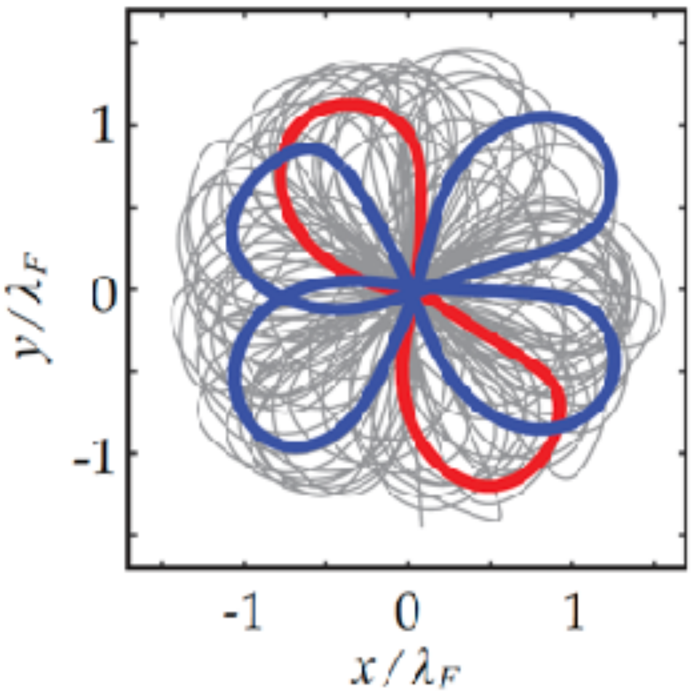

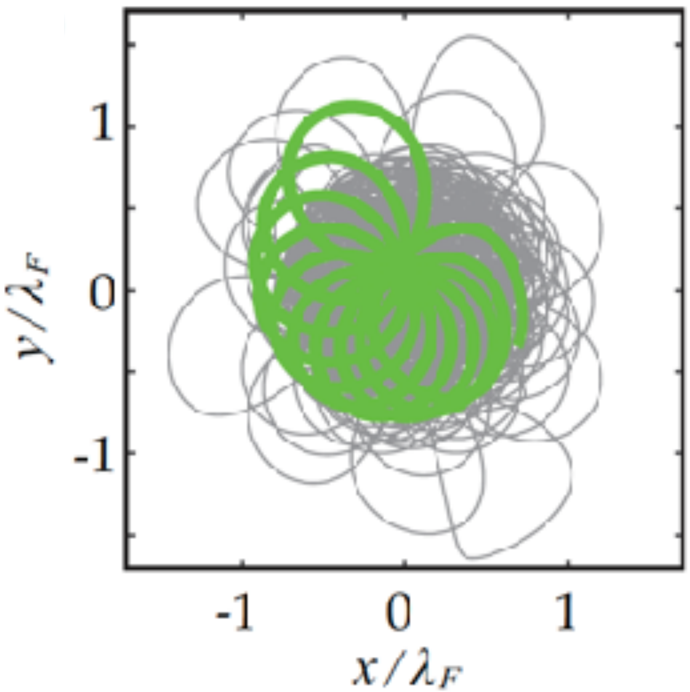

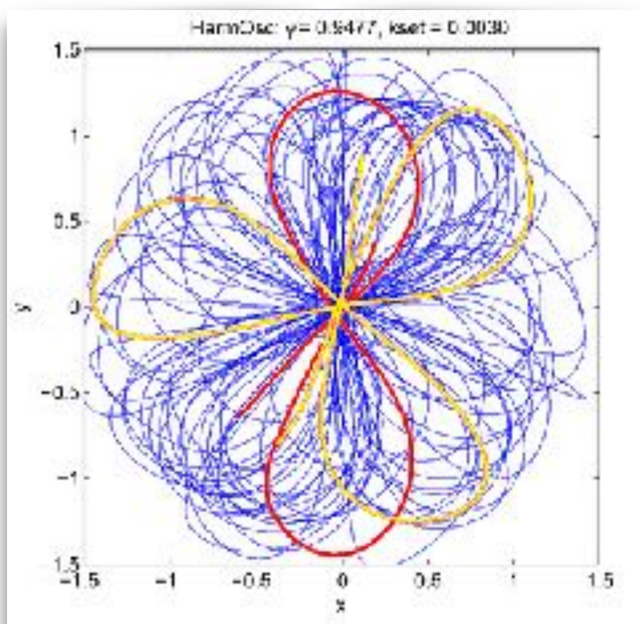

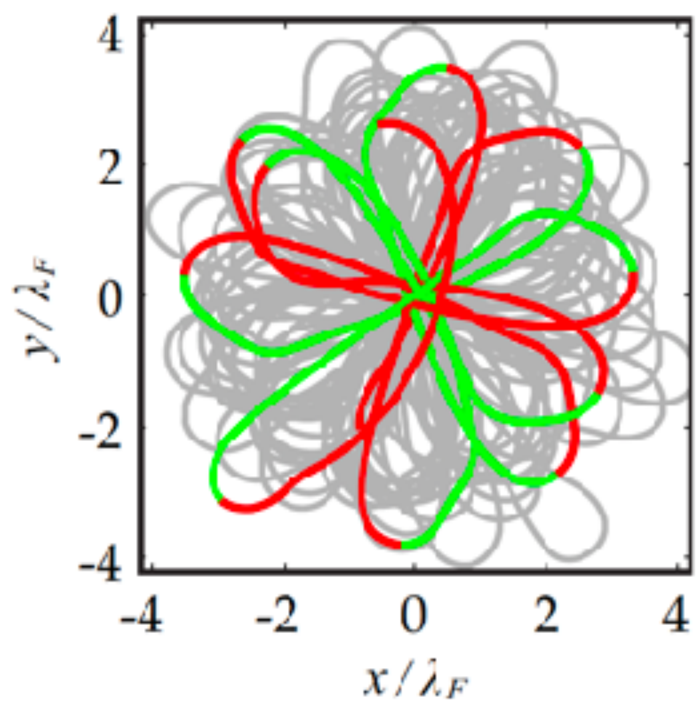

K-means clustering

Durey & Milewski (2017)
Dettmers et al. (2017)

- a means of characterizing quantization in the chaotic regime

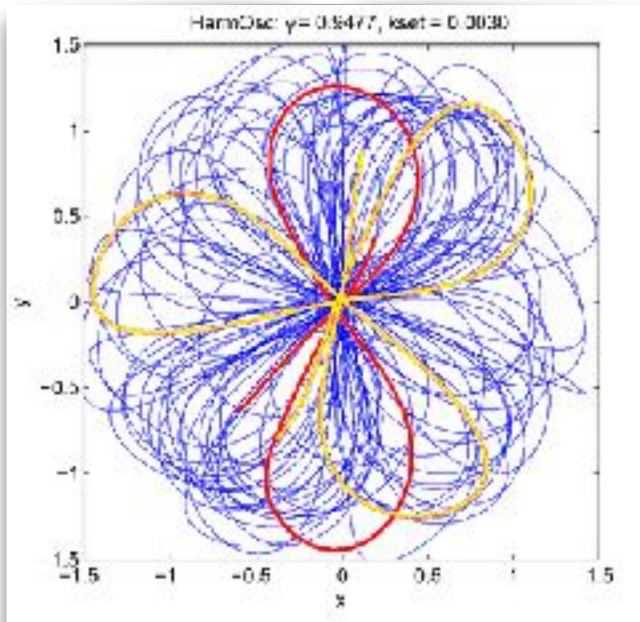

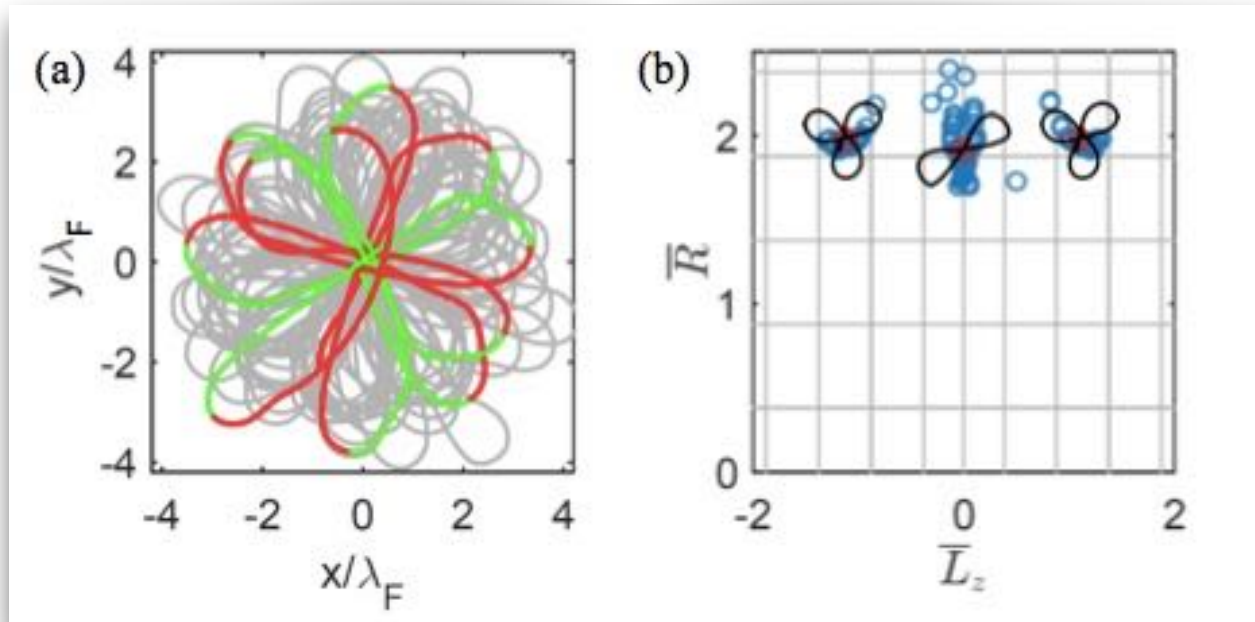

- snip chaotic trajectories at successive maxim, evaluate mean **R, L**
- each sub-trajectory yields a single blue dot
- applying K-means clustering produces means (red dots)

Quantization of chaotic orbits

Dettmers et al. (2017)

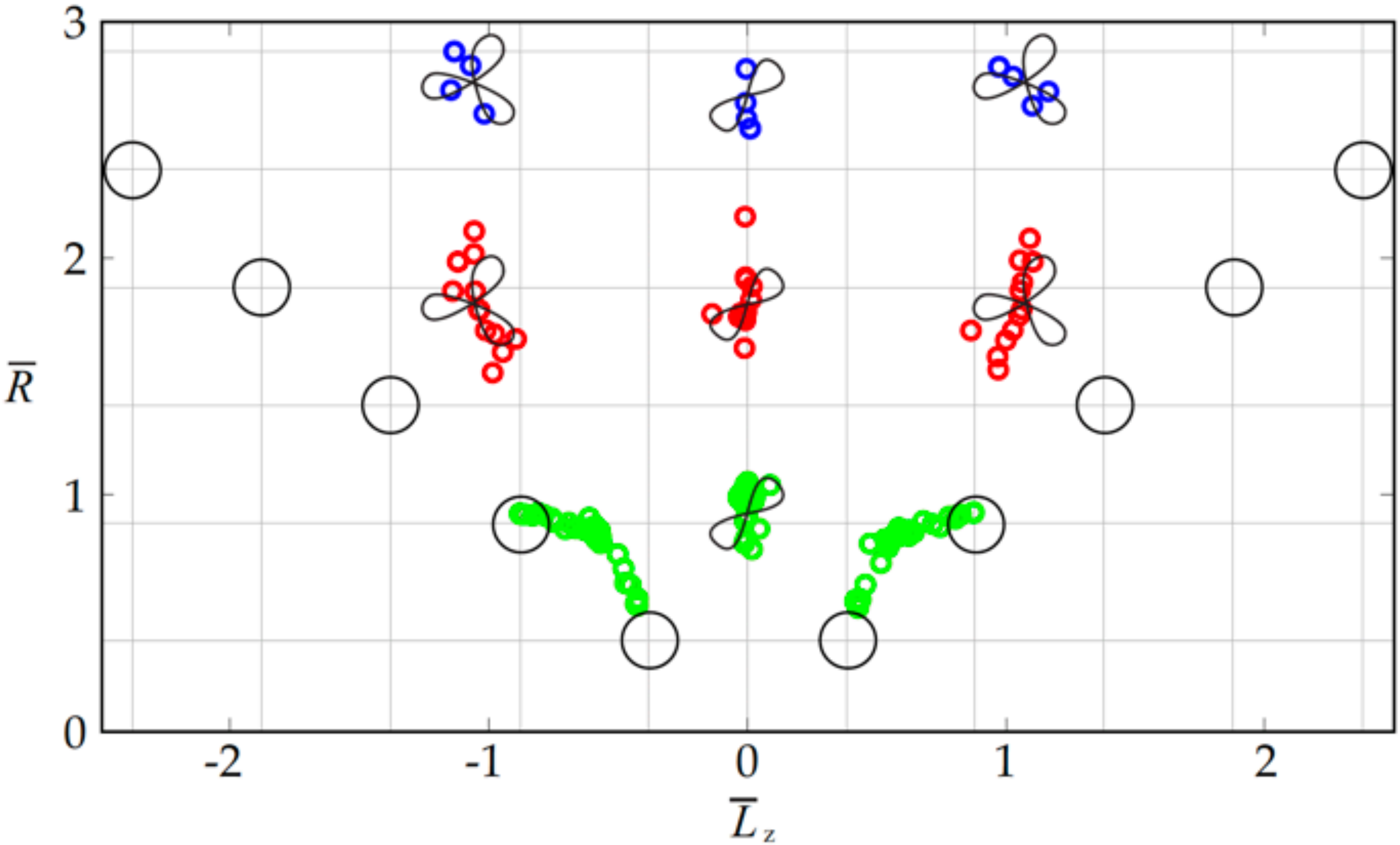

FIG. 9. Shown in green, red, and blue are centroids of clusters for chaotic trajectories at $\gamma/\gamma_F = 0.971$, for spring constants in the range $0.1 \leqslant k \leqslant 5.8$ μN/m, with corresponding Λ in the range $0.3986 \leqslant \Lambda \leqslant 3.254$. The blue, red, and green markers denote spring constants in the ranges $k < 0.57$ μN/m, $0.57 \leqslant k < 1.36$ μN/m, and $k \geqslant 1.36$ μN/m, respectively.

Tambasco et al. (2017)

The tongue diagram

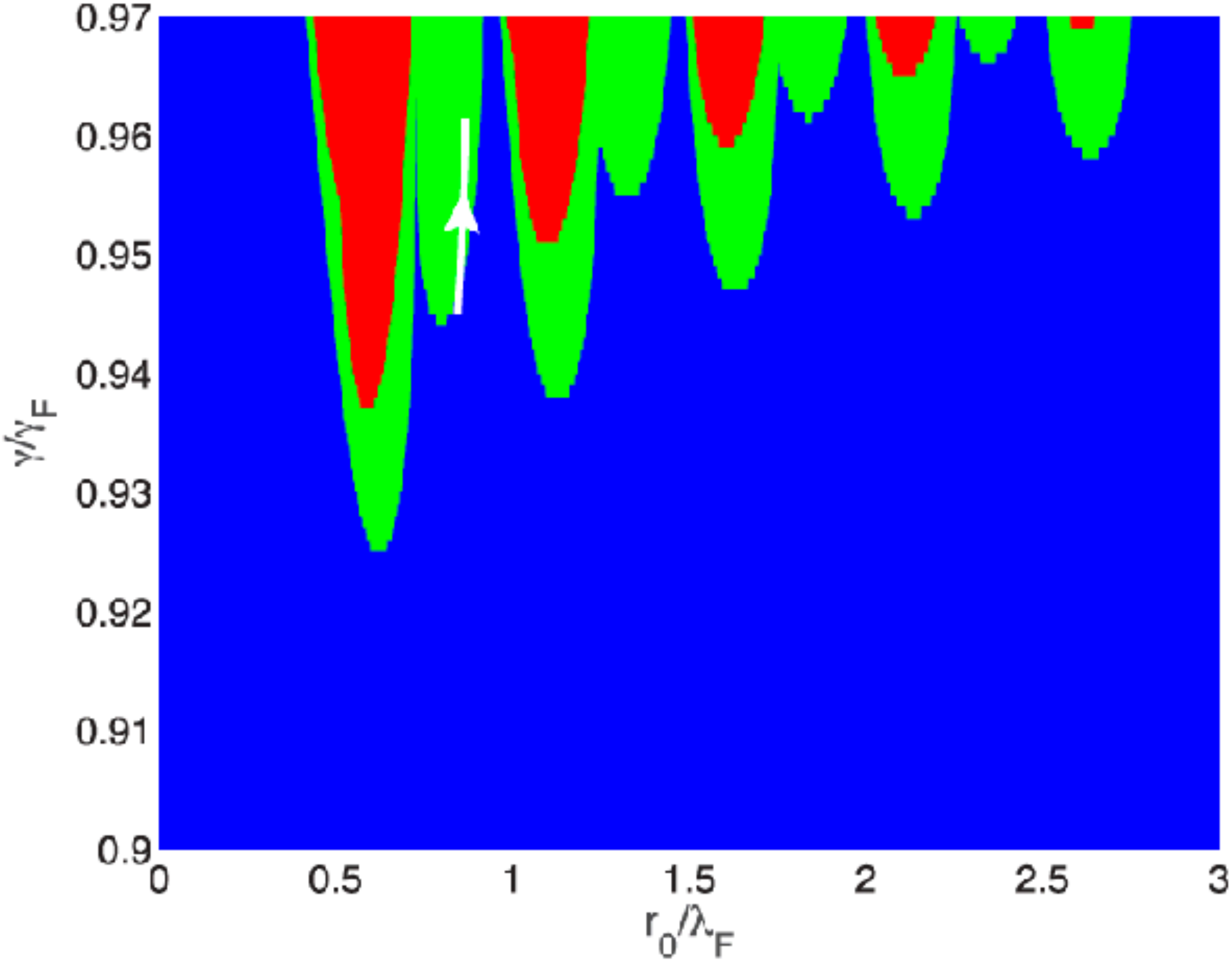

Onset of chaos

Tambasco et al. (2017)

- arises through the Ruelle-Takens-Newhouse route to chaos
- incommensurate frequencies appear in the spectrum

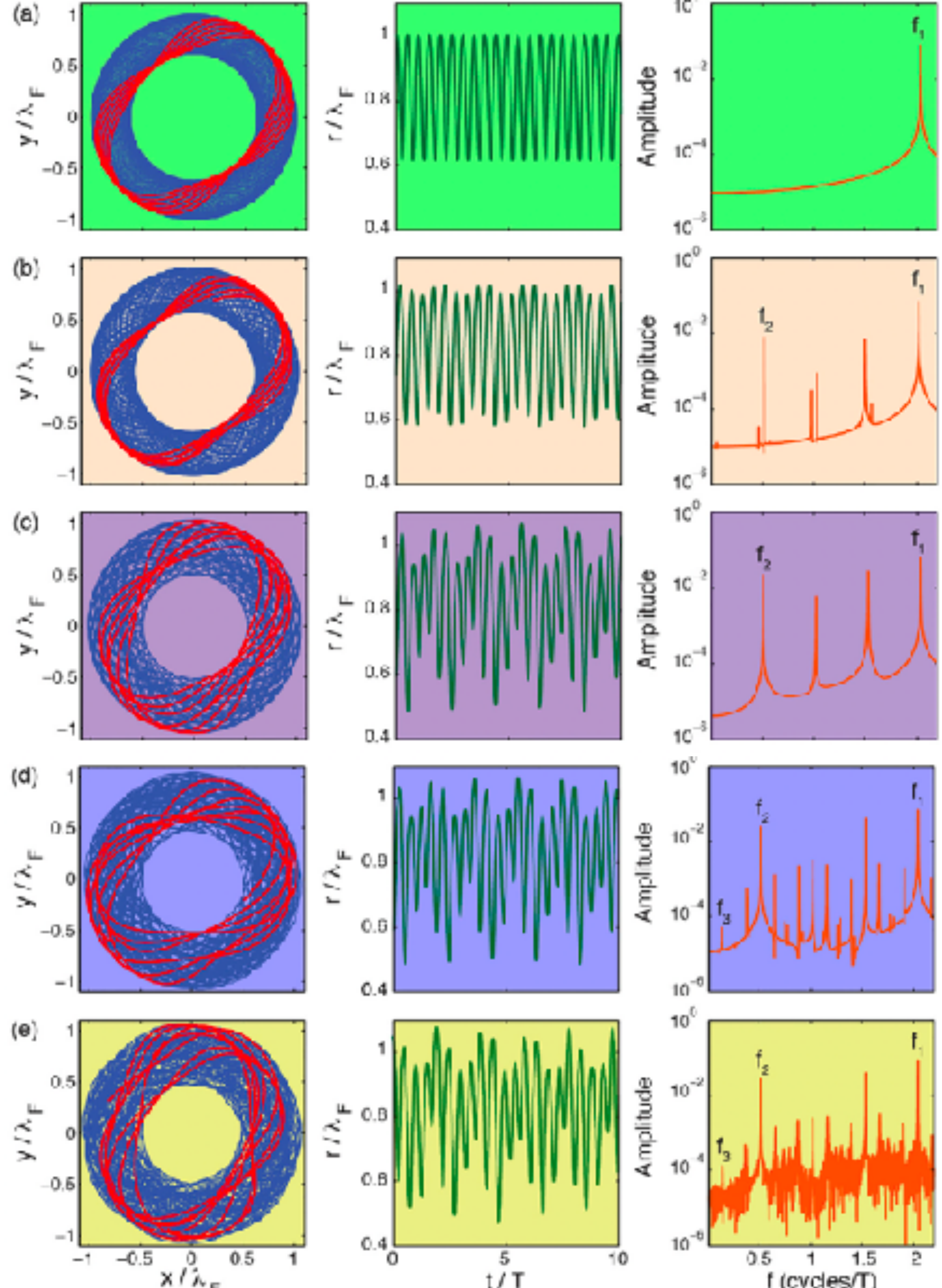

Orbital pilot-wave systems as `closed systems'

- walker motion confined by an applied force

Rotation: *Fort et al. (2010) , Oza et al. (2013, 2014), Harris & Bush (2014)*
SHO: *Perrard et al. (2014), Labousse et al. (2015), Durey & Milewski (2017)*

Quantization emerges provided:

$$T_M > u_0/R$$

MEMORY TIME **ORBITAL TIME**

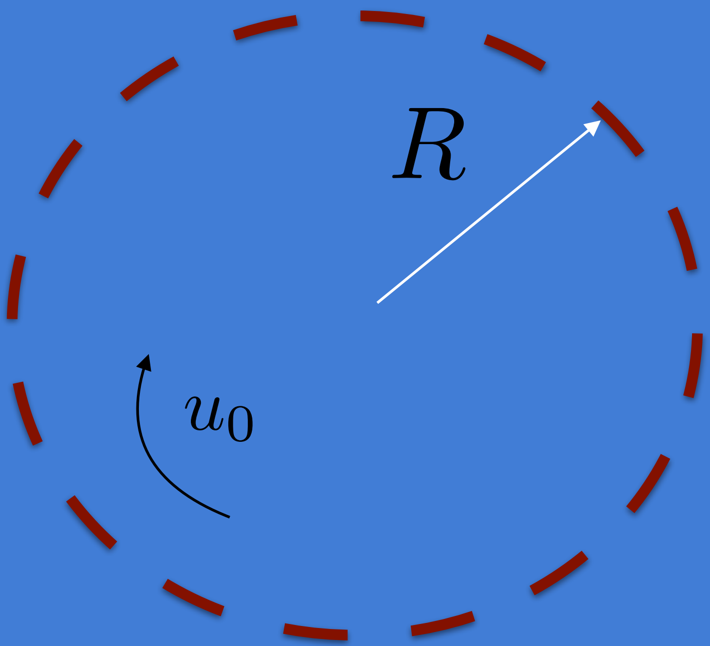

→ waves persist beyond characteristic orbital time

→ system is effectively `***closed***' and `***above threshold***'

The rotating frame as a `closed system'

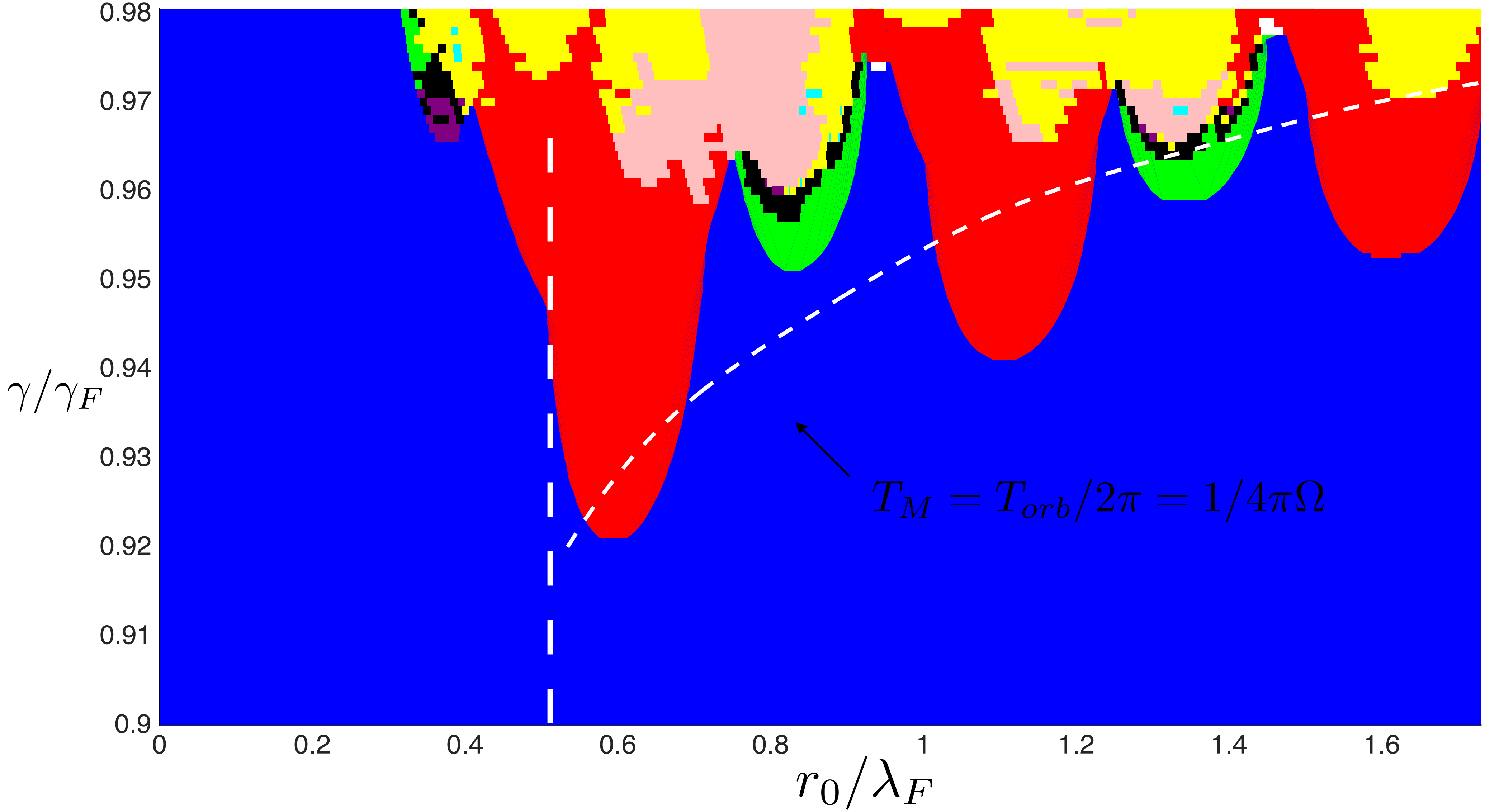

MEMORY TIME	ORBIT TIME	RANGE
$T_M \sim (2\nu k_F^2)^{-1}/(1-\gamma/\gamma_F)$	$T_{orb} = 1/2\Omega$	$R = u_0/2\Omega$

- **quantization emerges when system is effectively `closed'**

Orbital pilot-wave dynamics: summary

- particle motion in a monochromatic wave field is strongly constrained

→ ***quantization emerges from pilot-wave dynamics***

- chaotic pilot-wave dynamics emerging in the high-memory limit contains an imprint of the unstable orbital states

→ ***multimodal statistics emerge from chaotic pilot-wave dynamics***

- quantum-like behaviour emerges when the memory time exceeds the domain's crossing time: ***the drop surfs its self-generated potential***

- **superposition of statistical states may be seen as a manifestation of chaotic switching between accessible unstable periodic orbits**

Summary

- stroboscopic model captures salient features of orbital pilot-wave dynamics
- relatively minor discrepancies in stability characteristics, likely due to breakdown of assumption of drop-wave resonance
- has revealed a rich, multi-scale, multi-periodic dynamics

Physical picture

- quantization rooted in dynamic constraint imposed on the droplet by its monochromatic self-potential, its Faraday pilot-wave field
- at high memory, quantized orbits destabilize, chaotic trajectories emerge
- multimodal statistics reflect superposition of unstable dynamical states

The first paradigm for the emergence of quantum behavior

- quantum statistics underlaid by chaotic pilot-wave dynamics